

**DEVELOPMENT OF HYDROGEN-BASED PORTABLE POWER
SYSTEMS FOR DEFENSE APPLICATIONS**

by

Taylor Bryan Groom

A Dissertation

Submitted to the Faculty of Purdue University

In Partial Fulfillment of the Requirements for the degree of

Doctor of Philosophy



School of Mechanical Engineering

West Lafayette, Indiana

August 2020

**THE PURDUE UNIVERSITY GRADUATE SCHOOL
STATEMENT OF COMMITTEE APPROVAL**

Dr. Timothée Pourpoint, Chair

School of Aeronautics and Astronautics

Dr. Steven Son

School of Mechanical Engineering

Dr. Eric Dietz

Department of Computer and Information Technology

Dr. Robert Orth

School of Mechanical Engineering

Approved by:

Dr. Nicole L. Key

*For Max and Ellie. Being your dad will forever be my greatest joy and accomplishment.
And in loving memory of my dad, who showed me what it means to never give up.*

ACKNOWLEDGMENTS

I cannot overstate my gratitude to my advisor, Professor Timothée Pourpoint, for all he has done for my family and me over the past four years. It is because of his dedication and willingness to go beyond the typical responsibilities of an academic advisor that I was able to have the courage and resources necessary to continue pursuing my doctoral degree. I consider Professor Pourpoint a role model in many ways and look forward to continuing our friendship for years to come.

I would like to thank my committee members, Professors Steven Son and Eric Dietz and Dr. Robert Orth, for their time and commitment to my research. Professor Son was instrumental in convincing me that Purdue was the best place for me to further my education and I will forever be grateful that he did. From my first semester at Purdue, Professor Dietz has been an advocate for this research and a crucial resource in bridging the knowledge gap between academia and the needs of the United States military. Dr. Orth's contributions to my experience are too many to list, but I would especially like to thank him for his patience during our countless impromptu chemistry lessons. He has been a true friend and mentor both in and out of the lab and I appreciate the perspective that he provided me with throughout such a pivotal period of my life.

My experience at Purdue was greatly enriched by my colleagues and friends at Zucrow Laboratories, and specifically my peers in Professor Pourpoint's research group. There are too many names to list here, but I am confident these friendships will last long past our time at Zucrow. I owe a great debt of gratitude to Professor Pourpoint's staff, Mr. Jason Gabl, Mr. Benjamin Whitehead, and Dr. Alicia Carayon, for the many years they spent supporting my development as an engineer. I would also like to thank Zucrow's talented machinists, support staff, and the folks in the ME Graduate Office for supporting my research and always making Purdue feel like home.

The research for this dissertation was supported as part of Purdue's NEPTUNE Center for Power and Energy, funded by the Office of Naval Research under Award Numbers N000141613109 and N000141512833. I would like to thank Dr. Maria Medeiros, our program manager at ONR, for supporting and encouraging this work.

My wife, Marissa, has been my greatest support throughout my doctoral studies. This is truly *our* accomplishment. I cannot thank her enough for enabling this journey and for blessing me with the greatest joys of my life, Max and Ellie. I would also like to thank my incredibly supportive parents and sisters for always believing in me and encouraging me in all my endeavors.

TABLE OF CONTENTS

LIST OF TABLES	7
LIST OF FIGURES	8
TERMINOLOGY	11
ABSTRACT.....	12
1. INTRODUCTION	13
1.1 Motivation.....	13
1.2 Research Objectives.....	14
2. BACKGROUND.....	15
2.1 Fuel Cells	15
2.2 Solid State Hydrogen Storage.....	16
2.2.1 Metal Hydrides	16
2.2.2 Chemical Hydrides	17
2.2.2.1 Sodium Borohydride.....	17
2.2.2.2 Ammonia Borane.....	19
3. AMMONIA BORANE HYDROLYSIS CHARACTERIZATION	23
3.1 Burette Tests	23
3.1.1 Acid Screenings.....	24
3.1.2 Minimum Water Requirements	26
3.1.3 Influence of Water Purity	28
3.2 Hydrogen Purity Analysis.....	30
3.2.1 Preliminary Purity Analysis with Gas Chromatography and Dräger Tubes.....	31
3.2.2 Purity Analysis with FTIR Spectrometry	32
3.3 Comparison to Platinum-Based Catalysts.....	36
4. HYDROGEN REACTOR DESIGN.....	40
4.1 Envisioned System Use Case.....	40
4.2 Initial Design Requirements	40
4.3 Initial Hydrogen Reactor Prototype – The ABCharger	41
4.4 Updated Design Requirements	48
4.5 Second System Prototype – The ABCharger 2.0.....	50

5. ELECTRICAL HARDWARE INTEGRATION.....	56
5.1 Horizon H-30 PEMFC	56
5.2 Squad Power Manager	58
5.3 Programmable Electronic Load	60
6. INCREASED TEST DURATION WITH SIMULATED LOADS.....	62
6.1 System Testing with Ammonia Borane	62
6.2 System Testing with Sodium Borohydride	74
7. BATTERY CHARGING DEMONSTRATIONS	98
7.1 Cell Phone Battery Charging	98
7.2 BB-2590 Battery Recharging.....	101
8. WASTE MANAGEMENT	104
9. SYSTEM ENERGY DENSITY	106
9.1 Comparison to BB-2590 Batteries	106
9.2 Comparison to Other Energy Storage Systems.....	107
10. CONCLUSIONS	110
APPENDIX A. FTIR CALIBRATION CURVES	113
APPENDIX B. ABCHARGER MACHINE DRAWINGS	115
APPENDIX C. ABCHARGER 2.0 MACHINE DRAWINGS	121
REFERENCES	126

LIST OF TABLES

Table 3.1. Qualitative screening of various water sources for AB hydrolysis.	29
Table 3.2. Contaminant concentrations in acid-promoted AB hydrolysis gas products measured by GC and Dräger Ammonia Detection Tubes.....	32
Table 3.3. Contaminant concentrations in acid-promoted AB hydrolysis gas products measured by FTIR analysis.....	36
Table 3.4. Contaminant concentrations in AB hydrolysis gas products using maleic acid or Pt/C to promote gas release.....	38
Table 4.1. Initial hydrogen reactor design requirement matrix.	41
Table 4.2. Updated hydrogen reactor design requirement matrix.	49
Table 4.3. Dimensions of acrylic reaction vessels.....	54
Table 6.1. Contaminant concentrations in ABCharger hydrolysis gas products measured by FTIR analysis.....	72
Table 6.2. Contaminant concentrations in acid-promoted SBH hydrolysis gas products measured using FTIR analysis.	77
Table 9.1. Mass breakdown of ABCharger 2.0 system.	106

LIST OF FIGURES

Figure 3.1. Burette setup for benchtop hydrolysis experiments.	23
Figure 3.2. Screening of organic acids as potential AB hydrolysis promoters.....	24
Figure 3.3 Influence of temperature on maleic acid-promoted AB hydrolysis.	26
Figure 3.4. Tartaric acid-promoted AB hydrolysis using limited amounts of water.	28
Figure 3.5. Maleic acid-promoted AB hydrolysis using alternative water sources.	30
Figure 3.6. Gas chromatography system used for hydrogen purity analysis.	31
Figure 3.7. FTIR spectrums of gases evolved from acid-promoted AB hydrolysis using various water sources.....	34
Figure 3.8. Comparison of maleic acid and Pt/C as AB hydrolysis promoters.	37
Figure 3.9. Comparison of FTIR spectrums of gases evolved from either acid-promoted AB hydrolysis or platinum catalyzed AB hydrolysis	39
Figure 4.1. Initial hydrogen reactor prototype, the ABCharger.....	42
Figure 4.2. Simulated fuel transfer in the ABCharger using water and red dye.....	43
Figure 4.3. Fuel cell test stand at the Protonex facility.....	45
Figure 4.4. Hydrogen flow rate and pressure during Test AB-1.	46
Figure 4.5. PEMFC output during Test AB-1.....	47
Figure 4.6. P&ID of the ABCharger 2.0 on the hydrogen generation test stand.	51
Figure 4.7. ABCharger 2.0 on the hydrogen generation test stand.....	52
Figure 4.8. Hydrogen flow rate and pressure during Test AB-2.	53
Figure 4.9. ABCharger 2.0 acrylic vessel.	55
Figure 5.1. Electrical circuit used for testing the portable power generation system.	57
Figure 5.2. Example of how Horizon’s fuel cell water management techniques influence chamber pressure and hydrogen flow rate.	57
Figure 5.3. System used for preliminary BB-2590 battery recharge.	59
Figure 5.4. Hydrogen flow rate and pressure during Test AB-3.	60

Figure 5.5. P&ID of the modified hydrogen generation test stand.....	61
Figure 6.1. PEMFC output during Test AB-4.....	62
Figure 6.2. Hydrogen flow rate and pressure during Test AB-4.	63
Figure 6.3. PEMFC output during Test AB-5.....	64
Figure 6.4. Hydrogen flow rate and pressure during Test AB-5.	64
Figure 6.5. PEMFC output during Test AB-6.....	66
Figure 6.6. Hydrogen flow rate and pressure during Test AB-6.	67
Figure 6.7. PEMFC output during Test AB-7.....	68
Figure 6.8. Hydrogen flow rate and pressure during Test AB-7.	68
Figure 6.9. Hydrogen generation stand connected to FTIR for product gas analysis.....	70
Figure 6.10. FTIR spectrums of product gases generated in the ABCharger 2.0 system using the procedures developed for PEMFC testing.	71
Figure 6.11. Comparison of acid-promoted hydrolysis using maleic acid and either SBH or AB.	75
Figure 6.12. Hydrogen yield from maleic acid-promoted hydrolysis of SBH using low-quality water sources.....	76
Figure 6.13. FTIR spectrums of product gases generated by organic acid-promoted hydrolysis of SBH using low-quality water sources.....	77
Figure 6.14. PEMFC output during Test SBH-8.	79
Figure 6.15. Hydrogen flow rate and pressure during Test SBH-8.	79
Figure 6.16. PEMFC output during Test SBH-9.	80
Figure 6.17. Hydrogen flow rate and pressure during Test SBH-9.	81
Figure 6.18. Solution temperature inside reactor during Test SBH-9.	81
Figure 6.19. Reaction vessel following Test SBH-9. Solid particulate can be seen at the top and bottom of the reaction vessel.	83
Figure 6.20. PEMFC output using during Test SBH-10.....	84
Figure 6.21. Hydrogen flow rate and pressure during Test SBH-10.	84

Figure 6.22. Solution temperature inside reactor during Test SBH-10.	85
Figure 6.23. Temperature profiles from Test SBH-9 and Test SBH-10 representing solution temperatures for SBH hydrolysis using maleic acid and tartaric acid, respectively.....	86
Figure 6.24. Hydrogen flow rate and pressure during Test SBH-11.	87
Figure 6.25. PEMFC output during Test SBH-12.	89
Figure 6.26. Hydrogen flow rate and pressure during Test SBH-12.	90
Figure 6.27. Solution temperature inside reactor during Test SBH-12.	90
Figure 6.28. PEMFC output during Test SBH-13.	93
Figure 6.29. Hydrogen flow rate and pressure during Test SBH-13.	93
Figure 6.30. Solution temperature inside reactor during Test SBH-13.	94
Figure 6.31. PEMFC output during Test SBH-14.	96
Figure 6.32. Hydrogen pressure during Test SBH-14.	96
Figure 6.33. Hydrogen flow rate during Test SBH-14.	97
Figure 7.1. Flow diagram of the interface of key components during cell phone charging.	99
Figure 7.2. System used for charging cell phones with the ABCharger 2.0 on the hydrogen generation test stand.....	99
Figure 7.3. Hydrogen flow rate and pressure during Test SBH-15.	100
Figure 7.4. Hydrogen flow rate and pressure during Test SBH-16.	102
Figure 7.5. Solution temperature inside reactor during Test SBH-16	102

TERMINOLOGY

AB	=	Ammonia borane
GC	=	Gas chromatography
FTIR	=	Fourier-transform infrared spectroscopy
PEMFC	=	Proton exchange membrane fuel cell
SBH	=	Sodium borohydride
sLpm	=	Standard liters per minute
SOFC	=	Solid oxide fuel cell
SPM	=	Squad Power Manager
wt. %	=	Weight percent

ABSTRACT

This dissertation describes the design and characterization of a lightweight hydrogen reactor coupled to a proton exchange membrane fuel cell for portable power delivery. The system is intended to recharge portable batteries in the absence of an established electrical power supply. The presented work can be divided into two endeavors; the first being an investigation of various hydrogen generation pathways and the second being the design, fabrication, and testing of a system to house hydrogen generation and deliver electrical power.

Two hydrogen storage materials are considered for this work: ammonia borane and sodium borohydride. Organic acids are investigated for their ability to accelerate the hydrolysis of either material and generate hydrogen on-demand. In the case of ammonia borane, organic acids are investigated for a secondary role beyond reaction acceleration, serving also to purify the gas stream by capturing the ammonia that is produced during hydrolysis. Organic acids are found to accelerate the hydrolysis of ammonia borane and sodium borohydride with relative indifference towards the purity of water being used. This is advantageous as it allows the user to collect water at the point of use rather than transport highly pure water for use as a reactant. Collecting water at the point of use increases system energy density as only ammonia borane or sodium borohydride and an organic acid are transported with the system hardware.

A custom hydrogen reactor is developed to facilitate hydrolysis of ammonia borane or sodium borohydride. The reactor is paired with a fuel cell to generate electrical power. The rate of hydrogen being generated by the system is modulated to match the fuel cell's consumption rate and maintain a relatively constant pressure inside the reactor. This allows the system to satisfy a wide range of hydrogen consumption rates without risking over pressurization. The system is shown to produce up to 0.5 sLpm of hydrogen without exceeding 30 psia of hydrogen pressure or a temperature rise greater than 35°C.

The envisioned use for this system is portable battery charging for expeditionary forces within the United States military. This application informed several design choices and is considered when evaluating technological maturation. It is also used to compare the designed system to existing energy storage technologies.

1. INTRODUCTION

1.1 Motivation

Recent decades have seen technological advancements and cultural shifts make portable electronics a vital part of everyday life. These electronics are typically powered using either disposable or reusable batteries, with the latter being particularly useful as they can be recharged anywhere with access to a reliable electrical power supply. However, there are many high-risk scenarios in which dependable power sources are unavailable. In these situations, users who rely on electrical devices have limited power generation options and are typically forced to carry additional batteries to ensure they have adequate power to meet their demand. In settings where the user will be traveling by foot, the effort required to carry these batteries is significant and can limit the duration and effectiveness of their endeavor.

The conditions above apply to civilian applications such as backpacking, emergency response, and search and rescue efforts. However, expeditionary forces within the United States military have arguably the most to gain from high energy density portable power supplies. Often responsible for development and first adoption of cutting-edge technologies, the U.S. military has been significantly impacted by the technological revolution that has made portable electronics an integral part of daily activities. Today, dismounted ground combat troops in the U.S. military carry as much as 140 pounds of gear on foot patrols and expeditionary missions, which is far higher than the reported marching weight of any army in world history [1,2]. Depending upon the specialization of the soldier and the nature of the operation, an individual may carry as much as 40 pounds of batteries to power a variety of mission critical electronics [3].

The effects of carrying heavy loads are detrimental to the physical performance and situational awareness of U.S. warfighters [2]. In an interview conducted for this investigation, an Army Veteran confided that on several occasions his pack was so heavy that his lower arms and hands would go numb less than one hour into a foot patrol. This rendered him incapable of gripping his rifle, forcing him to take regular breaks and endangering his colleagues and himself. The impacts of carrying heavy loads often extend beyond the duration of a soldier's military career. In a 2006 study of veterans from Operations Iraqi Freedom and Enduring Freedom, 44% of veterans reported chronic back pain, while 45% reported chronic joint pain [4]. Electrical devices used for

communication, navigation, and other activities are critical to mission success and it is unlikely that they will be replaced in the near future. For the immediate and long term health and safety of America's warfighters, it is crucial that the energy for these devices be provided using the lowest mass possible.

The relationship between energy storage and mission success is so significant that the United States Marine Corps has set forth the objective to forge "an ethos that equates energy efficiency with combat effectiveness" [5]. Similarly, in the 2018 United States National Defense Strategy it was reported that the development of "ground [sic] forces that can deploy, survive, operate, maneuver, and regenerate in all domains while under attack" is one of United States' most pressing defense-related needs [6]. The ability to efficiently store energy and recharge batteries in remote locations is a critical aspect of a successful ground mission. For these reasons, it is clear that the development of a power delivery system with a higher energy density than currently fielded technologies would be a major advantage for the United States and its expeditionary ground forces.

1.2 Research Objectives

The overarching goal of this research is to develop a hydrogen storage and delivery system that can safely and reliably provide highly pure hydrogen gas for fuel cells or other end use applications. The hydrogen delivery system must be safe and robust, with particular importance placed on the ability to withstand the rigors of a combat environment as the envisioned use application is portable power generation for expeditionary warfighters. The novelty of this work lies in the development of a hydrogen generation pathway that can utilize low-quality water collected at the point of use to release hydrogen from solid state hydrogen storage materials.

Specific objectives of this work include:

1. Determine an efficient combination of hydrogen storage material(s) and reaction promoter(s) that is low cost, capable of facilitating rapid hydrogen release, and results in highly pure hydrogen gas regardless of the water source that is used.
2. Develop a robust and user-friendly hydrolysis control mechanism that can withstand the rigors of a combat environment.
3. Integrate the novel hydrogen generation system with commercially available fuel cells to create a highly efficient portable power system.

2. BACKGROUND

2.1 Fuel Cells

Although they are not the primary focus of this research endeavor, the utility of a hydrogen generation system cannot be fully described without first introducing fuel cells. Fuel cells are a family of electrochemical devices which directly convert chemical energy into electrical energy. Long considered as key elements of a hydrocarbon-free future, fuel cells produce electricity by reacting hydrogen and oxygen with the only byproducts being water and heat [7]. Fuel cells have commonalities to both batteries and internal combustion engines. Like batteries, fuel cells are electrochemical devices consisting of an anode, cathode, and electrolyte. They also both facilitate the direct conversion of chemical energy into electrical energy and are highly efficient. However, fuel cells differ from batteries in that they do not internally store energy. Instead, they are energy conversion devices that must be continuously fed by supplies of fuel and oxidizer and can essentially operate indefinitely if the reactants are replenished. In this regard, fuel cells are similar to internal combustion engines [8].

There are numerous types of fuel cells, with the fuel feedstocks and operating temperatures varying widely between the different designs. For example, proton exchange membrane fuel cells (PEMFC) typically operate below 80°C, while solid oxide fuel cells (SOFC) operate at temperatures as high as 1000°C [8]. The ability to operate at relatively low temperatures makes PEMFCs advantageous for mobile applications where high temperatures are prohibitive. Additionally, PEMFCs have been shown to scale favorably to mobile sizes and are expected to play a more prominent role in portable power delivery in the near future [8–12]. For these reasons, PEMFCs are the fuel cell of choice for this study.

The goal of this work is to develop a hydrogen storage and delivery system, not to advance fuel cell design or performance. However, integration of a PEMFC allows for the hydrogen generator to evolve from an energy storage device to a power delivery system with important real world applications and value. Pairing the system with a fuel cell also provides a use case through which the user interface and overall system maturity can be advanced and evaluated. This allows for demonstration of value and merit outside of a laboratory environment.

It is quite feasible that the hydrogen system described in this dissertation could be applied to other types of fuel cells beyond PEMFCs with comparable results. Alternatively, the generated hydrogen could instead be used to feed a hydrogen burner and produce high grade heat or to fuel an internal combustion engine. Combined fuel cell and burner systems have many applications, from residential combined power systems to space exploration. While PEMFCs provide a compelling use case for this investigation, they are not the only application which could leverage this technology in the future.

2.2 Solid State Hydrogen Storage

The fuel of choice for most fuel cell developers is hydrogen, primarily due to its high gravimetric energy density (120.0 MJ/kg) and the fact that it is a carbon-free energy carrier. However, hydrogen's low volumetric energy density (8.5 MJ/L for liquid hydrogen) and the complexities and inherent dangers associated with storing high pressure hydrogen gas present significant barriers for storage and transportation of pure hydrogen for mobile applications [14–17]. More efficient hydrogen storage can be achieved via materials-based methods, such as chemical or metal hydrides [18,19]. These materials are often easier and safer to store and transport than pure hydrogen.

2.2.1 Metal Hydrides

Metal hydrides are a family of solid state hydrogen storage materials which were initially discovered in the 1930s and have been investigated heavily starting in the late 1950s. By one account, more than 700 original articles investigating metal hydrides were published between 1955 and 1975, with innumerable more being authored since [20]. As the focus of such an abundance of investigation, metal hydrides have been considered for countless applications. Perhaps the most relevant to today's scientific challenges are cyclic applications such as on-board refueling of hydrogen powered automobiles. Metal hydrides are often considered for these applications as they can undergo a large number of hydriding and dehydriding cycles without performance degradation. These materials have also been proposed for thermal energy storage because the processes of hydrogen absorption and desorption are highly exothermic and endothermic, respectively [21,22].

The volumetric hydrogen densities of some metal hydrides exceed that of liquid hydrogen [23]. However, the gravimetric hydrogen density of metal hydrides is comparably low.

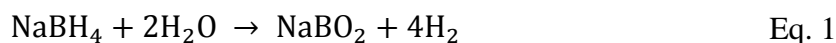
Even the most efficient commonly used metal hydride, lithium hydride (LiH), contains only 12.7 wt. % hydrogen [18,23]. For portable applications where mass is a limited resource, metal hydrides will typically compare poorly to other hydrogen storage technologies. There are also storage challenges to consider. Most metal hydrides must be packed and stored in the absence of air or moisture, which are conditions that would be difficult to maintain during military operations [24,25].

2.2.2 Chemical Hydrides

Chemical hydrides are another family of hydrogen storage materials that have been widely investigated in recent years. Chemical hydrides are particularly intriguing for their high hydrogen content, with gravimetric hydrogen capacities nearing 20%. They are also advantageous for their stability under atmospheric conditions and ability to evolve hydrogen at or near ambient temperatures and pressures. However, the process of releasing hydrogen from chemical hydrides is not readily reversible [26–29]. Currently, most proposed uses of chemical hydrides are single use scenarios. Two of the most investigated chemical hydrides, sodium borohydride and ammonia borane, are discussed below.

2.2.2.1 Sodium Borohydride

Sodium borohydride (SBH, NaBH₄) is a chemical hydride of great interest and has been the focus of extensive research since the 1950s. It has a hydrogen capacity of 10.6 wt. % and is highly soluble in water, dissolving at a rate of 550 g/L at 25°C to form a 35.4 wt. % solution. Aqueous SBH solutions are stable when the solution's pH is higher than 9.0, but will decompose and release hydrogen at lower pH values [30]. Hydrolysis of SBH can release as much as four equivalents of hydrogen gas, with half of the hydrogen atoms coming from two equivalents of water. SBH hydrolysis can be conducted at room temperature and pressure, with various metal catalysts and acid promoters having been shown to facilitate rapid kinetics [12,31–36]. The general reaction for SBH hydrolysis in the presence of a metal catalyst is shown in Eq. 1 below. More detail concerning the reaction pathway for this process, including the potential for hydration of the byproduct sodium metaborate, has been reported in great detail elsewhere [37,38].



The existing literature that is most relevant to the scope of this study is the use of organic acids to accelerate SBH hydrolysis, which was first reported by Schlesinger et al. in 1952 [32]. This topic has been further investigated by multiple groups in more recent years [33,35]. Organic acids have advantages over traditional metal catalysts in that they are inexpensive and water soluble, both of which are valuable for system level applications. Additionally, the catalytic performance of some metal catalysts have been shown to greatly diminish in the presence of low-quality water sources such as seawater, whereas organic acids are expected to be only minimally effected by water contaminations [39]. However, the mass loading of organic acid required for a given rate of hydrogen generation is quite high compared to most metal catalysts. Eq. 2 shows a generalized reaction for acid promoted SBH hydrolysis.



While metal catalyzed hydrolysis produces hydrogen and sodium metaborate, acid promoted hydrolysis results in hydrogen, boric acid, and the sodium salt of the acid's conjugate base [36,40]. It is imperative to understand these byproducts, particularly the sodium salts, when selecting an acid promoter for system level testing to ensure that all byproducts are fully soluble at the concentrations that will be used. It is also important to note that acid promoted hydrolysis does not result in sodium metaborate, which will hydrate under some conditions [38]. The hydration process consumes water and generates heat, both of which are challenges for portable applications.

Many attempts have been made to develop power delivery systems using hydrogen generated from SBH. Perhaps the most sophisticated system that has been developed was reported by Lapeña-Rey et al. in 2017 [41]. These authors used a hydrogen generator developed by Horizon Energy Systems to produced hydrogen via metal-catalyzed SBH hydrolysis. Despite several challenges being reported with the hydrogen generator, the system was paired with a fuel cell and used to power a small drone for flights over four hours long. While there are literature examples of hydrogen generators which use SBH and acid promoters, they have not yet reached the level of maturity that Lapeña-Rey et al. achieved. One example is the 2010 work by Moon et al., in which hydrogen was generated on-demand by introducing small amounts of acid solution into a NaOH stabilized SBH solution. The hydrogen was subsequently consumed by a single cell PEMFC to validate the system architecture [33]. A similar study was conducted in 2010 by Kim et al. with comparable results [35].

2.2.2.2 Ammonia Borane

Another chemical hydride, ammonia borane (AB, NH_3BH_3) has received considerable attention as a solid state hydrogen storage material due to its high hydrogen content of 19.6 wt.% [26,42–46]. It is soluble in water up to 350 grams per liter at 23°C, corresponding to a 26 wt.% solution [46,47].

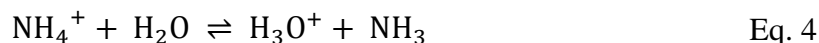
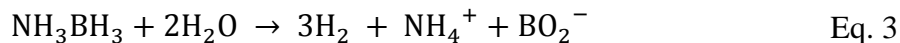
One of the most common procedures for AB synthesis is via salt metathesis of sodium borohydride with ammonium sulfate. Numerous routes have been developed using condensed ammonia, but the most recent developments have replaced this toxic reagent with environmentally benign water, marking its potential for widespread use [27,48–50]. Water-promoted salt metathesis, as reported by Ramachandran and Kulkarni, was used to produce much of the AB used in preparation of this report.

Limited investigations have been conducted concerning the stability of aqueous AB solutions, but the available data implies there is potential for short term stability without buffering. Such stability would provide an advantage when compared to SBH, which must be buffered to a pH greater than 9.0 in order to be stable in solution. Brockman et al. observed that the stability of AB solutions exposed to open air is largely dependent on the AB concentration. They found 10 wt. % solutions to evolve less than 3% of their total hydrogen capacity over 60 days, compared to more than 8% losses for 25 wt. % solutions [46]. This is an important relationship, as achieving useful energy densities will almost certainly require a system to use concentrated solutions for hydrolysis.

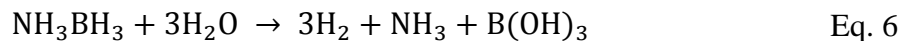
Perhaps the most highly cited investigation of AB stability is that of Chandra and Xu, in which the authors considered a 0.33 wt. % AB solution stored under argon [42]. Analyzing the sample with boron nuclear magnetic resonance before and after the aging study, the authors reported that the solution was unchanged after 80 days. However, the low AB concentration and the argon environment make this study largely irrelevant to a fielded system. Another data set for stability of aqueous AB solutions was reported in 2002 by T-Raissi. In this report, the author refers to “private correspondence with the Callery Chemical Co” when reporting stability of 10 wt. % AB solutions stored at room temperature [47]. The solutions were reported to have experienced 1.8% and 3.6% hydrogen loss after 4 days and 11 days, respectively, and up to 45.0% hydrogen loss after 18 months. Unfortunately, the storage configuration and test conditions are not reported, meaning direct comparison of this data set to those presented by Brockman et al. or Chandra and Xu is of little utility. However, when considered together, these data sets show minimal hydrogen

losses from solutions aged for 4-6 days. This allows for the possibility that AB solutions will not decompose appreciably during the relatively short periods (i.e. less than 10 hours) required to recharge batteries used by expeditionary forces.

Because the reaction of AB with water is quite slow, hydrolysis must be catalyzed to provide rapid hydrogen generation. For metal catalyzed hydrolysis, the overall reaction can be seen stepwise in Eq. 3-Eq. 5 [45].



Eq. 3 shows the release of three equivalents of hydrogen gas by reaction of AB with two equivalents of water, as well as the release of an equivalent of both ammonium and metaborate ions. The produced ammonium can react with water to form ammonia and hydronium, with the equilibrium depending on the pH, temperature, and concentration of the solution. A more basic pH will shift the equilibrium in favor of ammonia. Hydronium will readily react with metaborate anions to produce boric acid. The net reaction achieved by summing Eq. 3-Eq. 5 is represented by Eq. 6 [45].



Along with reaction kinetics and hydrogen yield, a critical property that will determine the utility of AB as a storage medium is the purity of the hydrogen being released. In addition to three equivalents of hydrogen gas, the reaction pathway described in Eq. 6 also results in the production of one equivalent of ammonia. Numerous reports have confirmed the presence of 27,000-174,000 ppm of ammonia in the gas stream when using various metal catalysts to promote hydrolysis [27,45,46,51,52]. Such high levels of ammonia present a significant problem as less than 10 ppm of ammonia can irreversibly damage PEMFCs [53–55]. As such, an ideal catalyst or reaction promoter for AB hydrolysis would promote complete ammonia sequestration. Acids are intriguing reaction promoters for this reason, as conducting hydrolysis a low pH solution will shift the equilibrium represented in Eq. 4 to favor ammonium and potentially prevent significant ammonia release. This is supported by the 2014 findings of Gabl, who reported that promoting AB hydrolysis with an acidic ion-exchange resin led to less than 100 ppm of ammonia in the hydrogen

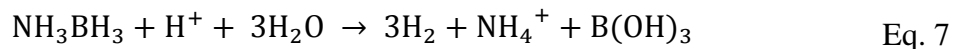
gas stream, compared to more than 36,000 ppm when using a platinum-based catalyst with the same conditions [51].

Other contaminants that can damage a PEMFC are carbon monoxide (CO) and carbon dioxide (CO₂). CO is of particular concern, as PEMFC performance has been shown to decrease in the presence of as little as 5 ppm of CO [56]. While CO₂ is not as detrimental as CO at low concentrations, significant PEMFC performance losses are observed with levels at or above 100,000 ppm [13]. While trace amounts of CO₂ are unlikely to directly damage a PEMFC, it is possible for CO₂ to indirectly contaminate a PEMFC via the reverse water-gas shift reaction, in which CO₂ and hydrogen react to form water and CO. If the conditions in the stack were favorable for this reaction to take place, it is possible that CO₂ concentrations far lower than 100,000 ppm could result in enough CO to damage PEMFCs. However, determining the upper threshold for CO₂ tolerance with respect to the reverse water-gas shift reaction is difficult because the equilibrium is highly dependent on stack operating conditions.

There is limited data reported concerning CO or CO₂ concentrations in hydrogen produced via AB hydrolysis, which is logical because in most cases neither AB nor the catalyst being employed contain carbon. The only mention found in literature of CO or CO₂ present after AB hydrolysis was published by Chandra and Xu, wherein the authors used carbonic acid generated *in-situ* from CO₂ in the head space above an aqueous AB solution to promote hydrolysis [42]. Following their experiment, the presence of both CO and CO₂ were confirmed via mass spectrometry, but the concentrations of either gas were not reported. The presence of CO₂ is to be expected because it was present in the system prior to the reaction, but the authors do not comment on whether the observed CO was an initial contaminant or a byproduct of the reaction.

Mineral acid-promoted AB hydrolysis was first reported by Kelly et al. in 1964 and then revisited by Kelly and Marriot in 1979 [43,57]. Following their initial work, there has been a relatively small amount of investigation concerning acid-promoted dehydrogenation of AB. Notable studies on the subject include those by Chandra and Xu in 2006, Stephen's et al. in 2007, and D'Ulivo et al. in 2004 and 2018 [42,58–60]. Kelly and Marriot suggested a potential reaction pathway for acid initiated hydrolysis, which was later supported with additional experimental evidence by Stephens et al. in 2007 [26]. In this pathway, an H⁺ from the acid replaces boron in AB's nitrogen-boron bond to form an ammonium cation and borane, with the borane rapidly

reacting with water to form boric acid and hydrogen gas. The global reaction pathway for acid promoted hydrolysis is shown in Eq. 7 below.



Previous investigations into acid-promoted hydrolysis of AB predominantly employed either strongly corrosive mineral acids or ion exchange resins. Organic acids have facilitated high yields and rapid hydrogen release during SBH hydrolysis, but similar studies with AB have not been found in existing literature. For this reason, initial work on this project focused on determining the validity of organic acid-promoted hydrolysis of AB as a hydrogen generation pathway for PEMFC systems.

3. AMMONIA BORANE HYDROLYSIS CHARACTERIZATION

3.1 Burette Tests

Using a gas burette to displace water and capture evolved gases is a simple, quick, and cost-effective method for measuring the yield of a gas evolution reaction such as AB or SBH hydrolysis. Water displacement techniques are advantageous because they allow for gas collection while preventing pressurization, which increases safety and permits reactions to be conducted in inexpensive glassware. Reaction kinetics can be determined from these tests by tracking the position of the meniscus in the burette as a function of time. Together, the rate and yield of hydrogen release can be used to quickly and efficiently screen combinations of hydrogen precursors, reaction promoters, and water sources. Additionally, this setup is easily adapted to accommodate temperature and pH measurements, as well as sample collection for purity analysis. A gas burette was used extensively in this investigation to compare organic acid-promoted hydrolysis of both AB and SBH with low quality water to similar reactions with more traditional catalysts and water sources. A schematic of the burette test setup is shown in Figure 3.1.

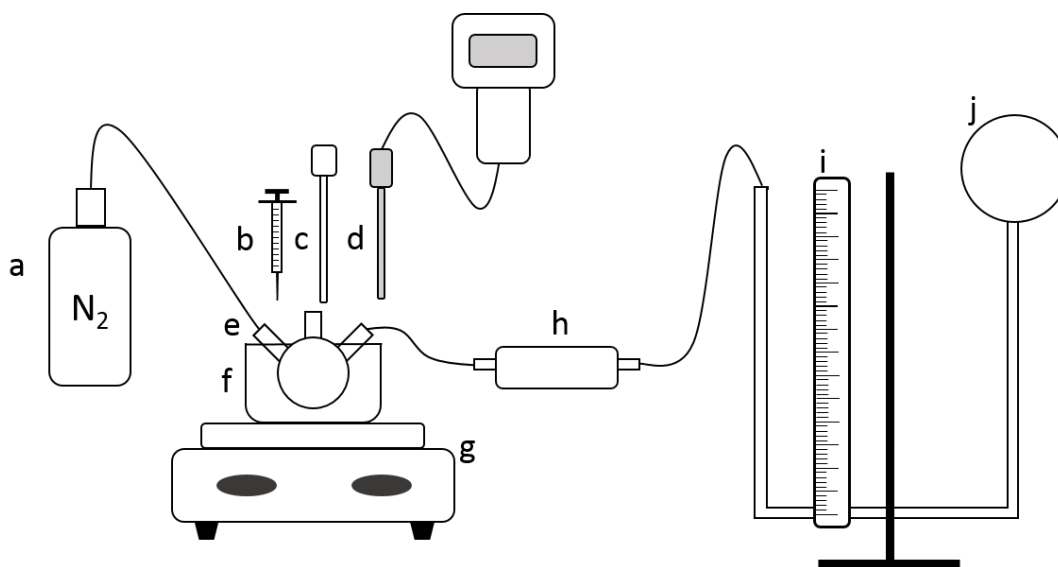


Figure 3.1. Burette setup for benchtop hydrolysis experiments. a.) Bulk nitrogen supply b.) Syringe for reactant addition c.) Thermocouple d.) pH probe e.) Reaction vessel f.) Water bath g.) Hot plate/stirrer h.) Gas sampling bulb i.) Burette j.) Leveling bulb. Not shown: Gas chromatograph, FTIR, Dräger tubes, circulating chiller, syringe pump.

3.1.1 Acid Screenings

Five different organic acids were selected due to their low cost and ready availability and investigated as AB hydrolysis promoters. The acids used for these and all subsequently reported tests were greater than 99% pure, purchased from Sigma Aldrich or Oakwood Chemical, and used as received. Screenings were conducted under pseudo-first order conditions with AB serving as the limiting reagent. These conditions were achieved using a 10 times molar excess of organic acid and a large excess ($\gg 100$ times the amount required by stoichiometry) of deionized water. The large excess of water was used to ensure the reaction was not water limited, as well as to provide enough heat sink to maintain a quasi-steady temperature during hydrolysis.

Hydrolysis screening tests were initiated by injecting 1 mL of 5 wt. % aqueous AB solution into approximately 50 mL of aqueous acid solution. The reaction was housed in a three-neck flask connected to a gas burette as shown in Figure 3.1. The flask was submerged in a 25°C water bath and a magnetic stir bar in the flask was used to vigorously mix the solutions. The results of the initial screening are shown in Figure 3.2 below.

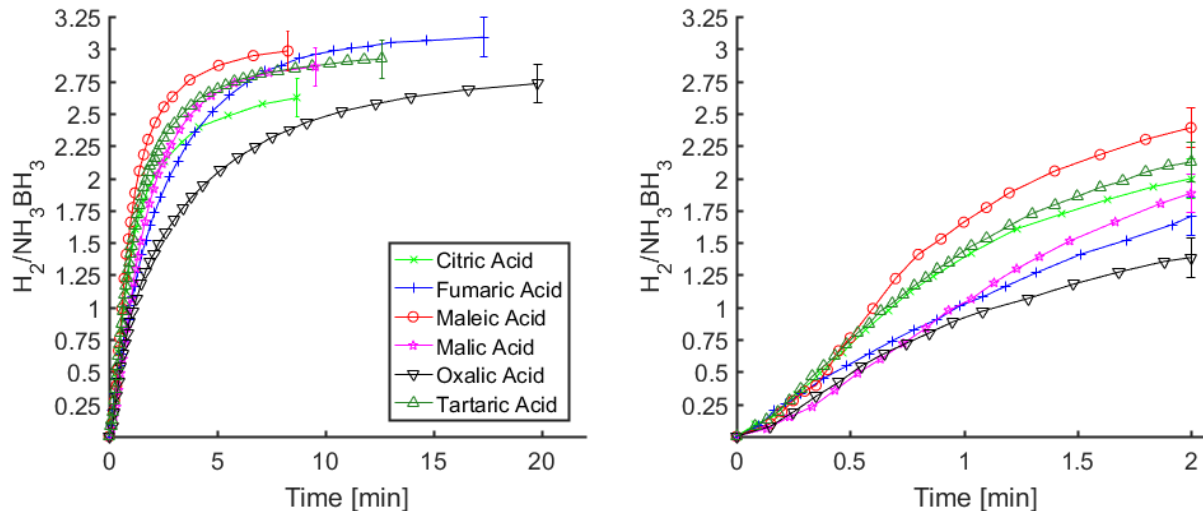


Figure 3.2. Screening of organic acids as potential AB hydrolysis promoters. Shown are the entirety of the hydrogen evolution reactions (left) and a detailed view of the first two minutes (right).

The uncertainty of the hydrogen yield in Figure 3.2 is approximately $\pm 5\%$, with the dominate contribution being uncertainty in injection volume due to syringe graduations.

Improvements were made to lower the uncertainty of future tests. These include using syringes with finer graduations and, when possible, limiting sample transfer by weighing the AB directly into the reaction vessel. The yields of tests conducted with these improved procedures have an uncertainty of $\pm 2.5\%$, with the major contribution coming from uncertainty in graduations on the gas burette.

All five of the acids that were screened facilitate the release of nearly 90% or more of the theoretical hydrogen yield in less than 20 minutes. Over that time period, fumaric, malic, maleic, and tartaric acids all allowed for near theoretical yields of gas release. With the exception of tests using fumaric acid, all reactants and reaction byproducts were fully soluble at the concentrations used and no precipitate was observed. Fumaric acid has poor water solubility compared to the other acids and is not fully soluble even at the highly dilute concentration used for this initial screening. While fumaric acid resulted in favorable hydrogen release and reaction kinetics, this author strongly recommends that it not be considered for system level applications. Fumaric acid's poor solubility would lead to many challenges that can be easily avoided by selecting one of the more water-soluble acids.

Of the screened acids, maleic acid and tartaric acid stand out as promising options for system level tests as they are both diprotic, highly soluble in water, and result in rapid hydrogen release. Maleic acid dissolves at a rate of nearly 0.5 kg/L, while tartaric acid dissolves at a rate of more than 1 kg/L. However, maleic acid has a lower molecular mass (116 g/mol) than tartaric acid (150 g/mol). Both of these acids have potential advantages as some applications could prioritize water solubility while others could be more sensitive to reactant mass. Moving forward, both of these acids were used to promote AB and SBH hydrolysis.

Additional testing was conducted using maleic acid in order to determine the activation energy required for acid-promoted hydrolysis. These tests closely mirrored those used for acid screenings, with the exception of the water bath temperature being held at 5, 25, 35, and 45°C to monitor the influence of temperature on reaction kinetics. Based on the results shown in Figure 3.3 below, the activation energy for maleic acid-promoted hydrolysis of AB was found to be 34 kJ/mol. By way of comparison, Gabl measured the activation energy of AB hydrolysis to be 11.6 kJ/mol in the presence of Amberlyst 15, and 49.3 kJ/mol in the presence of 20 wt.% platinum on carbon [51]. Other authors have reported activation energies ranging from 27.5 kJ/mol to

62 kJ/mol when using various metal catalysts [61,62]. This shows maleic acid is comparable in performance to previously investigated reaction promoters, both metal and acidic.

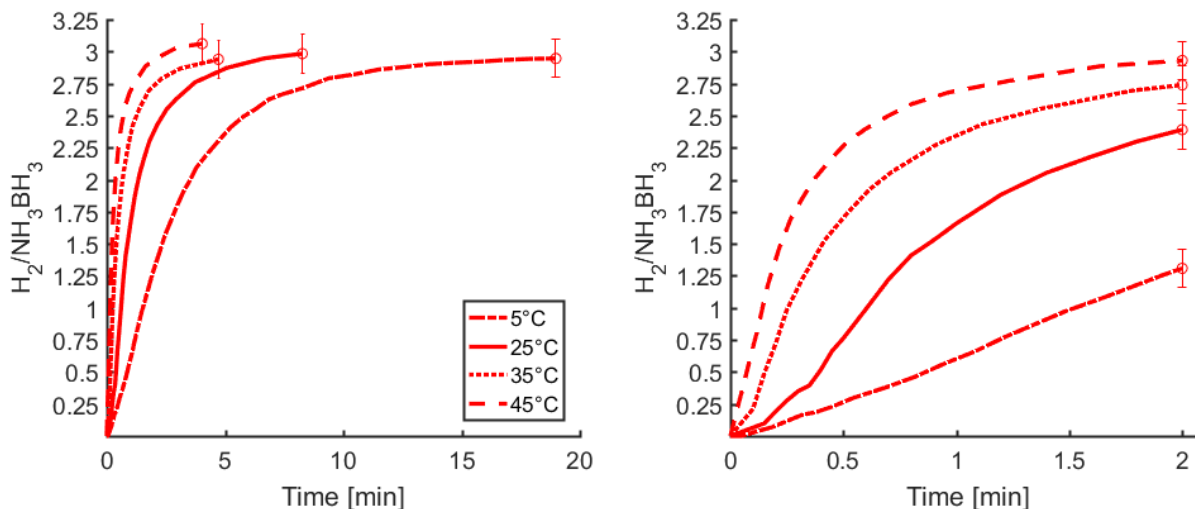


Figure 3.3 Influence of temperature on maleic acid-promoted AB hydrolysis. Shown are the entirety of the hydrolysis reactions (left) and a detailed view of the first two minutes (right).

The tests shown in Figure 3.3 were replicated a minimum of three times to demonstrate repeatability. The overall hydrogen yield remained constant within the bounds of uncertainty between duplicate tests, but the rate of hydrogen release appears to be rather sensitive to the degree of mixing in the reaction vessel. Factors such as the size of the stir bar being used, angular velocity of the stir bar, and even the location of the AB injection within the reaction flask all seemed to alter the initial hydrogen release rate. The sensitivity to mixing is likely related to the high dilution of the solutions being used. In an attempt to normalize mixing from one test to the next, future burette tests were conducted in smaller vials using higher solution concentrations and lower solution volumes. The mixing of future reactions was normalized by using a 0.125 x 0.5 inch PTFE coated stir bar rotating at 500 rpm.

3.1.2 Minimum Water Requirements

When considering a fielded system, the volume of water used for hydrolysis drives the minimum size of the reaction vessel and the overall system mass. Eq. 6 shows that three equivalents of water are required for hydrolysis, with additional water needed to fully dissolve all reactants and byproducts. In order to observe water lean reaction conditions, tests were conducted

by adding water to a dry mixture of four parts AB to three parts tartaric acid (on a molar basis) and monitoring the resulting hydrogen generation. The dry mixture was found to be stable, which allowed for the two to be well mixed prior to initiating the reaction by water addition. Interestingly, when a similar test was conducted by mixing dry oxalic acid with AB, the mixture spontaneously combusted with a green flame and audible “pop”. Schlesinger et al. reported that dry mixtures of SBH and oxalic acid also had a tendency to auto-ignite, while mixtures with other organic acids did not [32].

The hydrogen release when adding any amount of water to the dry mixture was instantaneous and vigorous, with the yield being highly dependent on the amount of water added. When approximately one equivalent of water was added, slightly more than one equivalent of hydrogen was evolved. The hydrogen yield doubled when using three equivalents of water, but only small increases in gas evolution were achieved by using six or ten equivalents. When using less than 6 equivalents of water, it was apparent that only a portion of the dry mixture was being wetted and that the gas generation was isolated to those wetted regions. It wasn't until enough water was added to fully dissolve all reactants (approximately 19 equivalents) that the hydrogen yield started to approach theoretical. This appears to be due to poor water transport and a lack of proper mixing in the slurries of AB and tartaric acid that are created when using less water than is required for full dissolution. For system level tests, enough water should be used to achieve full solubility of all reactants and products. Figure 3.4 shows the results of all water limited hydrolysis tests.

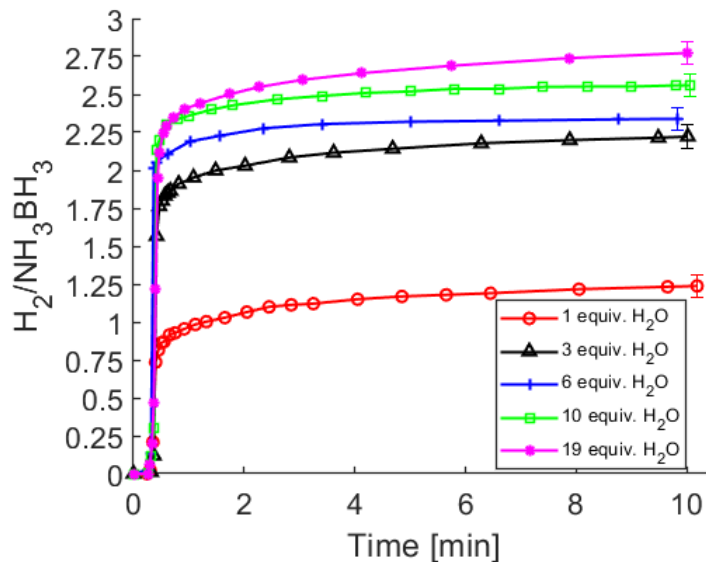


Figure 3.4. Tartaric acid-promoted AB hydrolysis using limited amounts of water.

3.1.3 Influence of Water Purity

It is proposed that the hydrogen generation system being developed will use water that is collected at the point of use as a reactant. Because it cannot be assumed that high purity water will be readily available everywhere the system is used, the hydrogen generation pathway must be indifferent towards water impurities. For this reason, water sources that are likely to be available in potential use environments were qualitatively screened for their potential to facilitate hydrolysis. In addition to various aqueous fluids, several non-aqueous fluids likely to be available at the point of use were screened for their ability to be used for AB hydrolysis. The non-aqueous fluids were primarily limited to alcohols and fluids that could be scavenged from a vehicle. The screening was conducted by first mixing small amounts of AB and tartaric acid together dry and then pipetting a few drops of liquid onto the mixture and monitoring for visible signs of reaction, such as bubbling and/or agitation of the mixture. As was described in Section 3.1.2, mixtures of dry AB and tartaric acid are quite stable, showing no signs of reaction after several minutes of constant mixing. The results of the water source screening are shown in Table 3.1 below.

Table 3.1. Qualitative screening of various water sources for AB hydrolysis.

Fluid	Visible Reaction Observed
10W-40 motor oil	No
Gasoline (up to 10% ethanol)	Yes
JP-8	No
Antifreeze (50/50 dilution)	Yes
Cola soft drink	Yes
Coffee	Yes
Dirty puddle water	Yes
Seawater	Yes
Isopropyl alcohol	No
Lemon juice	Yes
Vinegar	Yes
Ethanol (200 proof)	Yes
Vegetable oil	No
Synthetic urine*	Yes

* Synthetic urine was made in-house as a mixture of 94.8 wt.% water, 2.4 wt.% urea, 2.1 wt.% sodium chloride, 0.5wt.% potassium chloride, and 0.2 wt.% creatine. These same concentrations were used for all subsequent testing with synthetic urine.

The initial screening of alternative fluids indicates that any water-based liquid is capable of inducing gas evolution from an acid and AB mixture. Of the non-aqueous liquids, only ethanol and the gasoline/ethanol mixture resulted in a visible reaction when mixed with the dry powders. Alcoholysis of AB has been previously reported with methanol, and it is likely that in these cases a similar reaction was occurring with ethanol [27]. While various alcohols could be capable of facilitating hydrogen release from AB, moving forward this work will focus solely on water-based fluids.

Further investigation into potential water sources included rate and yield testing using the burette setup shown in Figure 3.1. For these tests, a small vial was loaded with 5 mL of 0.3 M AB solution made with the alternative water source of interest and sealed with a rubber septum. The vial was connected to the gas burette and 0.75 mL of 2 M solution of maleic acid and the water source of interest was injected into the vial to initiate the reaction. The molar ratio of acid to AB was 1:1, while the ratio of water to AB was in excess of 200:1.

As can be seen in Figure 3.5 below, there is virtually no difference in the rate or yield of hydrogen release from AB hydrolysis when using deionized water, seawater, synthetic urine, or puddle water. This indicates that these low-quality water sources are viable options for AB

hydrolysis. Using cola led to an initial rate of hydrogen release that was comparable to those observed when using other fluids, but resulted in only 84% hydrogen release. It is notable that gas evolution occurred as soon as AB and cola were mixed. Some of the evolved hydrogen was lost in the time between mixing the AB and cola and sealing the vial, which would at least partially account for the lower hydrogen yield. Additionally, using cola resulted in a great deal of foaming and left behind a sticky residue in the glassware. While sticky glassware is only a mild nuisance, excessive foaming in a fielded system could potentially lead to clogged orifices or moving parts becoming stuck. For these reasons, cola is not an ideal water source for hydrolysis, although it could likely be used in an emergency situation.

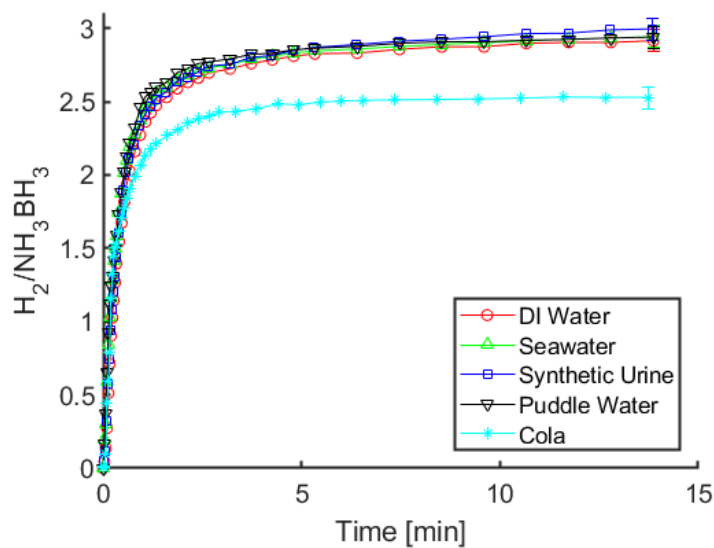


Figure 3.5. Maleic acid-promoted AB hydrolysis using alternative water sources.

3.2 Hydrogen Purity Analysis

As was introduced in Section 2.2.2.2, impurities in a hydrogen supply can permanently damage PEMFCs, even at low concentrations. The contaminant most likely to be released during AB hydrolysis is ammonia, which can account for as much as 25% of the gas stream by volume. For this investigation, several techniques have been employed to analyze hydrogen purity including gas chromatography, Dräger Ammonia Detection Tubes, and Fourier-transform infrared (FTIR) spectrometry.

3.2.1 Preliminary Purity Analysis with Gas Chromatography and Dräger Tubes

Initial product gas analysis was conducted using a Shimadzu GC-2014 gas chromatograph (GC) equipped with two separate flow paths. The first path, consisting of a custom-packed separation column (80/100 mesh, Haysep D, part number 0.50M x 1/8IN x 2.1MM SS) and a two-meter-long column packed with type 5A molecular sieve (part number 220-94714-20), was used to quantify CO levels. The second path was used to detect CO₂ levels and consisted of a two-meter-long custom-packed separation column (80/100 mesh, Haysep D, part number 2.0M x 1/8IN x 2.1MM SS). Both paths terminate with a thermal conductivity detector (TCD), a methanizer (to convert CO and CO₂ into methane for detection by combustion), and a flame ionization detector (FID). All GC hardware was purchased from Shimadzu Scientific. Ultra-high purity argon (99.999% pure) was used as a carrier gas and ultra-high purity hydrogen (99.999% pure) and commercial grade air (< 0.1 ppm hydrocarbon contaminations) were used as combustion gases for the FID. An image of the GC setup is shown below.

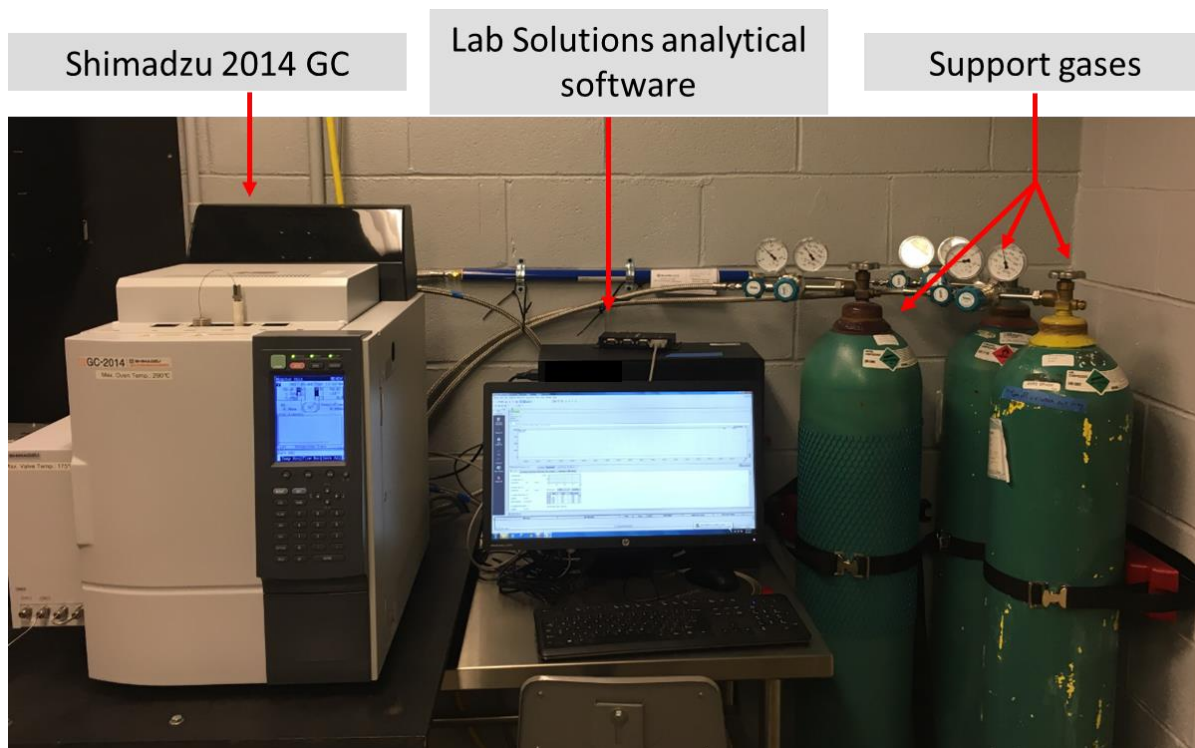


Figure 3.6. Gas chromatography system used for hydrogen purity analysis.

Gas products for GC analysis were generated using a 1:1 molar ratio of AB and either maleic acid or oxalic acid and a large excess of deionized water. 50 mL of acid solution were loaded into the reaction vessel before it was sealed and purged with nitrogen. The reaction vessel was held at 25 or 45°C using a water bath. Hydrogen generation was initiated by injecting 2 mL of AB solution into the vessel through a septum. Following reaction completion, samples were collected from the sample tube shown in Figure 3.1 using a 10 mL gas-tight syringe. The sample was then diluted with ultra-high purity argon to prevent GC-TCD signal saturation and loaded into the GC. Concentrations of CO and CO₂ were measured using the GC-FID, with concentrations never exceeding 1.8 or 2.4 ppm, respectively. These amounts are below the threshold of what would damage a PEMFC [13]. The uncertainty of these measurements is $\pm 5\%$, with the primary drivers of uncertainty being related to sample dilution.

In order to detect ammonia concentrations in the samples, gas analysis tests were repeated with the gas sampling bulb shown in Figure 3.1 being replaced with a Dräger Ammonia Detection Tube. These tubes are packed with a pH indicator that has a colorimetric response when exposed to ammonia. They are also quite sensitive, detecting levels of ammonia as low as 0.25 ppm. The tubes require a full liter of gas sample for quantitative ammonia detection. None of the gas samples tested with Dräger tubes triggered an indication of ammonia at concentrations above the lower detection limit of 0.25 ppm. The results of GC and Dräger tube analysis are summarized in Table 3.2.

Table 3.2. Contaminant concentrations in acid-promoted AB hydrolysis gas products measured by GC and Dräger Ammonia Detection Tubes.

Acid	Temperature (°C)	CO (ppm)	CO ₂ (ppm)	NH ₃ (ppm)
Oxalic Acid	25	< 1.8	2.4	< 0.25
	45	< 1.8	0.8	< 0.25
Maleic Acid	25	< 1.8	2.4	< 0.25
	45	< 1.8	1.2	< 0.25

3.2.2 Purity Analysis with FTIR Spectrometry

While GC-FID and Dräger tubes are both highly sensitive analysis tools, using separate analysis techniques to detect each compound is time consuming and ultimately requires a large

amount of gas sample to monitor a single set of reaction conditions. It would be more cost and time efficient to employ a gas analysis technique which requires less sample and can detect all potential impurities of interest in a single operation. FTIR spectrometry was ideal for this test campaign as it is highly sensitive and can detect a wide range of compounds using far less sample than is required when using Dräger tubes. It is also convenient for this study that the FTIR does not detect hydrogen, meaning only the impurities are observed and the spectrum is not saturated by the hydrogen response.

This investigation used an Agilent Cary 680 FTIR spectrometer and a Pike Technologies heated gas cell with a 10 m path length. The gas cell was heated to 150°C during testing and all samples were analyzed with the gas cell at atmospheric pressure. Quantitative calibration curves, shown in Appendix A, were created for ammonia, CO, and CO₂ using calibration gases purchased from GASCO Affiliates LLC. In order to generate gas samples for FTIR analysis, 0.19 g of AB and 20 mL of deionized water were loaded into a reaction vessel, at which point the entire system (including the FTIR gas cell) was evacuated to 3 psia and refilled to atmospheric pressure with ultra-high purity (99.999 ppm) nitrogen. This process was repeated four times to remove trapped air. With the system purged and evacuated to 3 psia, approximately 3 mL of 2 M aqueous maleic acid solution (enough to provide a 1:1 ratio of acid to AB) was injected into the reaction vessel and the evolved gases were allowed to flow directly into the evacuated FTIR gas cell. Nearly 0.02 moles of hydrogen were generated for each test, with the amount of collected sample being calculated from the ideal gas law using the pressure and temperature of the gas cell before and after gas addition. Following gas evolution, the sample was scanned 100 times and the results averaged in order to improve the signal to noise ratio and provide lower detection limits (LDL) that were low enough to ensure PEMFC compatibility. These tests were repeated by replacing the deionized water in the AB and acid solutions with various water sources. Spectrums for the gas samples collected using deionized water, seawater, synthetic urine, puddle water, and a cola soft drink are shown in Figure 3.7 below.

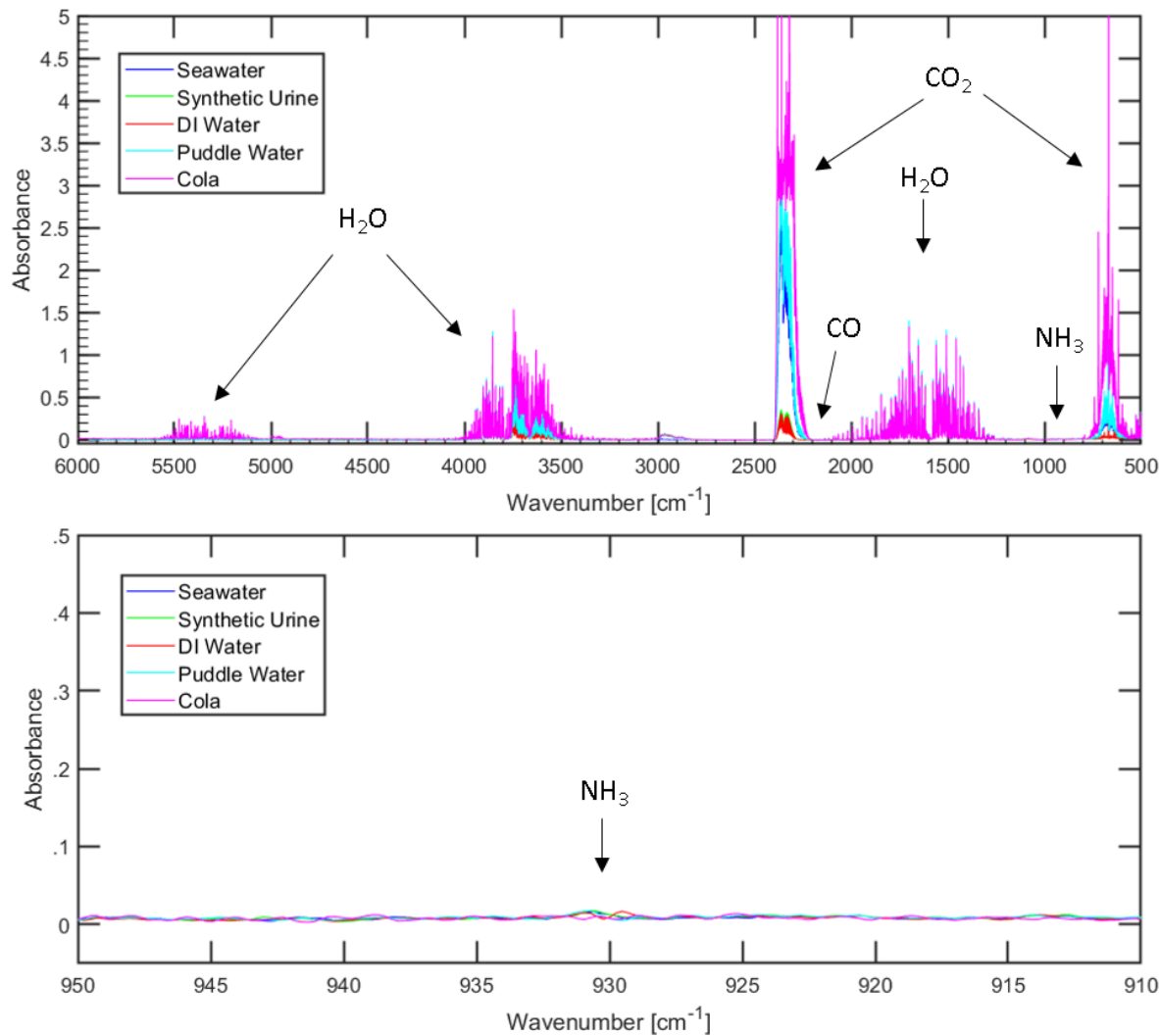


Figure 3.7. FTIR spectra of gases evolved from acid-promoted AB hydrolysis using various water sources. The top figure shows the entire spectra while the bottom figure shows a detailed view of the region where ammonia would be observed.

The spectrums in Figure 3.7 distinctly show the presence of water in all samples, as identified by the peaks in the vicinity of 5400, 4000-3500, and 1300-2000 cm^{-1} . This is not surprising as hydrolysis is exothermic and the formation and entrainment of water vapor is unavoidable. With the exception of the test using cola, the absorbance of water vapor was consistent despite changes to the water source. The water vapor levels were above the maximum concentration that could be calibrated for using available calibration samples, but extrapolation of the calibration curve shows water vapor levels of approximately 950 ppm using most water sources and 1300 ppm using cola.

The source of the water used for testing had a large influence on the amount of CO₂ collected during hydrolysis. Using seawater or puddle water resulted in approximately 1700-2000 ppm and cola resulted in 2500 ppm. In contrast, using deionized water or synthetic urine lead to no more than 360 ppm. The disparity in CO₂ concentrations observed when using different water sources appears to be related to the amount of time that the solutions were exposed to open air prior to use. Water will absorb CO₂ from air until the concentrations of gaseous and aqueous CO₂ reach a temperature, pressure, and pH dependent equilibrium. Aqueous CO₂ will react to form carbonic acid and/or bicarbonate based on the conditions of the system, allowing the solution to absorb additional CO₂ from the air before reaching equilibrium. If the solution is acidified, the equilibriums of aqueous species shift to favor CO₂. Increasing the concentration of aqueous CO₂ will in turn increase the concentration of gaseous CO₂ in the headspace as the system adjusts to maintain equilibrium. Thus, when the solutions used for hydrolysis are acidified a large fraction of the CO₂ that was previously stored as a variety of aqueous species will be converted into gaseous CO₂.

The deionized water and the synthetic urine samples were not exposed to open air for extended periods of time before use, so they likely contained minimal amounts of dissolved CO₂. Seawater and puddle water were both exposed to open air for multiple days prior to being collected, giving them ample time to become saturated with CO₂ and its aqueous products. The observed correlation between increased time of exposure to air and increased CO₂ concentrations in evolved gases implies that CO₂ primarily enters the system dissolved in the water used for hydrolysis. The CO₂ dissolved in the cola is not due to air exposure as it is an intentionally carbonated beverage, but the release of CO₂ from cola can be similarly attributed to the system shifting to maintain chemical equilibrium between gaseous CO₂ and its aqueous species.

The assumption that CO₂ enters the system dissolved in water can also be applied to explain why FTIR analysis detected an order of magnitude more CO₂ than GC-FID when analyzing samples generated using deionized water. For GC testing, 50 mL of acid solution was mixed in an open vessel which was then sealed prior to purging. The reaction was initiated by injecting 2 mL of AB solution into the purged vessel. This configuration allowed for CO₂ to be driven off from the bulk solution prior to sealing the system and without being collected with the product gases. For FTIR testing, the reaction vessel was loaded with 20 mL of AB solution and then sealed and purged before 3 mL of acid was injected into the vessel to initiate the reaction. In this case, any

gaseous CO₂ that was formed when the bulk solution was acidified was collected with the reaction's product gases. Considering system level operation, the FTIR measurements likely represent the worst-case scenario for CO₂ contamination. These conditions could be largely avoided by mixing the acid solution in open air prior to sealing the system. The GC-FID measurements represent the CO₂ concentrations that are more likely to be observed during steady-state operation after CO₂ has been driven off from the bulk solution.

None of the analyzed gas samples contained detectable amounts of either CO or ammonia. The lower detection limits were 19.3 ppm for CO and 7.4 ppm for ammonia. Their absence is especially encouraging as these compounds are the most detrimental to a PEMFC of any impurities likely to be found in hydrogen released from AB hydrolysis. The results of product gas analysis are summarized in Table 3.3.

Table 3.3. Contaminant concentrations in acid-promoted AB hydrolysis gas products measured by FTIR analysis.

Water Source	NH₃ [ppm]	CO [ppm]	CO₂ [ppm]
Deionized Water	< 7.4	< 19.3	291.5
Synthetic Urine	< 7.4	< 19.3	359.1
Puddle Water	< 7.4	< 19.3	2065.8
Seawater	< 7.4	< 19.3	1696.3
Cola	< 7.4	< 19.3	2502.5

3.3 Comparison to Platinum-Based Catalysts

The majority of previous work on AB hydrolysis has employed metal catalysts to promote hydrogen release. In an effort to compare the findings of this investigation to those of previous authors, metal-catalyzed hydrolysis was conducted using 10 wt. % platinum on a carbon support (Pt/C) purchased from Sigma Aldrich (part number 205958). The reaction was conducted using 0.047 grams of AB, a 1.8 wt. % loading of platinum (18 wt. % Pt/C), and approximately 25 mL of deionized water. The test was repeated with the Pt/C being replaced by one molar equivalent of maleic acid in order to allow for direct comparison between organic acid promoters and platinum catalysts, as can be seen in Figure 3.8 below. The burette setup shown in Figure 3.1 was used to measure rate and yield of hydrogen release.

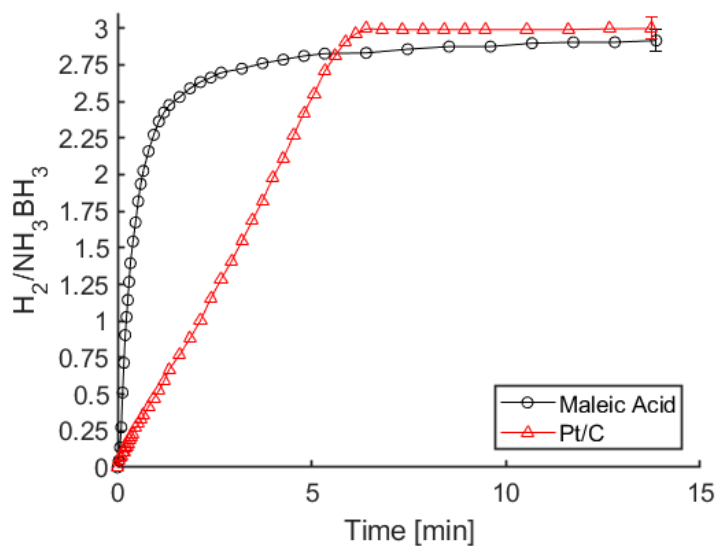


Figure 3.8. Comparison of maleic acid and Pt/C as AB hydrolysis promoters.

The initial hydrogen release rate is far more rapid in the presence of maleic acid than Pt/C, with the acid facilitating 80% completion before the Pt/C facilitates 25% completion. Aside from initial reaction rate, the largest difference between the two tests is the apparent reaction order, with maleic acid promoting first-order behavior and Pt/C promoting zero-order behavior. These observations are consistent with literature reports of acid-promoted and metal-catalyzed AB hydrolysis experiments. Despite the differences in apparent reaction order and initial hydrogen release rates, the two reaction promoters both result in immediate onset of hydrogen release and both achieve greater than 90% reaction completion in less than five minutes.

The FTIR analysis conducted in Section 0 was repeated for gas products generated by hydrolysis in the presence of Pt/C and either deionized water or seawater. Both tests resulted in greater than 1000 ppm of ammonia in the gas products, which is far more than a PEMFC can tolerate and would irreversibly damage the fuel cell after a few minutes [53]. It is interesting to note that these concentrations are lower than those observed in the products of metal catalyzed hydrolysis reported by Gabl, Brockman et al., Liu et al., and Demirci [45,46,51,52]. For a solution with a given temperature and pH, the partial pressure of ammonia in the solution's headspace is proportionate to the concentration of ammonia in the solution. Each of the earlier studies used far less water than what was used during this current work, which is likely why the previous authors detected higher ammonia concentrations in their gas products.

FTIR analysis shows that when using either deionized water or seawater, Pt/C-catalyzed hydrolysis results in the release of far less CO₂ than maleic acid-promoted hydrolysis. This strengthens the argument that CO₂ in the gas stream enters the system as aqueous CO₂ and is off-gassed when the water is acidified. Despite the decrease in CO₂ levels when using Pt/C, the detrimental levels of ammonia in the product gases prohibit the use of Pt/C as a reaction promoter without an additional ammonia trapping scheme. CO was not detected beyond the lower detection limit of 19.3 ppm using any combination of promoter or water source. A comparison of contaminant levels and spectrums from the products of Pt/C-catalyzed and maleic acid-promoted hydrolysis using either seawater or deionized water can be seen in Table 3.4 and Figure 3.9.

Table 3.4. Contaminant concentrations in AB hydrolysis gas products using maleic acid or Pt/C to promote gas release.

Water Source	Promoter	CO [ppm]	CO ₂ [ppm]	NH ₃ [ppm]
Deionized Water	Maleic Acid	< 19.3	291.5	< 7.4
	Pt/C	< 19.3	< 26.2	1102.8
Seawater	Maleic Acid	< 19.3	1696.3	< 7.4
	Pt/C	< 19.3	356.1	1067.6

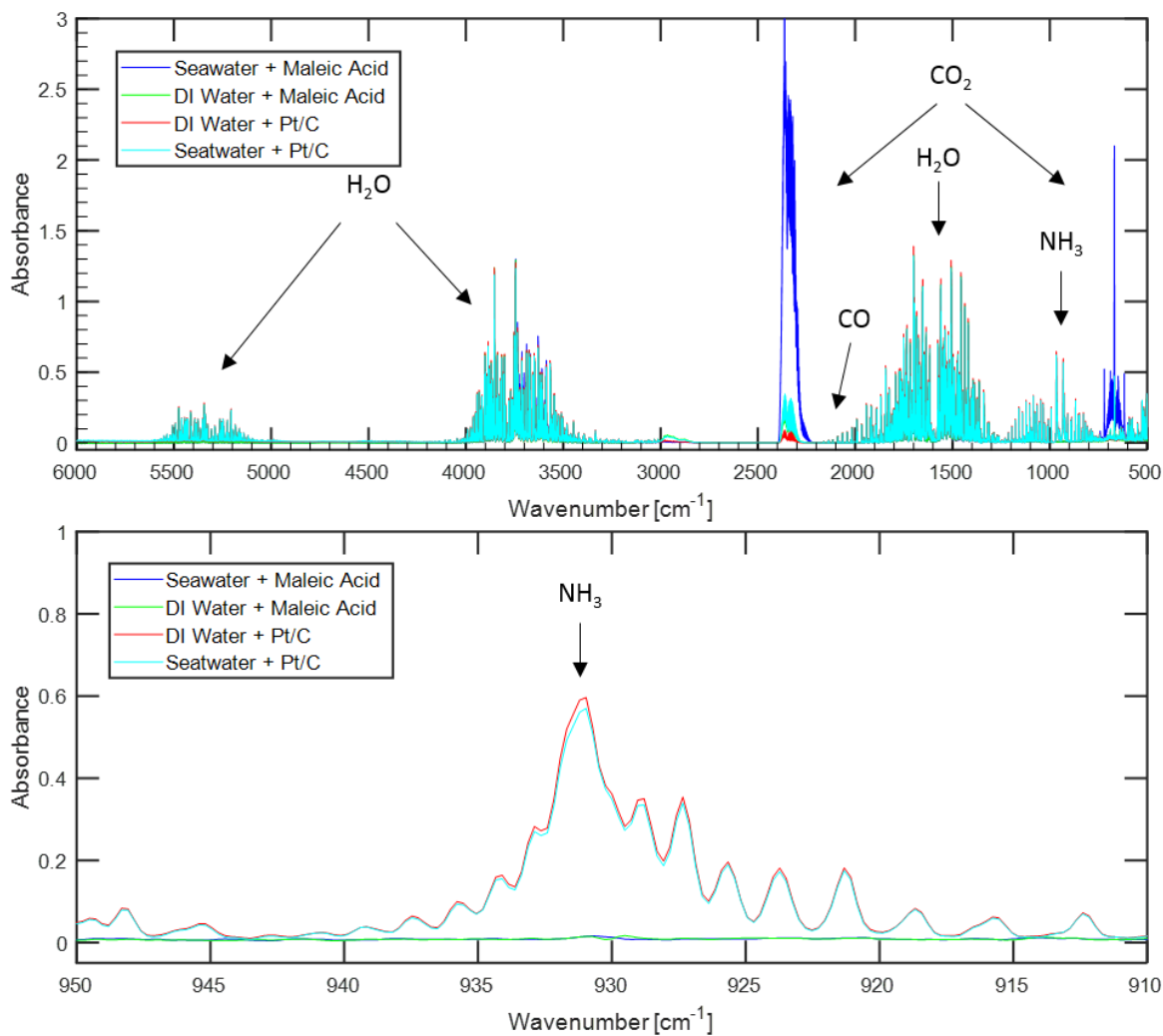


Figure 3.9. Comparison of FTIR spectra of gases evolved from either acid-promoted AB hydrolysis or platinum catalyzed AB hydrolysis. The top figure shows the entire spectrum while the bottom figure shows a detailed view of the region where ammonia is observed.

4. HYDROGEN REACTOR DESIGN

4.1 Envisioned System Use Case

The results discussed in Sections 3.1 and 3.2 demonstrate the potential to generate highly pure hydrogen gas using organic acid-promoted hydrolysis of AB. Based on these results, the next step towards a portable power system that leverages this hydrogen storage and delivery architecture is to design a reactor to house and regulate hydrogen generation. This reactor will eventually be interfaced with a PEMFC for power production. As was discussed in Section 1.1, the system is designed and evaluated based on the envisioned use case of recharging lithium-ion (Li-ion) batteries used by members of the United States military during foot patrols and expeditionary missions.

The BB-2590 is a class of rechargeable Li-ion batteries manufactured in accordance with the Military Performance Specification MIL-PRF-32383/3 [63]. The BB-2590 has been selected as the benchmark battery against which the designed portable power generation system will be compared. This battery was selected based on feedback from current military members who reported it to be widely used for communications, robotics, and more by each branch of the United States military. The BB-2590 weighs 1.4 kg, is 2.4 x 4.4 x 5.0 inches, and has a nominal energy capacity of 225 Wh (810 kJ) [64].

4.2 Initial Design Requirements

With any design project, the first step towards development of a successful product is to clearly define critical design requirements. For this endeavor, these requirements were initially based on a rudimentary understanding of expeditionary warfare. This understanding was informed by a handful of conversations with veterans and active duty military members concerning their experiences with energy storage technologies currently available to soldiers. The following design requirement matrix was created to evaluate reactor designs for their ability to address the challenges associated with expeditionary energy storage and power delivery.

Table 4.1. Initial hydrogen reactor design requirement matrix.

Quantifiable Metrics		Units	Target Value
1	Required electrical input	W	0
2	Hardware mass	g	< 1000
3	Operating pressure	psia	< 30
4	Max hydrogen generation rate	sLpm	> 0.5
5	Time to load reactants	min	< 5
6	Max system temperature rise	°C	40
7	Reactant shelf life	years	> 5
Pass/Fail Metrics			
8	Fuel delivery system capable of starting and stopping	Pass/Fail	Pass
9	Fuel delivery system resilient to changes in fluid properties	Pass/Fail	Pass
10	Housing material compatibility (AB, acid, water, ammonia)	Pass/Fail	Pass
11	Hydrolysis takes place in acidic environment	Pass/Fail	Pass
12	Hardware is robust and easy to use	Pass/Fail	Pass

When considering the design of initial reactor prototypes, it was desired that soldiers could leave the reactor, a fuel cell, and spare reactants unattended in their pack for years at a time. In order to satisfy these conditions, the requirements that were believed to be most pressing were: 1) reactant shelf life, and 2) no dependence on electrical inputs. The second requirement is important as it was believed that this would simplify the system and make it more stable during long term storage. To accommodate these requirements, a system architecture was envisioned in which AB and an organic acid are kept separate and dry until the time of use. Storing both reactants individually and isolating them from moisture protects them from one another and from environmental conditions to provide virtually indefinite shelf life.

4.3 Initial Hydrogen Reactor Prototype – The ABCharger

The initial hydrogen reactor prototype, referred to as the Ammonia Borane Charger or ABCharger for short, is designed to meet the requirements shown in Table 4.1. The ABCharger is a single cylindrical vessel divided into two chambers by a spring-loaded piston head. The bottom chamber houses the AB solution and the top chamber houses the acid solution and hydrolysis reaction. The system is machined out of polycarbonate, a plastic with high machinability, good chemical compatibility, and outstanding impact resistance. Reactants are loaded into the ABCharger by removing the end caps and adding solid acid and AB to the top and bottom

chambers, respectively. Water can be added through ports in the top and bottom end caps and the system shaken to mix the solutions. Alternatively, the solutions can be mixed outside of the chamber and added through the ports. An image of the ABCharger and a CAD cross section are shown below. Detailed machine drawings of the ABCharger are included in Appendix B.

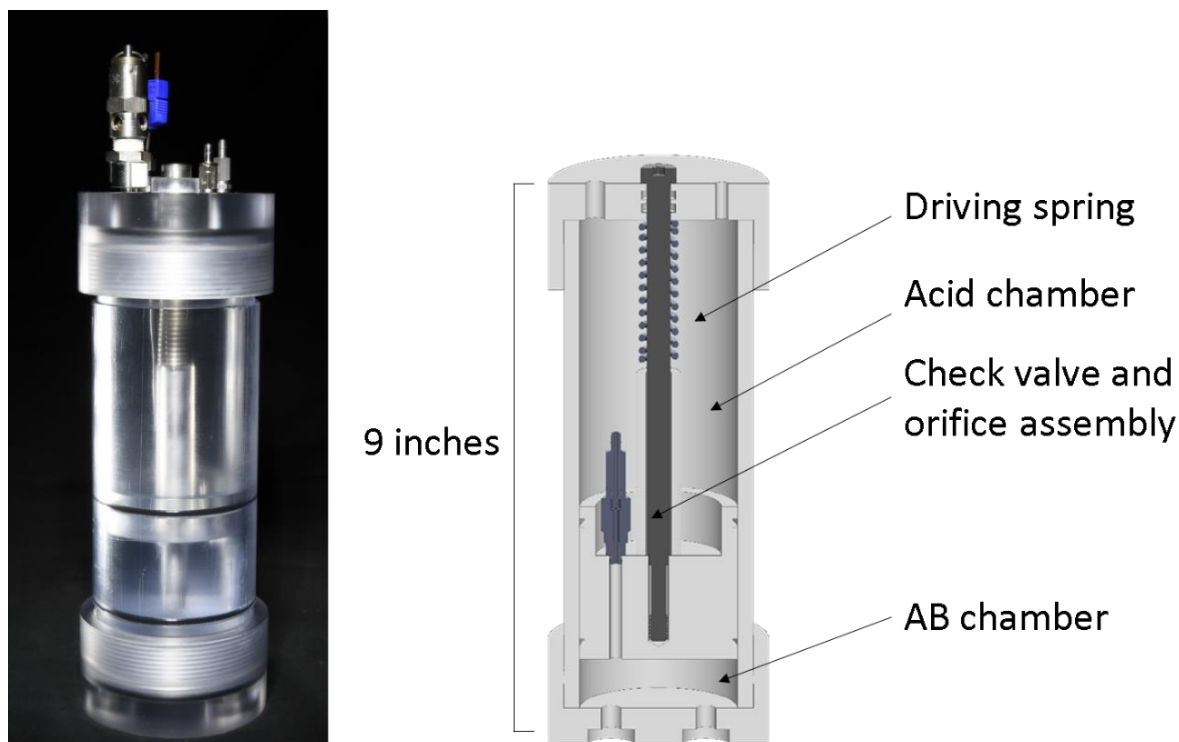


Figure 4.1. Initial hydrogen reactor prototype, the ABCharger. Photo of system on left, CAD cross section on right.

The ABCharger's piston is energized by tightening the center bolt and compressing the spring between the piston head and the top cap. To initiate hydrolysis, the center bolt is loosened to allow the spring to act on the piston and force AB solution through a flow path in the piston head. This flow path terminates in a check valve and an orifice to prevent backflow and regulate the rate of AB addition. The system is designed such that the center bolt maintains thread engagement with the piston head throughout the entirety of operation, which allows for AB addition to be stopped mid-test by tightening the center bolt. To illustrate metered solution mixing, AB transfer was simulated using water that had been dyed red for improved visualization. The results can be seen in Figure 4.2 below.

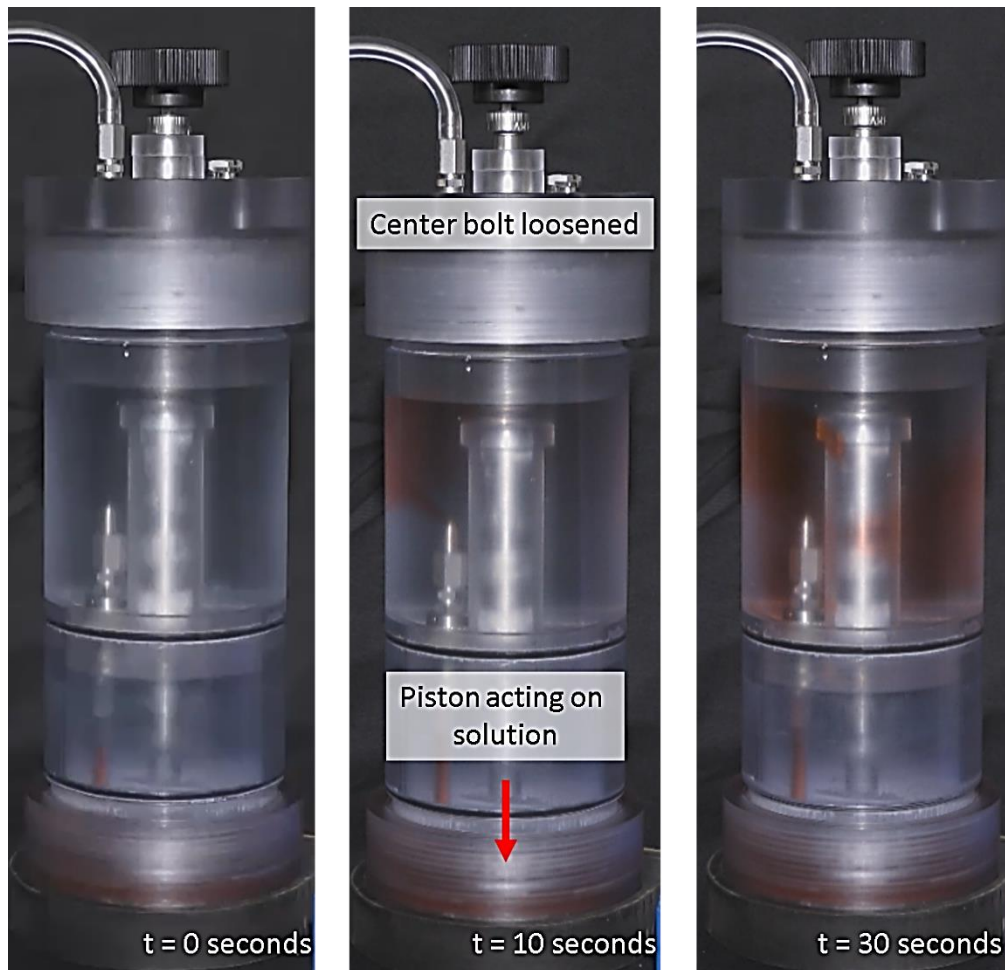


Figure 4.2. Simulated fuel transfer in the ABCharger using water and red dye.

Hydrogen generation in the ABCharger is regulated by controlling the rate at which AB solution is transferred to the reaction chamber. This is achieved using different combinations of springs and orifices to choke the flow of AB solution at the desired flow rate. In order to meet the design requirement of 0.5 sLpm of hydrogen, the ABCharger must transfer nearly 1 mL of saturated AB solution every minute. This translates to a piston head velocity of approximately 0.3 mm/minute. The target flow rate was attained with reasonable repeatability during water calibration using a 0.005 inch orifice. However, the transfer of AB solution proved more difficult to regulate. Fine particulate in the AB solution had a tendency to clog the orifice and residue from the solutions would interfere with lubrication on the piston's O-rings. Replacing the 0.005 inch orifice used for water calibration with a 0.02 inch orifice allowed for consistent AB solution transfer, but at a flow rate much higher than the target of 1 mL/min.

The next three chapters of this dissertation include several tests conducted in the ABCharger and its subsequent design iterations. In order to present and compare these tests in an efficient and clear manner, they are referred to by the hydrogen source they used and the order in which they are reported. For example, the first test used AB and is referred to as Test AB-1. Similarly, the eighth test used SBH and is referred to as Test SBH-8. The test number is only incremented for tests that are discussed in detail and not for repeats of a set of conditions that are not reported or are only briefly mentioned.

The ABCharger was used to generate hydrogen and fuel a PEMFC at the Protonex testing facility in Southborough, Massachusetts. Protonex (recently purchased by Ballard power Systems) is an industry leader in PEMFC design and testing. The custom air-breathing PEMFC used for these tests was a 12 cell stack with 9.5 cm² of active area and was capable of producing up to 35 W of power. An electronic load was used to simulate a constant current demand, with tests being conducted at set points of 2 A and 4 A. Air was provided to the fuel cell at rates of 1.3 and 2.6 sLpm for the 2 A and 4 A tests, respectively. The charger was loaded with tartaric acid and AB at ratios between 0.6:1 and 0.75:1. An orifice with a diameter of 0.02 inches was placed between the two chambers to meter the AB solution flow rate. Under these conditions, the ABCharger fueled a PEMFC producing as much as 34.9 W of power and met various load demands during tests ranging between 5-20 minutes. An image of the Protonex testing setup is included below.

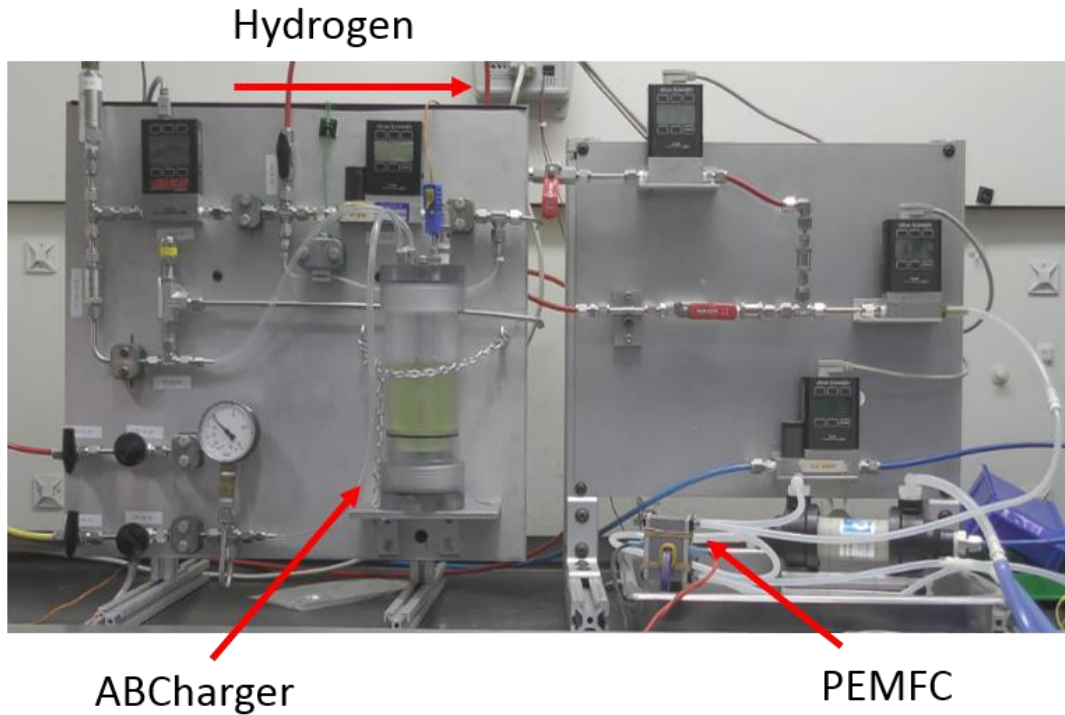


Figure 4.3. Fuel cell test stand at the Protonex facility. Note: green dye added to AB solution to visualize flow.

The orifice in the ABCharger piston head was oversized to mitigate the clogging issues described previously, which meant the rate of AB flow was not tailored to match the fuel cell's hydrogen consumption rate. As can be seen in Figure 4.4 below, the chamber pressure spiked immediately following initiation of Test AB-1 and then slowly decayed as hydrogen was consumed. This appears to indicate that a majority of the AB solution was injected rapidly at the onset of the test, almost as if in a singular injection event. There was also a small pressure increase after 240 seconds when test operators pressed on the center bolt to check if it was fully depressed, causing the remaining AB solution to be transferred. The pressure spike at the beginning of the test violated the third design requirement in Table 4.1 which requires the system to never exceed 30 psia of hydrogen pressure.

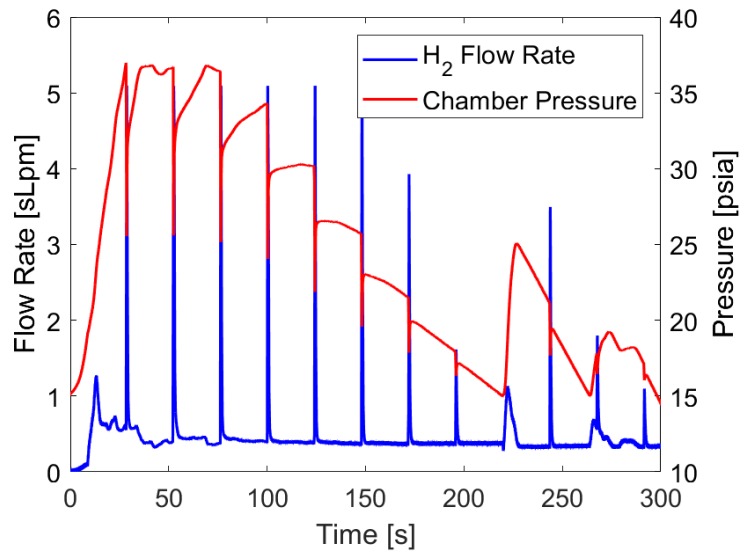


Figure 4.4. Hydrogen flow rate and pressure during Test AB-1. Testing conducted at the Protonex facility in Southborough, Massachusetts

The PEMFC output shown in Figure 4.5 below depicts relatively steady power generation. The stack initially produced 34.9 W before slowly decaying to 33.8 W by the end of the test. The power decay seen in Figure 4.4 closely mirrors the decline in hydrogen pressure supplied to the stack as seen in Figure 4.5, including the slight increase seen in both at 240 seconds. The Protonex test engineers believed the power decay was solely due to the decreasing hydrogen supply pressure. Similar results were observed in the other four tests conducted at the Protonex testing facility.

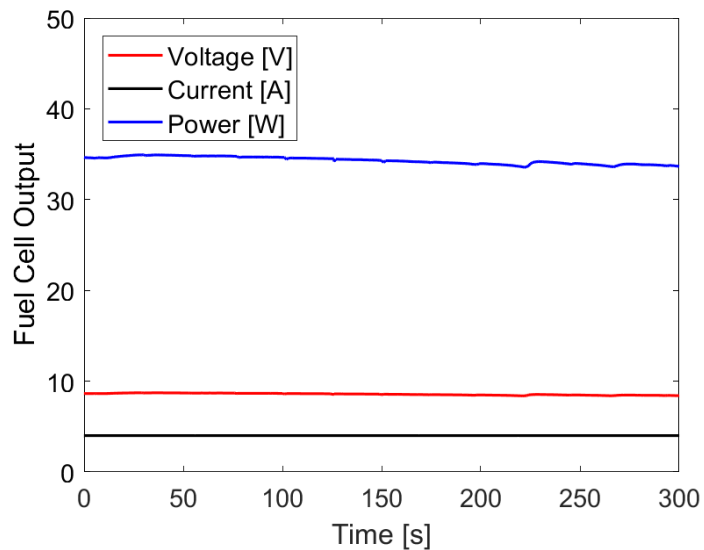


Figure 4.5. PEMFC output during Test AB-1. Testing conducted at the Protonex facility.

Testing the ABCharger with the Protonex fuel cell stack identified the need for increased control over the rate of hydrogen evolution. It was observed that perhaps the biggest shortcoming of the ABCharger design is the use of a spring and orifice to provide a constant flow rate of AB solution. It was originally envisioned that if the spring and orifice were properly selected to match the stack's presumably constant hydrogen consumption rate, then the entire system would operate at a steady state pressure for long test durations. However, it became apparent during testing that the rate at which the PEMFC consumes hydrogen is highly dependent on test conditions such as load demand, stack temperature, and hydrogen and air humidification. Even if the spring driven AB delivery mechanism is improved to where it is impervious to particulate in the solution, it would still be incapable of adjusting hydrogen generation rate during operation to match fuel cell demand. For this reason, the system design was revisited to implement a control loop that modulates hydrogen generation based on instantaneous consumption. Such control will allow for prolonged test durations with relatively steady chamber pressures. The new design also built on the lessons learned concerning orifice clogging and lubrication challenges in order to improve the user interface and increase resiliency towards non-ideal conditions.

4.4 Updated Design Requirements

While initial ABCharger design, fabrication, and testing was taking place, a great deal of effort was put into better understanding the relationship between energy storage and expeditionary warfare. The motivation for this endeavor was to validate and/or update the design requirements listed in Table 4.1. This process was guided by a series of design methodologies developed for startup companies who need to innovate rapidly, operate with limited funding, and bring products to market as quickly as possible. Adaptations of this methodology have been called Lean Launchpad, User-Oriented Design, and Hacking for Defense. Regardless of the name or specific industry focus, each of these approaches are similar in that their core belief is end users should be involved with every step of the design process. The champions of these methodologies believe that truly innovative products are created when the designer has an intimate understanding of the problem at hand. They would argue that only then can one identify and address the primary cause of the customer's problem, rather than simply trying to alleviate the pain that it causes.

User-oriented design was implemented for this effort because of the relative disconnect between academic research and military operations. The challenges faced by today's expeditionary warfighters cannot be identified by a typical academic literature review, but must instead be uncovered through "customer discovery". This process took place in the form of interviews with individuals who are intimately aware of how energy storage impacts the efforts of the United States Military. Over 50 interviews were conducted with veterans and active duty military members representing the Army, Navy, Marines, and Air Force as well as representatives from various special operations forces such as Marine Reconnaissance Forces, Navy SEALs, and Army Rangers. Interviewees also included DoD program managers, scientists from national laboratories, and defense contractors with experience in design, testing, and certification of energy storage systems.

The results of this customer discovery process led to a refinement of several user requirements. Most notable was the requirement that the system not rely on electrical inputs for operation. While a completely mechanical system has its advantages, repeatability and reliability were consistently confirmed to be by far the most important considerations for military use. If electrical input could improve those factors, it would be welcomed as a favorable trade off. Similarly, the original requirement that the system have a virtually indefinite shelf life such that it could sit forgotten in a pack for several years before use was found not to be as important to

potential users as was previously imagined. Discussions with veterans and active duty military members revealed that their packs are meticulously prepared before each mission and that every item placed in their pack is routinely confirmed to be in operational condition. While logistical considerations benefit from reactants that can be stored for several years, potential users had no concerns over the lifetime of a small battery used only during start up transients before the fuel cell reaches nominal operating conditions. These updated requirements allow for more sophisticated AB solution delivery methods which provide far better control over hydrogen generation rates. An updated design requirement matrix that considers the findings from customer discovery is included below.

Table 4.2. Updated hydrogen reactor design requirement matrix.

Quantifiable Metrics		Units	Target Value
1	Average continuous electrical input	W	< 2
2	Startup transient electrical input	W	< 5
3	Hardware mass	g	< 1000
4	Operating pressure	psia	< 30
5	Max hydrogen generation rate	sLpm	> 0.5
6	Time to load reactants	min	< 5
7	Max system temperature rise	°C	40
8	Reactant shelf life	years	> 1
Pass/Fail Metrics			
9	Fuel delivery system capable of starting and stopping	Pass/Fail	Pass
10	Fuel delivery system resilient to fluid properties	Pass/Fail	Pass
11	Fuel delivery system resilient to particulates	Pass/Fail	Pass
12	Housing material compatibility (AB, acid, water, ammonia)	Pass/Fail	Pass
13	Hydrolysis takes place in acidic environment	Pass/Fail	Pass
14	Hardware is robust and easy to use	Pass/Fail	Pass

4.5 Second System Prototype – The ABCharger 2.0

A second hydrogen reactor prototype, referred to as the ABCharger 2.0, was designed to build on the lessons learned from testing the initial ABCharger and meet the updated requirements listed in Table 4.2. A significant deviation from the original design is the use of two separate vessels for storing AB and acid solutions. The AB solution is stored in a thin walled vessel that is open to air such that it cannot be pressurized. The reaction chamber is a sealed vessel designed to withstand internal pressures of 35 psia or higher. Initially, the original ABCharger prototype served to store the acid solution and house hydrolysis reactions before a more compact and lightweight vessel could be designed and fabricated.

The most notable deviation from the original design is that in this new configuration AB solution is transferred into the reaction chamber using a peristaltic pump. The pump was purchased from The Williamson Manufacturing Company (part number 100-035-006-008/2). The system is designed with an intentionally oversized pump to allow for intermittent operation. The ABCharger 2.0 can accommodate a wide range of hydrogen consumption rates by varying the frequency and duration of pumping cycles. A 9 V battery is used to power the pump during shorter tests, while tests longer than three hours use a benchtop power supply. However, in a fielded system, the use of external power sources could be limited to the startup transient. Once the system reaches nominal operational conditions power output from the fuel cell could be used to drive the pump and transfer AB solution as needed.

The peristaltic pump is controlled based on the pressure inside the reactor. A control mechanism was used to provide power to the pump and transfer AB solution whenever the hydrogen pressure in the reactor dropped below a set point, typically 22-24 psia. Initial tests used a LabVIEW program to monitor a pressure transducer on the hydrogen supply line and power the pump accordingly. For later tests, a normally closed low pressure switch replaced the LabVIEW program to allow for passive system control. The pressure switch operates in a similar way as the digital controller, completing the circuit between the pump and the power supply whenever the pressure in the vessel drops below a set point. Either control mechanism allows for a pressure-informed delivery system that generates hydrogen based on instantaneous consumption and accommodates a wide range of hydrogen generation rates. This architecture is self-limiting and prevents the buildup of large amounts of hydrogen.

A hydrogen generation test stand was built to facilitate and standardize system testing. This simple and easily adaptable test stand allows for measurement of temperature (Omega T-type thermocouple, $\pm 2^\circ\text{C}$ accuracy), pressure (Unik 5000 pressure transducer, 0-50 psia range, $\pm 0.2\%$ full scale accuracy), and hydrogen flow rate (Alicat M-Series mass flow meter, accurate to ± 0.01 sLpm $\pm 0.8\%$ of reading). The stand is equipped with a digital flow controller (Alicat MC Series flow controller) which is used to simulate a fuel cell's hydrogen consumption for initial tests. The test stand is connected to an ultra-high purity hydrogen bottle (99.999% pure), and to the facility bulk nitrogen supply to allow for purging the system prior to hydrogen generation. A relief valve between the flow controller and the reaction vessel is set to 40 psia to protect against unexpected over pressurization. A plumbing and instrumentation diagram (P&ID) of the system in its nominal configuration used for the initial testing campaign is shown in Figure 4.6, and an image of the ABCharger 2.0 (using the original ABCharger for a reaction vessel) on the hydrogen generation test stand is shown in Figure 4.7.

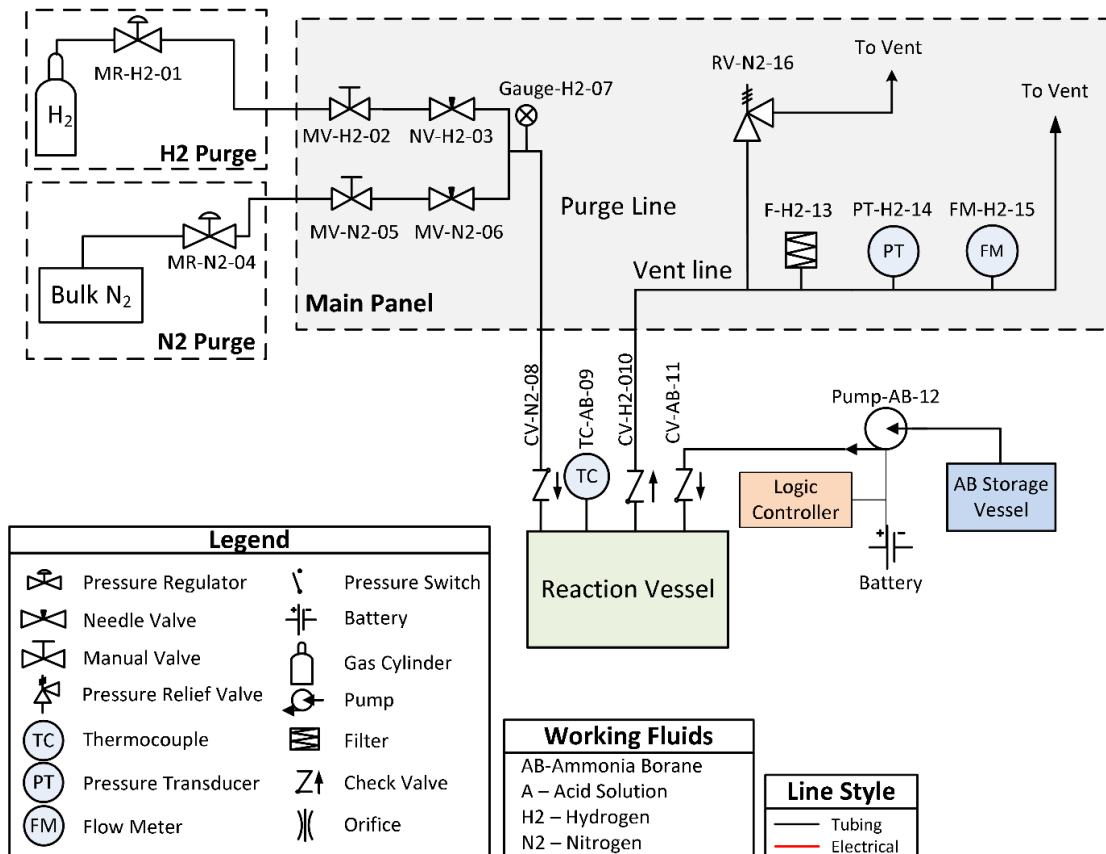


Figure 4.6. P&ID of the ABCharger 2.0 on the hydrogen generation test stand.

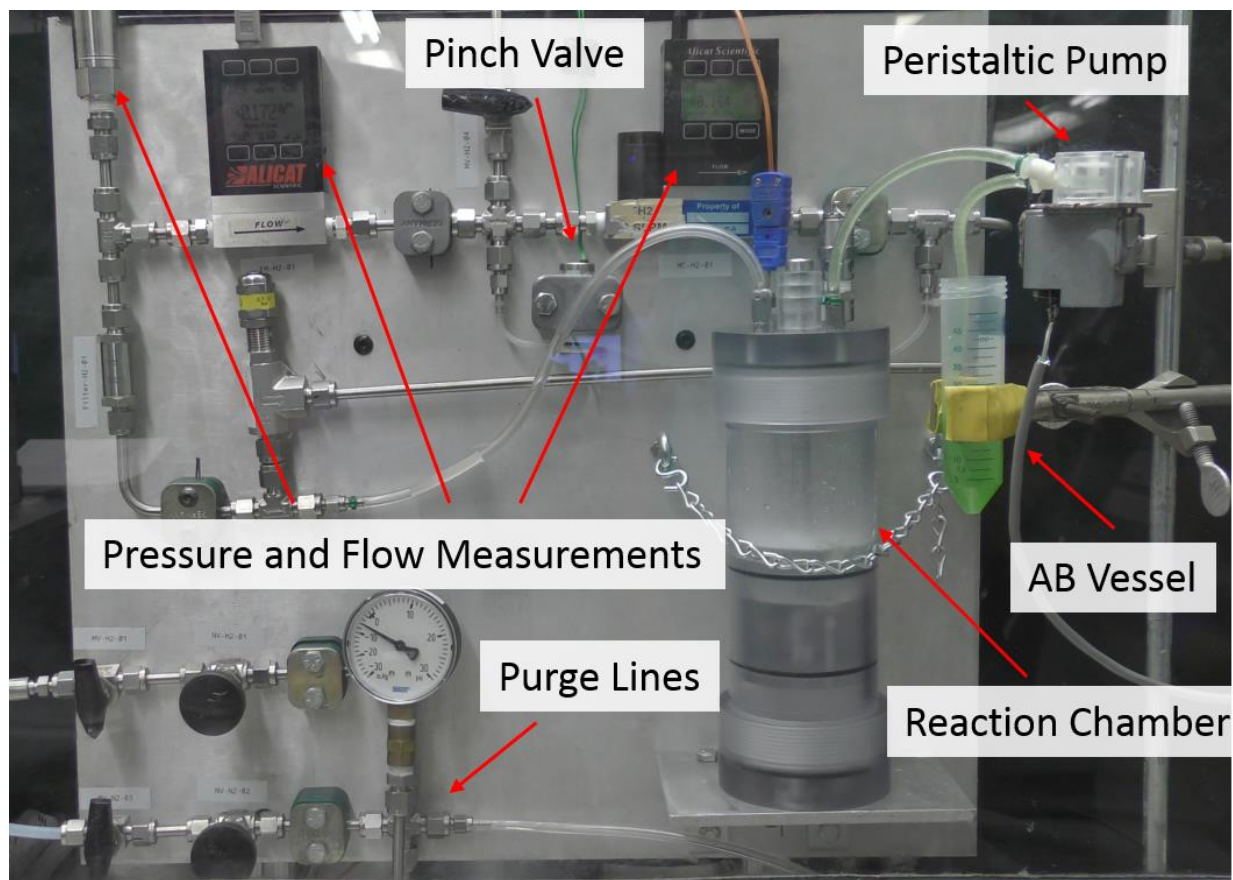


Figure 4.7. ABCharger 2.0 on the hydrogen generation test stand. Green dye was added to the AB solution to improve flow visualization.

The test stand shown above was used extensively to test hydrogen reactor prototypes and was later modified to accommodate subsystem integration. The general procedures for using the test stand are as follows:

1. Load acid solution into the reactor and AB solution into an open vessel
2. Connect reactor to purge gasses and vent line
3. Connect peristaltic pump inlet to AB solution vessel using flex tubing
4. Connect peristaltic pump outlet to reactor using flex tubing
5. Purge system with nitrogen
6. Purge system with hydrogen
7. Connect 9 V battery to peristaltic pump to initiate hydrogen generation
8. Use load controller to modify hydrogen demand as appropriate

Using the procedures listed above and the stand as shown in Figure 4.7, several tests were conducted to demonstrate the system's ability to provide various hydrogen flow rates for extended periods. The first demonstration, Test AB-2, was prepared using 2.5 g of AB (synthesized in-house) in 12 mL of deionized water and 5.6 g of maleic acid in 60 mL of deionized water. The molar ratio of acid to AB was 0.6:1. The LabVIEW program controlling the peristaltic pump was set to maintain a chamber pressure of 22 psia, and the flow controller was set to a flow rate of 0.16 sLpm. The results of this test can be seen in Figure 4.8.

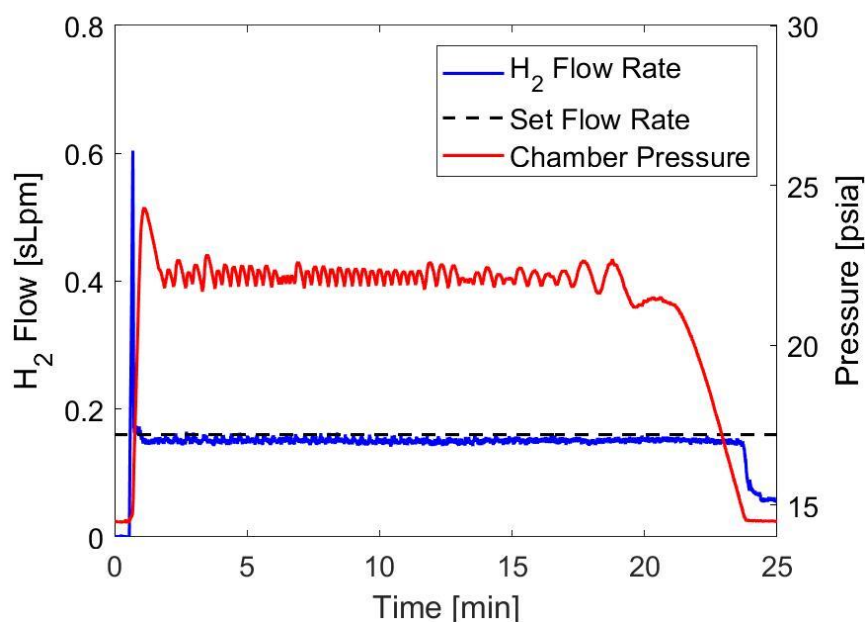


Figure 4.8. Hydrogen flow rate and pressure during Test AB-2.

The target flow rate for Test AB-2 was provided for just shy of 25 minutes, with the pressure holding within ± 2 psi of the 22 psia set point for the first 20 minutes. Given the theoretical hydrogen release from 2.5 g of AB and the target flow rate of 0.16 sLpm, this test could have operated for a maximum of 34 minutes. Once a large fraction of the acid had been consumed by the hydrolysis reaction, the reaction kinetics began to slow. This caused the pump to operate for longer intervals to recover hydrogen pressure, leading to the larger pressure oscillations observed starting after 17 minutes. Eventually, the kinetics were too slow to keep up with hydrogen demand and the chamber pressure could no longer be maintained. After delivering 0.16 sLpm of hydrogen for ~23 minutes, the system continued to operate at a lower flow rate with the yield

reaching nearly 80% of theoretical after 30 minutes. This test was repeated several times with the hydrogen flow rate and chamber pressure demonstrating good repeatability. Despite attaining only 80% yields, the results of these tests are a large improvement over the previous ABCharger configuration. The 0.6:1 ratio of maleic acid to AB was used because, despite the low overall yield, it provides the highest ratio of delivered hydrogen to reactant mass of any acid and AB combination that was considered. However, for future tests a 1:1 ratio of maleic acid was used as to not waste AB during laboratory tests.

An updated reaction vessel design was implemented prior to additional testing. This design uses an acrylic vessel rather than polycarbonate like the original ABCharger because of the wider range of stock acrylic tube dimensions available from commercial vendors. Making the vessel walls from stock tube is economical and the cost savings allowed for the vessel to be made in three sizes to accommodate longer tests and larger volumes of solution. The end caps were machined from acrylic rod and adhered to the vessel walls using a methylene chloride-based solvent. It should be noted that polycarbonate has far better impact resistance than acrylic and is recommended for field prototypes. However, the cost of fabricating acrylic vessels was favorable for laboratory testing where impact resistance is not an issue. The dimensions of the various reaction vessels are shown in Table 4.3.

Table 4.3. Dimensions of acrylic reaction vessels.

	Small Vessel	Medium Vessel	Large Vessel
Outer Diameter [inches]	2.5	2.5	3.5
Wall Thickness [inches]	0.125	0.125	0.125
Internal Height [inches]	4	9	9.5
Internal Volume [inches ³]	15.9	35.7	78.8
Internal Volume [mL]	260	590	1290

The updated vessel design is sealed using a PTFE plug. The plug was produced by modifying a bushing purchased from Chemglass Life Sciences (part number CG-363-05). Four ports were added to the bushing, but it was otherwise used as received. The ports were used to connect the vessel to purge gases, a hydrogen vent line, the AB solution supply, and for inserting a thermocouple into the reactor. The same PTFE plug was reused for each of the three vessels. Machine drawings for the smallest acrylic vessel and the PTFE plug are shown in Appendix C. Drawings are not included for the larger reactors as the only dimensions that changed are the outer

diameter and height of the vessel as shown in Table 4.3. An image of the smallest reaction vessel is shown in Figure 4.9 below.

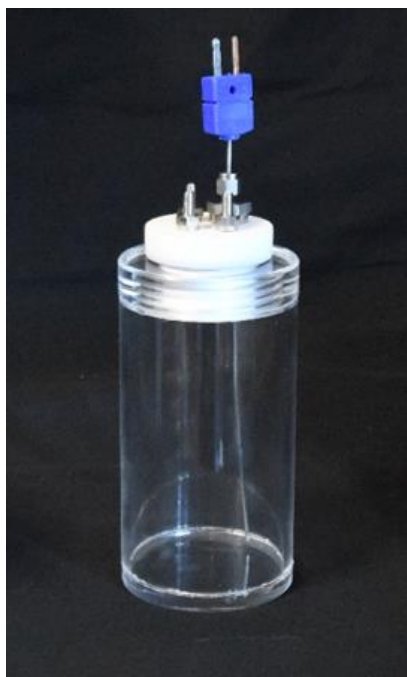


Figure 4.9. ABCharger 2.0 acrylic vessel.

5. ELECTRICAL HARDWARE INTEGRATION

5.1 Horizon H-30 PEMFC

The fuel cell testing conducted at the Protonex facility and reported in Section 4.3 suggested that the proposed hydrogen generation system is compatible with PEMFCs and justified the development of fuel cell testing capabilities at Purdue's Zucrow Laboratories. The fuel cell used for this investigation, is a Horizon H-30 Fuel Cell Stack purchased from Horizon Fuel Cell Technologies. This unit is an air-breathing, self-humidified PEMFC stack rated for a nominal power output of 30 W. The H-30 operates in a deadheaded configuration.

Water management for the H-30 includes a periodic purge event in which the electronic valve that deadheads the system is cycled open and closed every 10 seconds to allow internal hydrogen pressure to remove product water that is built up inside the stack. The unit is self-humidified and keeps its membranes moist by generating water vapor inside the stack using a short circuit event every 10 seconds (out of phase with the purge event). This is a common humidification technique that has been described in detail elsewhere [65]. Both water management events are regulated by a control unit provided by the fuel cell manufacturer.

Because of the periodic purge and short circuit events, the electrical output of the fuel cell is briefly interrupted every five seconds. In order to smooth these interruptions and provide a more consistent power output, a 2 F, 16 V capacitor can be placed in parallel between the fuel cell and the load with a diode preventing back flow from the capacitor to the fuel cell as shown in Figure 5.1. The capacitor and diode are useful when powering a system that can be negatively impacted (i.e. shut off or sustain permanent damage) during brief power outages. For example, this simple circuit is typically required for powering consumer electronics. However, for safety and simplicity, the capacitor and diode were not used for tests where the fuel cell was powering a load that was resilient towards power interruptions. Unless otherwise noted, fuel cell testing for this dissertation did not include the capacitor and diode circuit.

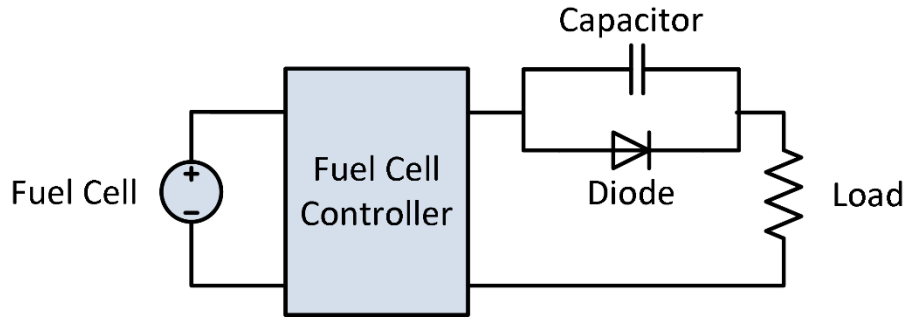


Figure 5.1. Electrical circuit used for testing the portable power generation system.

The water management events described above influence the system's hydrogen flow rate and internal pressure. When the purge valve is opened, a rush of hydrogen escapes the vessel and causes a dip in hydrogen pressure. Likewise, the fuel cell consumes more hydrogen during the short circuit event than it does at steady state. The frequency of these events makes it difficult to visualize flow rate and pressure trends for tests that last longer than several minutes. Figure 5.2 below shows chamber pressure and hydrogen flow rate when using hydrolysis to fuel the H-30 PEMFC (the details of this test will be discussed later). The image on the left shows a zoomed view of the humidification events and the image on the right demonstrates the difficulties of analyzing trends over long periods using the raw data. To allow for trend visualization, all pressure and flow rate data reported for tests using the H-30 stack will be smoothed over 30 second intervals.

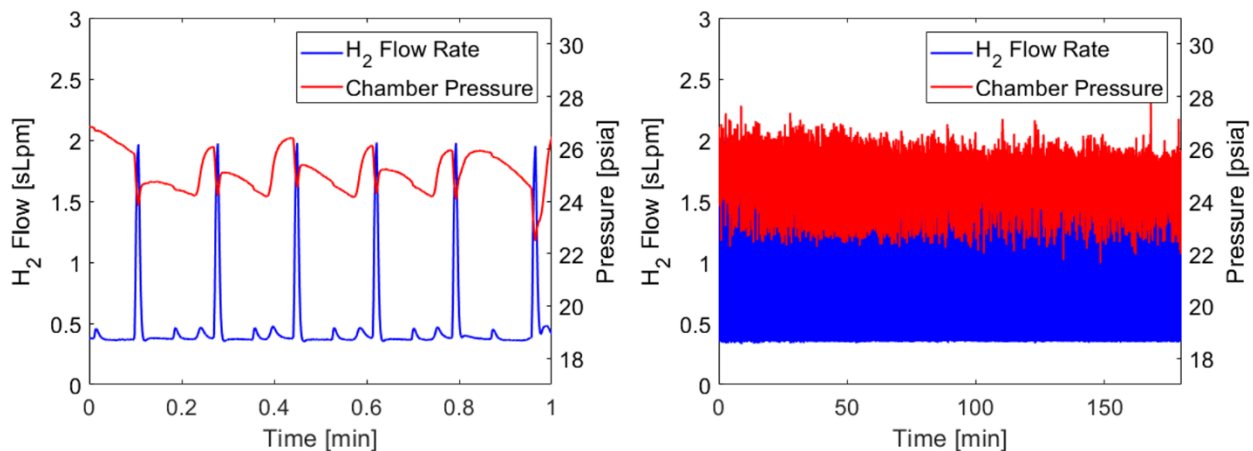


Figure 5.2. Example of how Horizon's fuel cell water management techniques influence chamber pressure and hydrogen flow rate.

5.2 Squad Power Manager

Recharging a battery using the Horizon H-30 PEMFC requires that its electrical output be conditioned to match the charging profile of that specific battery. This can be done using a smart battery charger like the Squad Power Manager (SPM), which is already in use by the U.S. military. The SPM was designed by Protonex and is currently sold by Galvion [66]. It accepts a wide range of AC and DC electrical power sources and outputs DC power to match the charge profile for an assortment of consumer electronics and batteries. Of particular interest to this study, the SPM is capable of conditioning the Horizon H-30 PEMFC power output and using it to safely recharge BB-2590 batteries.

Procurement of a SPM can take several months and cost in excess of \$5,000. In order to ensure compatibility prior to purchase, a SPM was loaned from Ballard Power Systems. The unit was used to conduct a partial recharge of a BB-2590 battery using the ABCharger and Horizon H-30 PEMFC. Integration of the subassemblies was assisted by Dr. James Sisco, Principle Engineer at Ballard Power Systems (formerly Protonex).

Test AB-3 was the first attempt at integrating all of the subassemblies required for the envisioned field-ready system. The objective of the test was to demonstrate a partial recharge of a BB-2590 battery using AB hydrolysis, the Horizon H-30 PEMFC, and the SPM. Hydrolysis was conducted in the second generation ABCharger vessel using 4 g of AB (synthesized in-house) and 15 g of maleic acid (1:1 molar ratio) and approximately 150 mL of deionized water split between the two solutions. The hydrogen generation test stand shown in Figure 4.6 was used to monitor hydrogen feed pressure and flow rate, with three modifications being made to the stand. First, rather than flowing hydrogen through the flow controller and exhausting to vent, the flow was instead directed to the deadheaded H-30 PEMFC. Second, the logic controller was replaced with a low pressure switch installed on a branch in the line between the reaction vessel and the fuel cell. And finally, a 0.01 inch orifice was placed downstream of the purge valve to conserve hydrogen during purging. Testing procedures followed those outlined in Section 4.5. The only modification to the testing procedures was to allow the fuel cell to operate on facility hydrogen for several minutes following the hydrogen purge but prior to initializing hydrolysis to allow the stack to warm up and reach steady state operating conditions. Tests were initiated by connecting a 9 V battery to the peristaltic pump and isolating the stand from the facility hydrogen supply. A schematic of the test setup is shown in Figure 5.3 below.

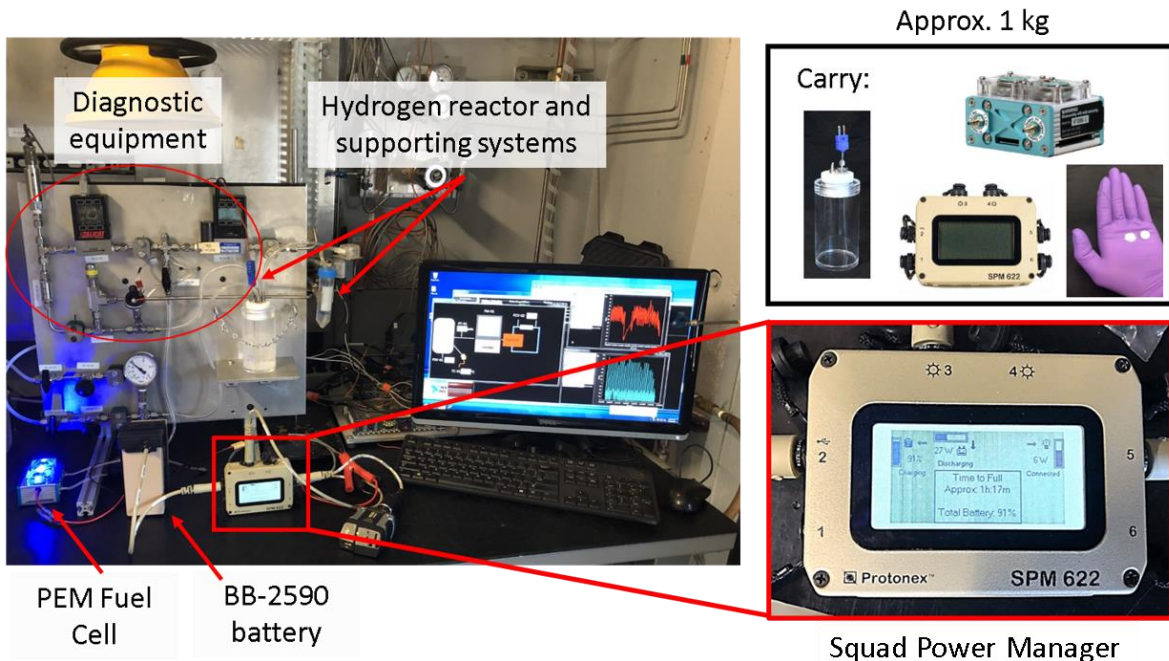


Figure 5.3. System used for preliminary BB-2590 battery recharge.

Evolved hydrogen was fed to the H-30 PEMFC with the power output from the stack being conditioned by the SPM and used to charge a BB-2590 battery. The test lasted just over 15 minutes and resulted in a 3% increase in BB-2590 charge level, corresponding to an average power output of 25-30 W. This test was repeated with the deionized water being replaced by puddle water collected from the Zucrow Laboratories parking lot and similar results were observed. The hydrogen pressure and flow rate for the puddle water test are shown in Figure 5.4. As was mentioned above, the data in Figure 5.4 has been smoothed over 30 second intervals to allow for trend visualization without flow spikes and pressure dips from water management events. Hydrogen pressure was consistent throughout the test, with the smoothed pressure holding within ± 1 psi of the 20 psia set point after the initial startup transient.

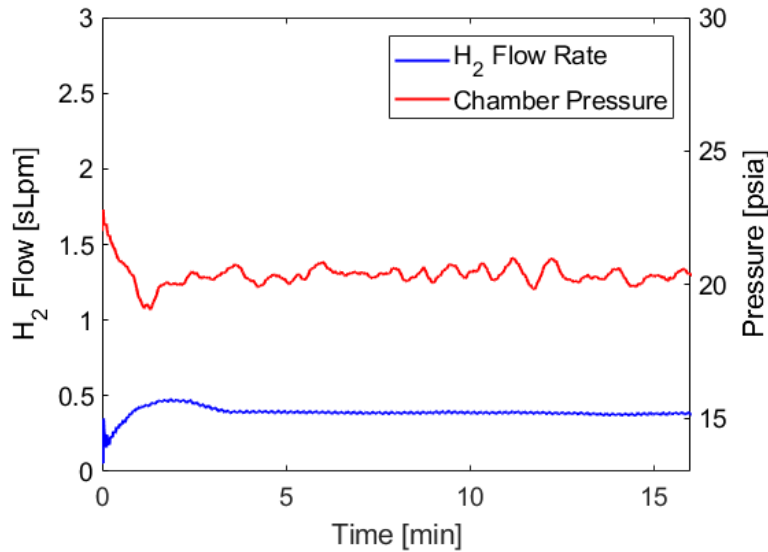


Figure 5.4. Hydrogen flow rate and pressure during Test AB-3.

5.3 Programmable Electronic Load

Initial testing with the SPM was deemed to be successful enough to warrant purchasing a unit for additional tests. During the lengthy lead time for receiving the SPM, efforts were focused on extending test duration to provide more power and subjecting the system to abrupt changes in load demand. In order to test the system under wide ranging load conditions, an 8600 Series Programmable DC Electronic Load was purchased from B&K Precision [67]. This unit can simulate virtually any load that the portable power system being developed would be subjected to during field use. Notably, it can create constant current, voltage, and power loads and can simulate charging profiles for many common batteries. The electronic load can draw up to 30 A and 120 V with a max power draw of 150 W. It also allows for monitoring and recording of fuel cell power output at a rate of 10 Hz, which is important for monitoring PEMFC health over time.

Updates were made to the test stand shown in Figure 4.6 to accommodate the H-30 PEMFC and the electronic load. These changes include those previously described in Section 5.2 such as replacing the flow controller with the H-30 PEMFC stack and the LabVIEW-based logic controller with a normally closed pressure switch. Other improvements were made based on lessons learned during testing with the SPM, most notably the addition of a miniature single stage pressure regulator between the flow meter and the fuel cell to protect the stack against unintended over

pressurization. After analyzing initial tests with the pressure regulator, a pressure transducer was installed downstream of the regulator to monitor the fuel cell feed pressure. A 0.01 inch orifice was also installed downstream of the purge valve to minimize hydrogen loss during purging. An updated P&ID is shown in Figure 5.5 below.

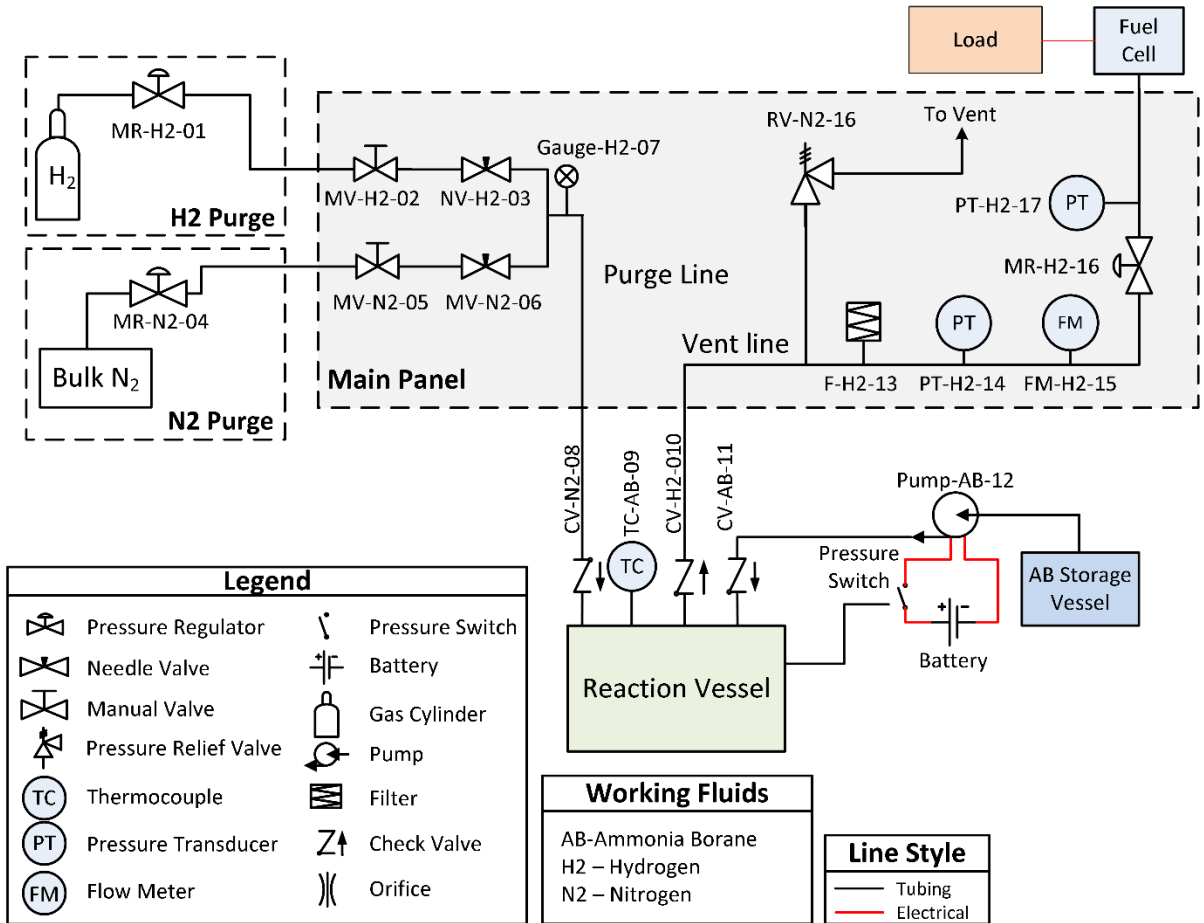


Figure 5.5. P&ID of the modified hydrogen generation test stand.

6. INCREASED TEST DURATION WITH SIMULATED LOADS

6.1 System Testing with Ammonia Borane

The electronic load described in Section 5.3 was used to demonstrate the ABCharger's ability to modulate hydrogen generation rate and satisfy varying load demands while maintaining a steady chamber pressure. For Test AB-4, 7.5 g of AB (synthesized in-house) and 28 g of maleic acid (1:1 molar ratio) were dissolved into 30 and 145 mL of deionized water, respectively. The electronic load was programmed to demand constant current draws of 2 A, 3 A, and 4 A, each being held for 10 minutes. The operating procedures used for initiating Test AB-3 were also used for this test. The power output is shown in Figure 6.1 while the hydrogen pressure and flow rate, which have been smoothed over 30 second intervals, are shown in Figure 6.2.

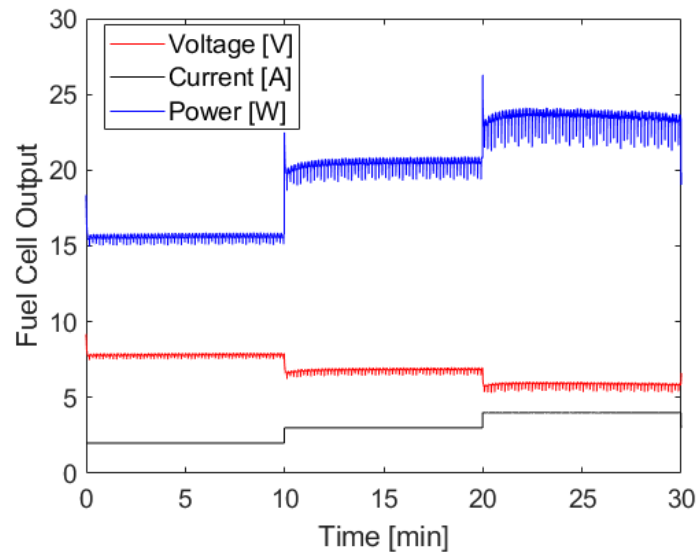


Figure 6.1. PEMFC output during Test AB-4.

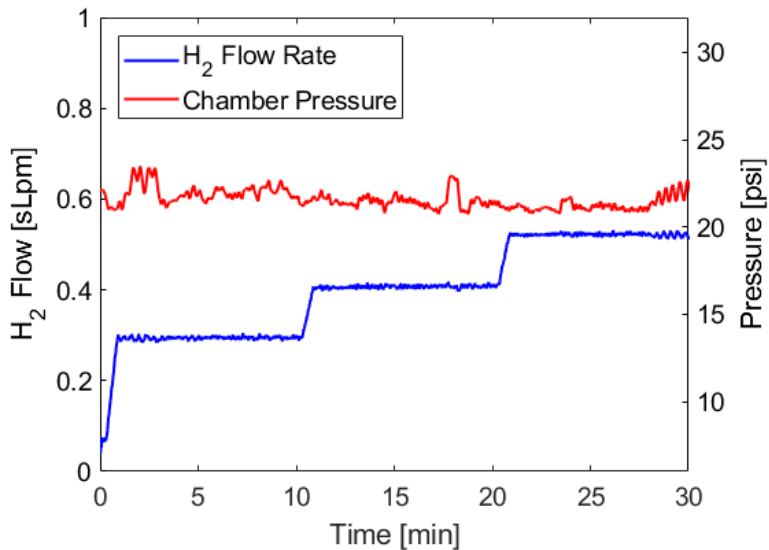


Figure 6.2. Hydrogen flow rate and pressure during Test AB-4.

For the first 10 minutes of Test AB-4, the electronic load drew 2 A of current and the fuel cell generated ~15 W power while consuming nearly 0.3 sLpm of hydrogen. When the load was changed to 3 A, the stack generated ~20 W of power and consumed 0.4 sLpm of hydrogen. Over the final 10 minutes, the load increased to 4 A and the stack produced ~23 W while consuming 0.55 sLpm of hydrogen. Under these conditions, the hydrogen generation system was able to nearly double its output while maintaining a chamber pressure of 22 ± 2 psia. The ability to adjust hydrogen generation rate to match load demand is important for system safety and versatility.

Test AB-5 was prepared with the intent of extending test duration. The system was loaded with 8 g of AB (synthesized in-house) and 30 g of maleic acid (1:1 molar ratio) which is enough reactants to power a 4 A load for up to 45 minutes. The AB and acid were dissolved into 35 mL and 120 mL of deionized water, respectively. The test was initiated using the procedures described for Test AB-3. The fuel cell output for Test AB-5 is shown in Figure 6.3 while hydrogen pressure and flow rate are shown in Figure 6.4 below.

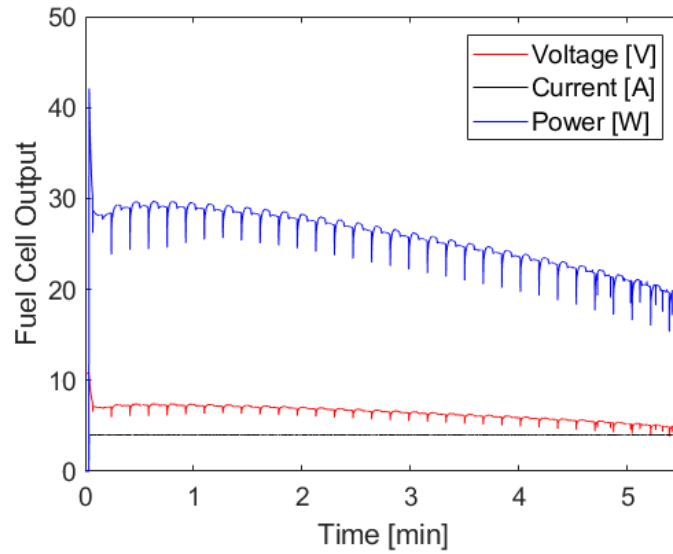


Figure 6.3. PEMFC output during Test AB-5.

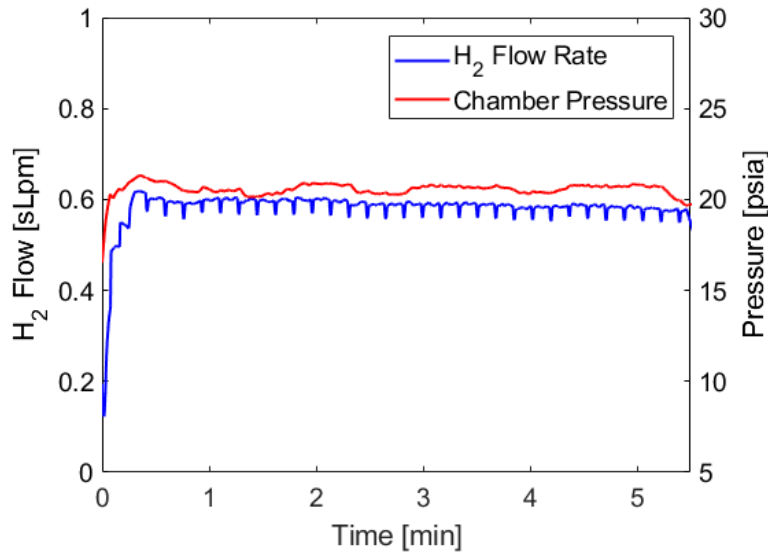


Figure 6.4. Hydrogen flow rate and pressure during Test AB-5.

One minute after closing the bottled hydrogen supply and switching over to generated hydrogen, the PEMFC's power output slowly began to decay. After five minutes, the power output had dropped significantly and the test was aborted. Two potential explanations have been considered for this performance loss. The first is that the PEMFC could have been starved of hydrogen. The pressure in the chamber held relatively constant throughout the test, but it is

possible that the pressure regulator between the reaction chamber and the PEMFC was knocked out of calibration during system setup and was supplying a lower hydrogen pressure than intended. The second possible explanation is that a contaminant, potentially ammonia, was present and poisoning the stack. Gas pockets were observed in the line between the AB reservoir and the reaction vessel and seemed to grow larger while moving from one end of the tube to the other. Assuming relatively constant pressure in the tube, this would imply that a reaction was taking place and generating gas before the AB solution was introduced to the acid solution. If the AB solution was self-hydrolyzing in the tube it would be generating some amount of ammonia that could reach the fuel cell without passing through the acid solution to be trapped. Future testing focused on investigating whether either of these potential explanations were responsible for PEMFC degradation.

An attempt was made to revive the fuel cell after observing performance loss. This included operating the stack on bottled hydrogen for several hours while applying a low current demand of 1-2 A. The stack was then disconnected from the load and hydrogen supply and flushed with deionized water, per the manufacturer's procedures in the H-30 user manual. The process was repeated several times, alternating between operating at low current draw and flushing with deionized water. The revival effort resulted in improved stack performance, but repeating the procedures achieved diminishing returns after several cycles. Full recovery was never achieved and the stack was used for additional testing with slightly lower performance than was previously attainable.

Before additional testing, the hydrogen generation system was disassembled, thoroughly cleaned, and leak checked following reassembly. The conditions used for Test AB-5 were then repeated to determine if the stack would once again be damaged. The results were quite similar to the first attempt using these conditions, with PEMFC output decaying after one minute of operating on generated hydrogen supply and the test being aborted after five minutes. After aborting the test, the PEMFC revival procedures detailed above were repeated. The stack again showed some performance improvement, but did not fully recover to the performance observed prior to this test.

Two modifications were made to the test setup in an attempt to diagnose the cause of PEMFC performance decline and prevent further damage. First, a Unik 5000 pressure transducer (0-50 psia range, $\pm 0.2\%$ full scale accuracy) was added between the pressure regulator and the PEMFC to monitor feed pressure. Second, a dip tube was added to the reaction vessel such that

the AB supply was injected at the bottom of the acid solution rather than being dripped from the top of the vessel. This orientation ensures that gases generated in the transfer tube are bubbled through the acid solution to trap any ammonia that may be present. A check valve and 40 micron filter were added to the dip tube to prevent backflow of acid solution and disperse incoming fluids to improve mixing and gas retention time.

The conditions from Test AB-5 were repeated for Test AB-6 using the system modifications described above. Figure 6.5 below shows that the power output still decays over time, but at a slower rate than was observed during previous tests. The output remains relatively constant for the initial several minutes, and then drops rapidly over the next 15 minutes before the test is aborted. Figure 6.6 shows an initial drop in pressure at the onset of the test, seemingly due to the line between the AB supply and the reactor not being completely primed. Once hydrogen generation commences, the pressure supplied to the PEMFC stack is consistent throughout the test, with no apparent correlation between feed pressure and fuel cell performance decay. Once the system reached nominal operating conditions, it maintained a constant chamber pressure and hydrogen flow rate throughout the test. The one exception is the step in flow rate at seven minutes, which occurred when the orifice downstream of the purge valve was removed to ensure that performance decay was not related to water build up in the stack. Removing the orifice did not improve stack performance.

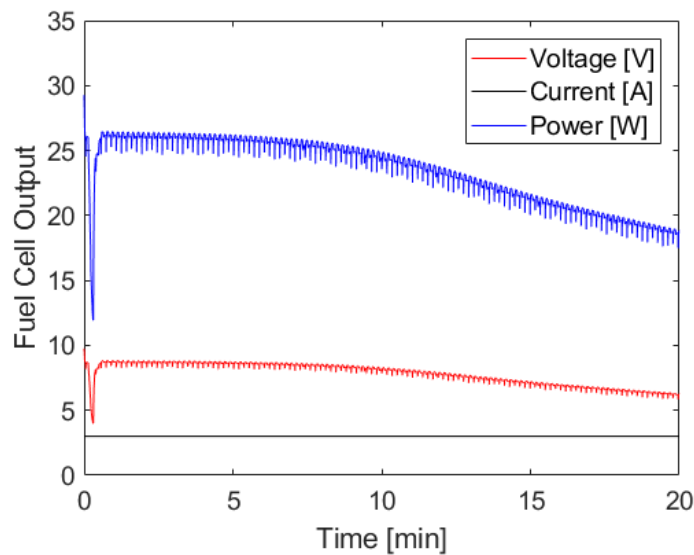


Figure 6.5. PEMFC output during Test AB-6.

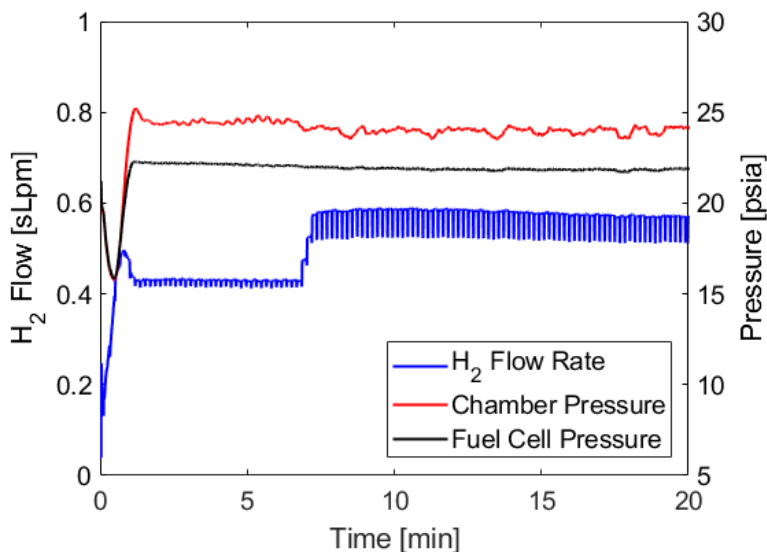


Figure 6.6. Hydrogen flow rate and pressure during Test AB-6.

All of the system level tests reported thus far have been conducted with AB synthesized in-house using the method of Ramachandran and Kulkarni [48]. The next test, Test AB-7, was conducted with >97% pure AB purchased from Sigma Aldrich to determine if PEMFC degradation is related to the AB source. The molar ratio of AB to acid was held constant at 1:1, but the mass of reactants used was scaled to 60% of the amounts used for Test AB-6. The decision to scale the test down was made due to the cost and availability of commercial AB, which can have a lead time of 4-6 months. The solution concentrations were diluted by a factor of two to increase the liquid depth in the vessel with the goal of increasing retention time and improving ammonia sequestration. The test was conducted in the medium-sized acrylic reaction vessel to accommodate the larger solution volumes. The results of this test can be seen in Figure 6.7 and Figure 6.8 below.

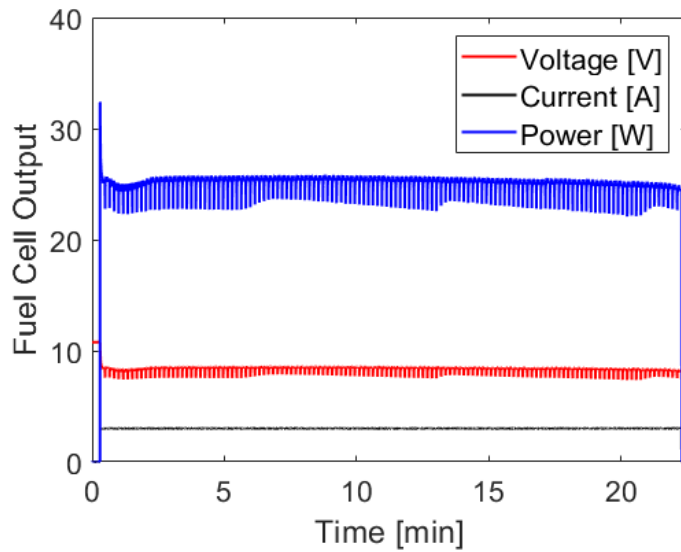


Figure 6.7. PEMFC output during Test AB-7.

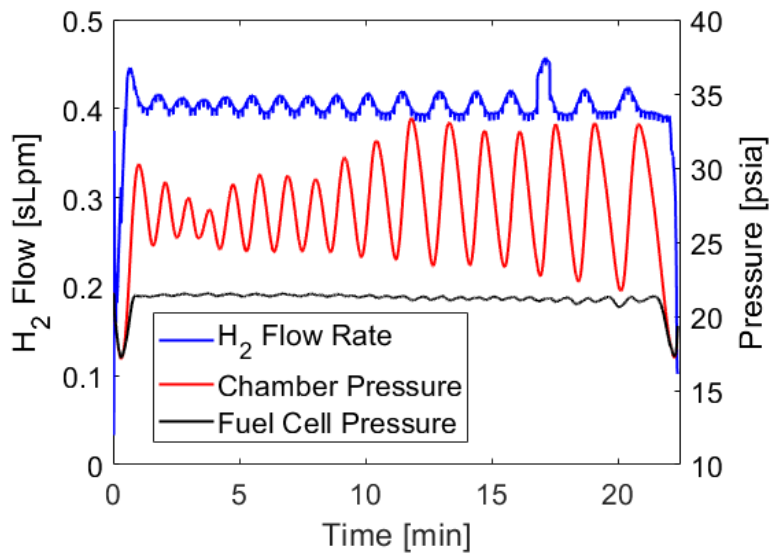


Figure 6.8. Hydrogen flow rate and pressure during Test AB-7.

The pressure profile in the reaction chamber fluctuated more during Test AB-7 than it has in previous tests. This can be attributed to dilution of the solutions and the large volume of headspace in the medium-sized acrylic vessel. Diluting the solutions slowed reaction kinetics considerably and increased the amount of time required for AB to fully react after being transferred to the reaction vessel. This latency dampened the control system's response to a pressure drop and

resulted in longer pumping cycles. More AB is transferred during these cycles than is required to recover pressure to the set point, leading to the pressure fluctuations shown in Figure 6.8. The large amount of headspace in the reaction vessel intensified this behavior. Future tests used a higher concentration of acid and largely avoided such significant pressure fluctuations.

The power generation during Test AB-7 is far better than the power output of Test AB-6. The power decay observed after more than 20 minutes when using Sigma Aldrich AB is less than 3% of the starting output, compared to almost 30% decrease over the same time during Test AB-6. While this represents improvement, it is problematic that degradation is still occurring. It is also important to note that the observed fuel cell degradation appears to be cumulative and partially irreversible. This implies that while the AB purchased from Sigma Aldrich allows for slower decay, it will still eventually result in complete loss of the fuel cell.

PEMFC performance degradation does not appear to be related to hydrogen feed pressure or stack flooding due to buildup of product water. Therefore, the most likely cause for decay is a gas contaminant in the generated hydrogen stream. It was shown in Section 3.2 that acid-promoted hydrolysis of AB results in highly pure hydrogen gas. However, the procedures used to generate hydrogen for gas analysis differ slightly from those used to test the ABCharger. The primary difference is that system level testing exposes highly concentrated AB solutions to open air before and during testing, whereas gas analysis employed relatively dilute AB solutions that were promptly used without more than a few minutes of air exposure. Chandra and Xu reported that exposure to a CO₂ atmosphere will facilitate hydrogen release from an AB solution, while Brockman et al. found that the concentration of AB solutions has a large impact on their stability in open air [42,46]. Together, these reports suggest that exposure to CO₂ in ambient air and the use of higher AB concentrations would tend to decrease the stability of AB solutions. This could explain why the solutions and procedures used for system level testing appear to be less stable than those used for gas analysis.

To measure hydrogen purity while accounting for system level testing procedures, the hydrogen test stand was connected directly to the FTIR apparatus described in Section 0. Rather than delivering generated gases to the PEMFC, the stand was connected to the heated gas cell such that all generated gases were collected. The flow controller simulated the fuel cell's consumption to ensure that hydrolysis occurred at a similar rate to what was observed when testing with the fuel

cell. An image of the hydrogen generation test stand connected to the FTIR is shown in Figure 6.9 below.

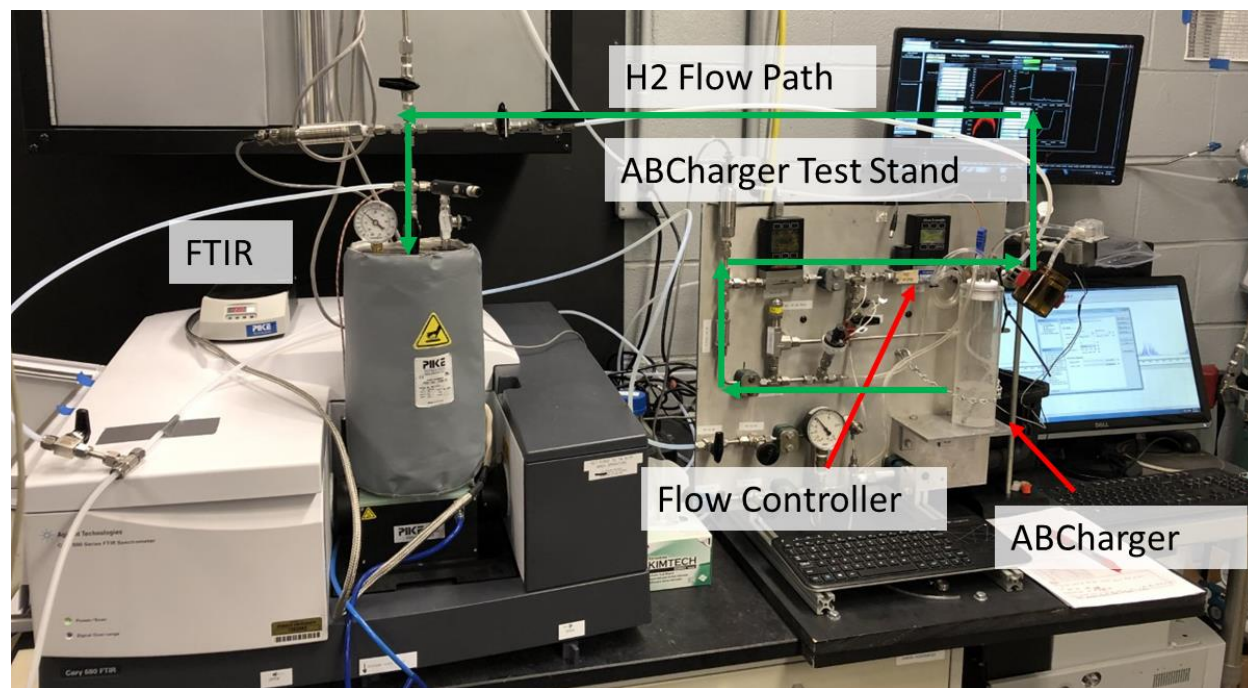


Figure 6.9. Hydrogen generation stand connected to FTIR for product gas analysis.

System level hydrogen purity tests were conducted using >97% pure AB from Sigma Aldrich. During testing with the H-30 stack, AB from Sigma Aldrich appeared to result in better PEMFC performance than AB synthesized in-house. These tests also used the dip tube and muffler to approximate the experimental conditions that resulted in the least amount of PEMFC decay during fuel cell integration. The ratio of AB to maleic acid was 1:1 and the solution concentrations were similar to those used for Test AB-6. The gas cell was heated to 150°C, purged with ultra-high purity nitrogen, and then evacuated to 3 psia. Gas sample was loaded by initiating hydrolysis and allowing the pressure in the cell to increase by approximately 8 psi. The gas cell was then isolated from the hydrogen generation system and brought to atmospheric pressure using ultra-high purity nitrogen before the sample was analyzed. After analysis, the cell was evacuated and purged before being loaded with additional sample. This process was repeated a total of four times to investigate how hydrogen purity changes as the test progresses. Figure 6.10 shows the FTIR spectrums from the four fills, including a zoomed view of the region where an ammonia response

would be detected. Two calibration samples representing 3 ppm and 22.5 ppm of ammonia are included for comparison to the generated samples. Table 6.1 presents the concentrations of ammonia, CO, and CO₂ that were measured following each of the fills.

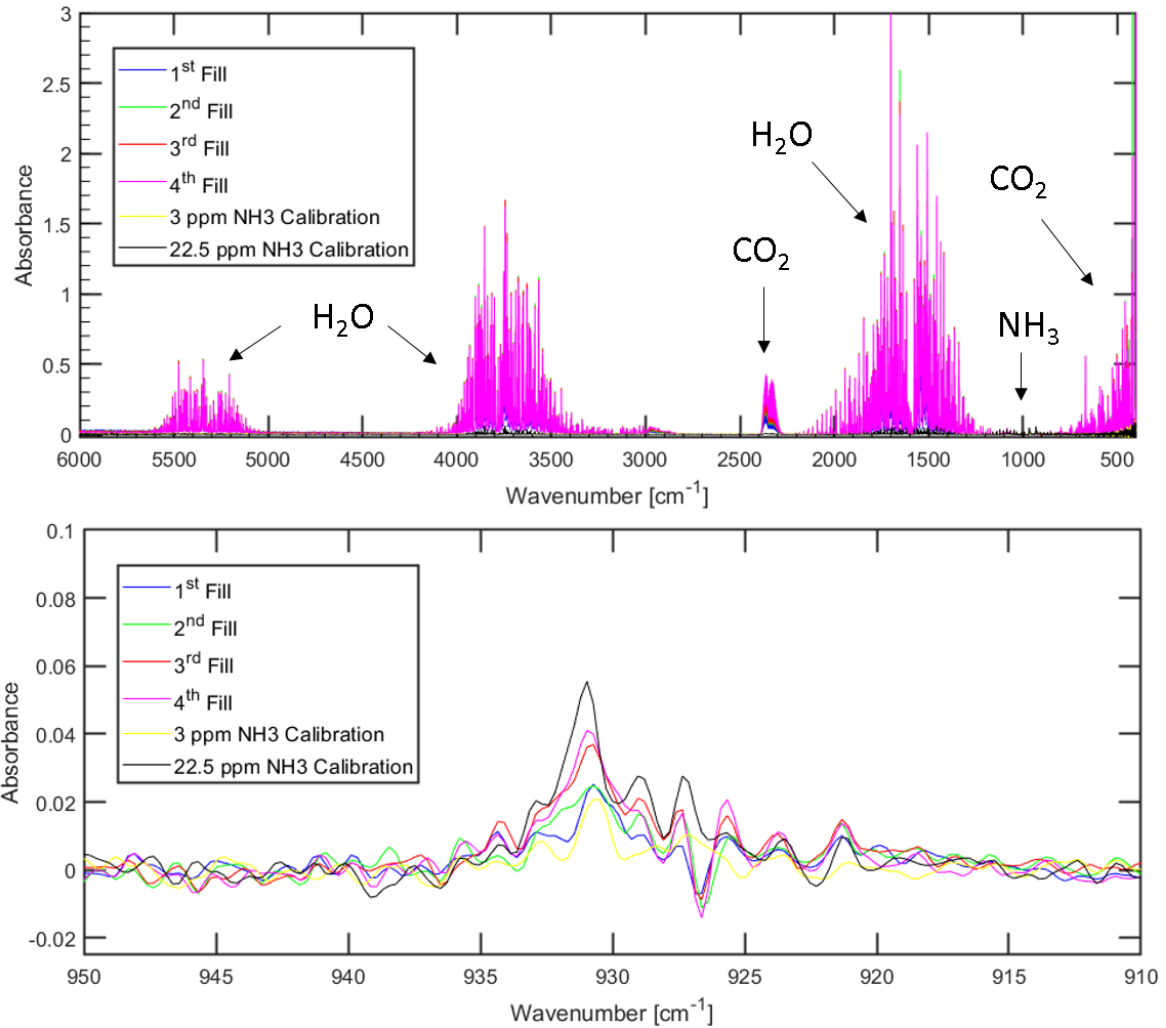


Figure 6.10. FTIR spectrums of product gases generated in the ABCharger 2.0 system using the procedures developed for PEMFC testing. The top figure shows the entire spectrums, while the bottom figure shows a detailed view of the region where an ammonia response would be observed.

Table 6.1. Contaminant concentrations in ABCharger hydrolysis gas products measured by FTIR analysis.

Sample	NH₃ [ppm]	CO [ppm]	CO₂ [ppm]
Fill 1	< 8	< 17	44
Fill 2	< 8	< 17	92
Fill 3	17	< 17	109
Fill 4	21	< 17	164

Table 6.1 shows that the concentration of CO₂ increases with each subsequent test. It was proposed in Section 0 that CO₂ enters the system dissolved in water and is released when the water is acidified. This explanation is consistent with the results of system level testing that show more CO₂ entering the system the longer the AB solution is exposed to open air. It is important to note that despite the system level tests using more than 10 times the amount of water as tests reported in Section 0, the levels of CO₂ measured in these samples is on the order of 10 times less than what was previously measured. When generating gas samples for earlier FTIR tests, the bulk of the water was acidified after the system was sealed such that released CO₂ was captured and quantified. Conversely, using system level procedures, the bulk of the water is acidified before the system is sealed and CO₂ is not collected. This is the same order of operations reported in Section 3.2.1 and used to generate samples for GC-FID analysis that measured similarly low levels of CO₂. This confirms that CO₂ release is rapid upon acidification and that system testing procedures allow only the CO₂ dissolved in the AB solution to actually be delivered to the PEMFC. Levels of CO in each sample were below the lower detection limit.

The concentrations of ammonia in the first and second samples were below the lower detection limit of 8 ppm, while the third and fourth samples contained 17 and 21 ppm of ammonia, respectively. This trend of increasing ammonia concentration as the test progresses is consistent with the hypothesis that AB solutions begin to react when exposed to air and are generally unstable over time. Similarly to previous tests, small bubbles were observed in the tubing between the reaction vessel and the AB storage vessel, indicating that gas is indeed being generated prior to mixing the two solutions. Based on the rate of PEMFC decay when using AB synthesized in-house and AB from Sigma Aldrich, it is likely that the concentrations of ammonia released using the former would be higher than the 21 ppm or less detected in the gas products of Sigma Aldrich AB.

If 21 ppm were considered to be the maximum amount of ammonia that could be released, the generated gas stream would still contain a level of ammonia that has been previously reported to cause permanent damage to a PEMFC. In studies investigating exposure of PEMFCs to 30 ppm or less of ammonia, previous authors found that it took up to eight hours for performance decay to be observed [52,53,55]. This implies it would take several hours for the concentrations of ammonia detected in hydrogen generated by the ABCharger to noticeably damage the fuel cell. It is then logical that the initial tests shown in Figure 5.4 and Figure 6.1 did not result in observable performance decay, but that subsequent tests did after the stack's resiliency towards ammonia had been compromised.

To confirm that ammonia is released from AB solutions before they are added to the acid solution, aqueous AB samples were prepared in open air and sealed in vials. The vials were then connected to Dräger Ammonia Detection Tubes and left over night. Multiple solutions were prepared using deionized water and AB either purchased from Sigma Aldrich or synthesized in-house. Each solution resulted in a positive ammonia detection from the Dräger tubes. The ammonia concentration cannot be quantified from this experiment as the solutions did not generate enough gas to satisfy the Dräger tube calibration conditions. However, the experiment does verify that the AB solutions are unstable in air and will react to release ammonia before they are added to the acid solution.

To summarize the results presented thus far in this dissertation: AB hydrolysis can be accelerated using organic acids to achieve near theoretical hydrogen yields and less than 7.4 ppm of ammonia. However, the hydrogen generation system that has been designed requires AB solutions to be exposed to open air prior to and during testing, resulting in levels of ammonia release that are detrimental to PEMFCs. The presence of ammonia in hydrogen generated using the ABCharger system has been confirmed at levels as high as 21 ppm using FTIR spectroscopy. Dräger tube analysis has verified that the AB solutions are releasing ammonia prior to being introduced to the acid solutions. The system could be modified to include additional ammonia sequestration techniques and to prevent the AB solution from being exposed to open air, but the purpose of this initial investigation was to determine whether or not organic acids could facilitate the release of hydrogen that met PEMFC purity requirements without purification. As currently designed, the system could only be considered single-use and used to power a PEMFC for less than eight hours. Additional ammonia sequestration mechanisms or a modified system design

would be required to operate a PEMFC for longer durations. Rather than modify the system to accommodate AB, alternative hydrogen sources that do not contain ammonia were investigated.

6.2 System Testing with Sodium Borohydride

Perhaps the most obvious solution to prevent ammonia poisoning is to remove the ammonia source from the system altogether. The most logical replacement for AB is SBH, which not only does not contain ammonia, but is also cheaper and more readily available than AB. Organic acids were selected as the reaction promoter of choice for SBH hydrolysis despite there no longer being an obvious need for ammonia sequestration. This was motivated by literature reports of metal catalysts lacking durability for prolonged use in SBH hydrolysis [39,41,68]. Of particular concern are the findings of Glad and Becker-Glad who observed less than 20% hydrogen yields when using seawater and CoCl_2 for SBH hydrolysis. This is a stark contrast to the greater than 97% yields they reported when using seawater and an acid accelerator. Because the proposed application for the system being designed requires the use of water collected in the field of operation, it is imperative that the reaction promoter be indifferent towards water contaminants.

There are several additional reasons why organic acids were selected as SBH hydrolysis promoters. As was discussed in Section 2.2.2.1, when considering portable applications, the byproducts of SBH hydrolysis are more favorable when using an acid accelerator than a metal catalyst. This is because acids do not lead to the formation of NaBO_2 , which will exothermically hydrate in the presence of excess water, leading to higher operating temperatures and increased water consumption [69]. The use of a homogenous reaction accelerator also makes the system simpler to load and operate and prevents the need to stir the contents of the reactor or pump solution through an immobilized catalyst bed. Finally, organic acids are far cheaper and more readily available than metal catalysts.

Before conducting system level testing with SBH, it was necessary to repeat many of the small scale tests previously reported using AB to ensure hydrogen could be generated at the required rate and purity. SBH solutions used for testing were stabilized with a 10:1 mass ratio of SBH to sodium hydroxide (NaOH). The SBH used for this investigation was purchased from Alfa Aesar and was >98% pure.

The initial effort towards SBH investigation was to compare hydrogen release rate from AB and SBH when using a 1:1 molar ratio of maleic acid. The results, which have been normalized to

show hydrogen yield as a percentage of the theoretical maximum for each material, can be seen in Figure 6.11 below. Hydrogen release rates were similar using either source. SBH had the slightly faster initial rate, but after five minutes the yields matched to within experimental uncertainty. After 15 minutes, the yields for each source were between 97% and 98% of theoretical.

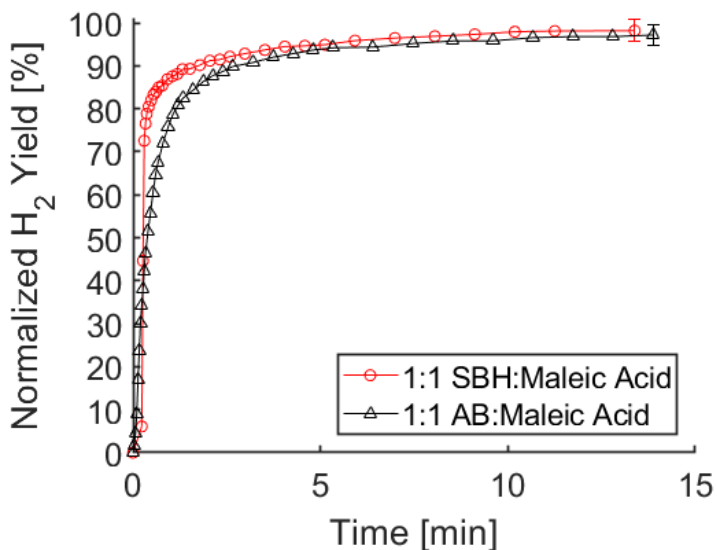


Figure 6.11. Comparison of acid-promoted hydrolysis using maleic acid and either SBH or AB.

The influence of common water contaminants was investigated by preparing acid solutions and NaOH stabilized SBH solutions using a variety of low quality water sources. These solutions were combined to generate hydrogen and their performance compared to that of solutions made with deionized water. As can be seen in Figure 6.12 below, the rate and yield of hydrogen release was essentially unaffected when switching between the various water sources. Each water source allowed for instantaneous hydrogen release and final yields within experimental uncertainty of 100%.

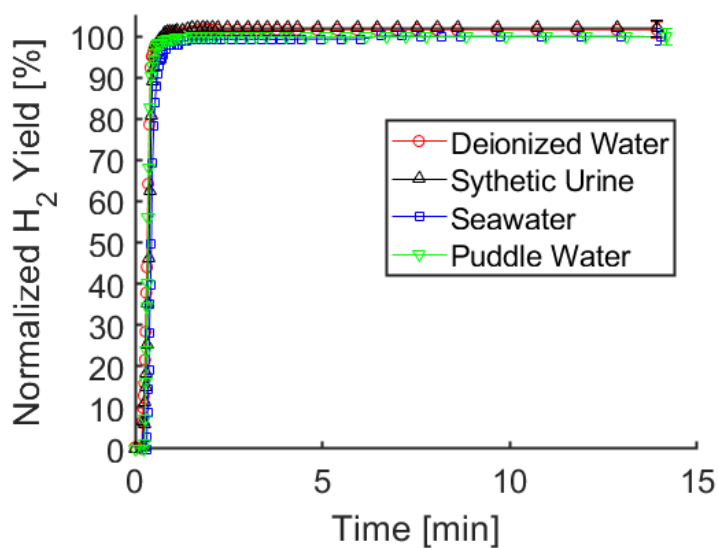


Figure 6.12. Hydrogen yield from maleic acid-promoted hydrolysis of SBH using low-quality water sources.

Although the likelihood of SBH hydrolysis releasing ammonia is extremely low, there are other contaminants that could be released that need to be quantified to ensure PEMFC compatibility. The procedures for FTIR analysis of AB hydrolysis products outlined in Section 0 were repeated for samples generated using a 1:1 molar ratio of SBH and maleic acid and various water sources. The results are included in Figure 6.13 and Table 6.2 below.

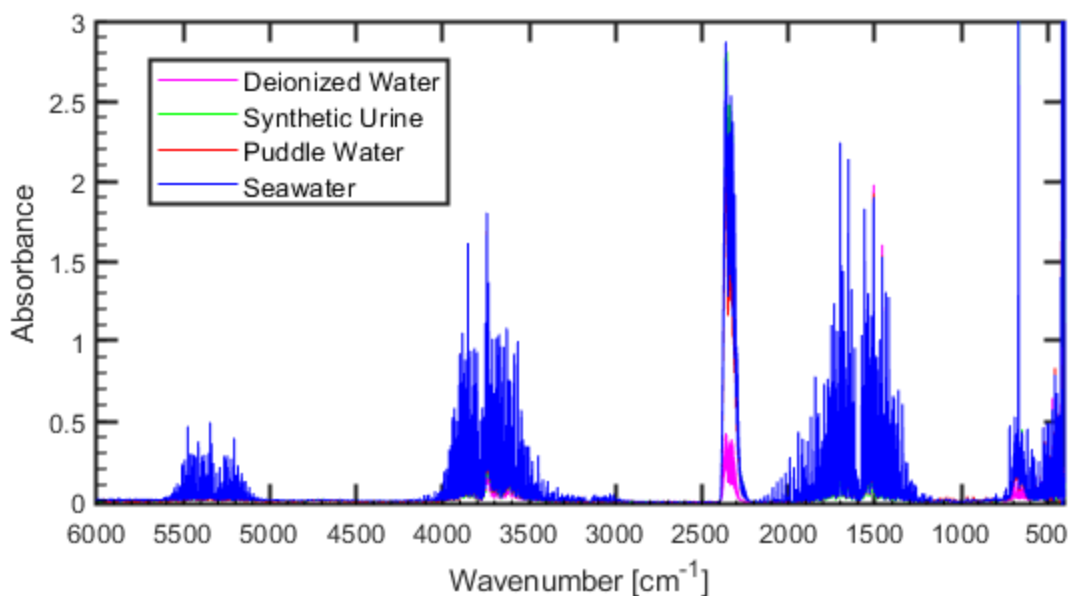


Figure 6.13. FTIR spectrums of product gases generated by organic acid-promoted hydrolysis of SBH using low-quality water sources.

Table 6.2. Contaminant concentrations in acid-promoted SBH hydrolysis gas products measured using FTIR analysis.

Water Source	NH₃ [ppm]	CO [ppm]	CO₂ [ppm]
Deionized Water	< 13	< 28	319
Synthetic Urine	< 13	< 28	1266
Puddle Water	25	< 28	1308
Seawater	< 13	< 28	1215

Interestingly, Table 6.2 shows that gas products from tests using puddle water contained 25 ppm of ammonia. This ammonia is unlikely to have been generated during the reaction given the reactants being used, and is more likely to have been dissolved in the puddle water prior to testing. A sample of the puddle water used for these tests was analyzed for dissolved ammonia using a Thermo Fisher Scientific Ion Selective Electrode and found to contain 0.1 ppm of ammonia. Nearly half a mole of water was used to make the solutions that generated this gas sample, meaning there was approximately 5.0×10^{-8} moles of ammonia dissolved in the solutions. The FTIR gas cell was loaded with 1.9×10^{-5} moles of gas for analysis, so a 25 ppm concentration would translate to 4.7×10^{-10} moles of ammonia in the gas cell. This is less than 1% of what was dissolved in the

puddle water at the beginning of the test. It is therefore reasonable to assume that the ammonia detected in the product gases entered the system dissolved in the puddle water and was not a product of hydrolysis. If ammonia was dissolved in the puddle water, it is unlikely to have come out of solution after the puddle water was made acidic. Instead, it is more probable to have evolved when the stabilized (i.e. basic) SBH solution was in the reaction vessel following the purge prior to acid injection. However, designing the fielded system in such a way that gasses evolved from a basic solution must pass through an acidic solution before reaching the fuel cell, as is done in the ABCCharger 2.0, would likely eliminate this problem altogether. The potential for ammonia to be dissolved in naturally occurring water sources supports the decision to use acid promoters rather than metal catalysts for this system.

The CO₂ concentrations shown in Table 6.2 are generally consistent with those reported in Table 3.3 for samples generated using AB hydrolysis and similar water sources. Using either AB or SBH, tests with deionized water resulted in approximately 300 ppm of CO₂, while using seawater or puddle water and either hydrogen source resulted in concentrations between 1300 and 2100 ppm. CO₂ levels were not as consistent when using synthetic urine, with less than 400 ppm for AB tests compared to more than 1300 ppm using SBH. The synthetic urine was prepared shortly before testing with AB, with these tests resulting in CO₂ levels similar to tests using deionized water. The urine was then stored for several months prior to SBH testing. During this time, the storage container was opened on several occasions to collect samples for testing, with fresh air entering the container each time. After repeated air exposure, the urine was used for SBH hydrolysis and resulted in CO₂ concentrations consistent with those detected when using seawater or puddle water. This seems to suggest that the urine samples were collecting CO₂ from the air and eventually approached an equilibrium of dissolved CO₂ similar to what was attained by the seawater and puddle water prior to testing.

With the exception of the ammonia detected when using puddle water, the hydrogen generated using SBH and any of the water sources considered was PEMFC compatible. This justified testing with the H-30 PEMFC by replacing AB solutions with NaOH stabilized SBH solutions. The first SBH test, Test SBH-8, used 4 g of SBH dissolved in 30 mL of deionized water and stabilized with a 1:10 mass ratio of SBH to NaOH. One molar equivalent of maleic acid was dissolved into 120 mL of deionized water. The electronic load was set to demand 3 A of current and the test was

expected to run for 25 minutes based on an expected hydrogen consumption rate of 0.4 sLpm. Results of the test can be seen below.

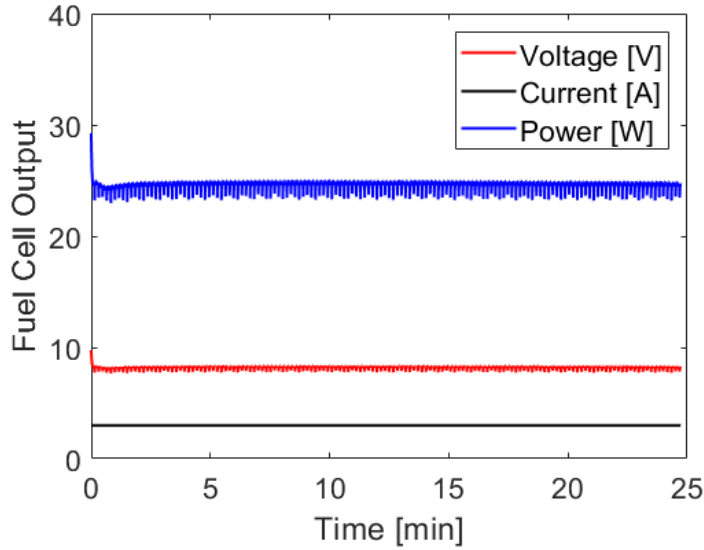


Figure 6.14. PEMFC output during Test SBH-8.

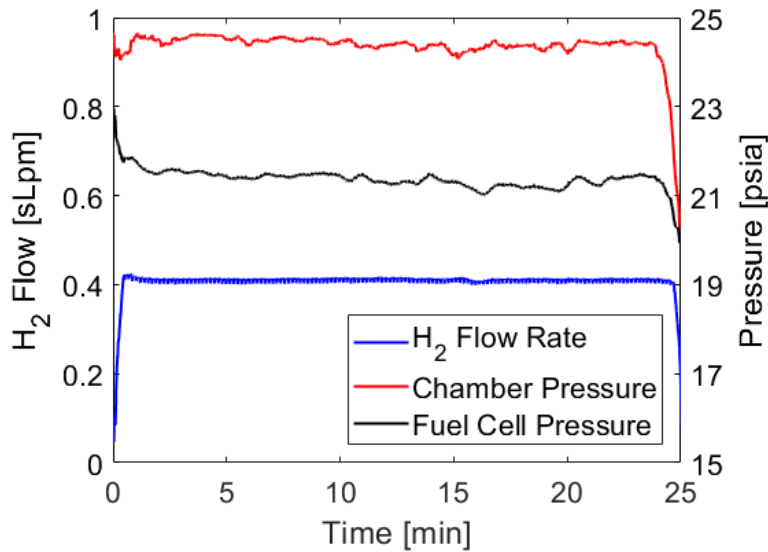


Figure 6.15. Hydrogen flow rate and pressure during Test SBH-8.

The power production observed in Figure 6.14 is more consistent than any of the previously reported tests conducted using AB. The PEMFC produced approximately 25 W of power for nearly

25 minutes, consuming an average of 0.41 sLpm of hydrogen. The system maintained a consistent chamber pressure of nominally 24 psia until all SBH had been transferred to the reaction chamber. All reactant byproducts were fully dissolved following the test.

The test conditions used for the test above were gradually scaled up to increase system capacity. The system responded well to each increase, continuing to maintain consistent chamber pressure and fuel cell output as test duration surpassed three hours. As the test duration increased, the temperature rise in the reaction solution became much more significant, such that it merits being reported for these longer tests. The results for Test SBH-9, the first of the three-hour tests, are shown in Figure 6.16, Figure 6.17, and Figure 6.18 below. The system was loaded with 34.3 g of SBH dissolved in 75 ml of deionized water and stabilized with 3.4 g of NaOH. The reaction vessel was loaded with 105.3 g of maleic acid (1:1 molar ratio to SBH) dissolved in 300mL of water. The electronic load was set to demand a constant 3 A load.

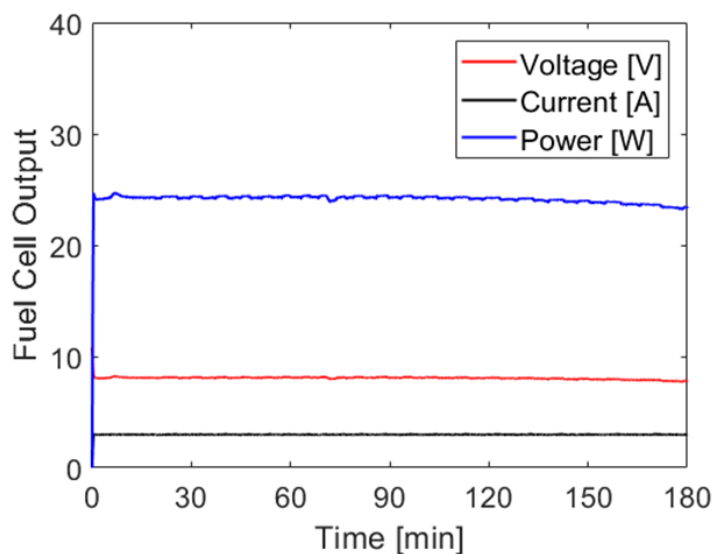


Figure 6.16. PEMFC output during Test SBH-9.

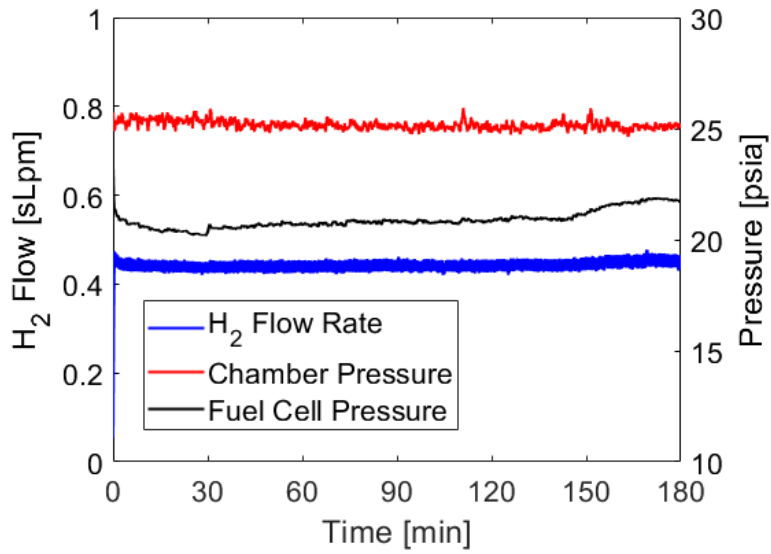


Figure 6.17. Hydrogen flow rate and pressure during Test SBH-9.

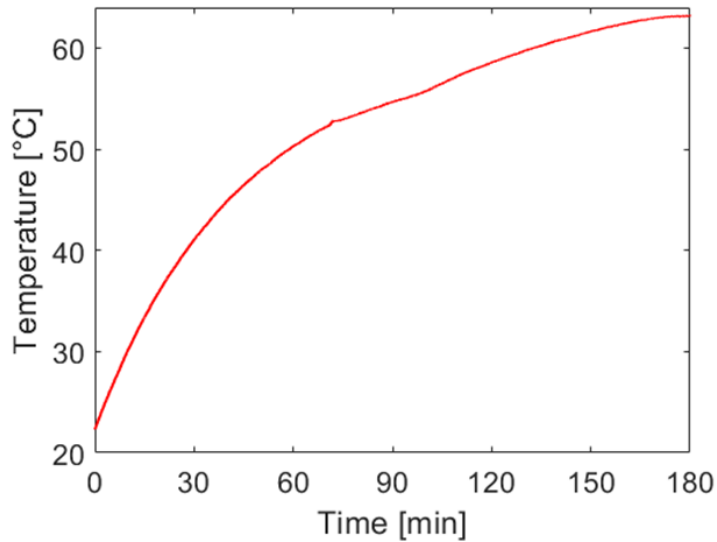


Figure 6.18. Solution temperature inside reactor during Test SBH-9.

Throughout the duration of Test SBH-9, the chamber pressure and hydrogen flow rate held steady at 25 psia and 0.45 sLpm, respectively. The fuel cell feed pressure, measured immediately downstream of the pressure regulator, fluctuated between 20 and 22 psia, which is within the range of acceptable feed pressures prescribed by the fuel cell manufacture. The power output held steady at an average of 24.2 W for the first 120 minutes, before slightly decreasing to 23.4 W over the

final 60 minutes. It is interesting to note that the decrease in power output occurred only after the temperature in the reactor neared 60°C. It is plausible that the decay could be related to the increase in water vapor in the hydrogen gas stream, which would block some of the fuel cell's active catalysts sites. The power decay was quickly reversed after purging the system and operating the PEMFC on bottled hydrogen (which is virtually free of moisture) for several minutes, indicating the performance decay was not related to stack poisoning. Future tests were closely monitored to see if similar decay was observed.

Solution temperature inside the reactor appeared to be approaching steady state conditions between 55 and 60°C after 90 minutes, at which point there is an inflection in the temperature curve and the solution continues to heat to beyond 60°C. The temperature inflection point coincided with the observation of solid particulate forming in the reaction vessel. Additional solids developed as the test went on. As can be seen in Figure 6.19 below, a large fraction of the reaction vessel was filled with solids by the end of the experiment. A sample of the particulate was collected following the test and was found to be easily dissolved in water. While some solids were loose and suspended in the solution, a large portion were fixed to the diffuser through which SBH enters the reaction vessel. The solids attached to the muffler were difficult to remove by scraping or brushing, and instead had to be removed by dissolving them in water. It appears that after 90 minutes the solution became saturated with reaction byproducts, likely sodium maleate, and that the solids crashed out of solution. While the temperature inflection point appears to be directly linked to the formation of solid byproducts, it is unclear whether crystallization is exothermic or if the thermodynamic properties of the system were altered, or both.



Figure 6.19. Reaction vessel following Test SBH-9. Solid particulate can be seen at the top and bottom of the reaction vessel.

Investigating the relationship between solid byproducts and solution temperature was not of primary interest to this work as the formation of solids jeopardizes system reliability and reusability and should be avoided. Instead, the logical step was to replace maleic acid with a reaction accelerator that will not result in solid byproducts. Of all the organic acids that were considered as AB or SBH hydrolysis promoters, tartaric acid is the most water soluble and was therefore investigated as an alternative to maleic acid with potentially improved byproduct solubility.

Maleic acid was replaced with tartaric acid for Test SBH-10. This test used 34.5 g SBH in 75 mL of deionized water stabilized with NaOH. The tartaric acid solution was prepared using 137.0 g tartaric acid, a 1:1 molar ratio to SBH, dissolved in 250 mL of deionized water. The remaining test conditions and operating procedures were held constant within experimental uncertainty to those that resulted in solid byproducts when using maleic acid. Results of the test can be seen below.

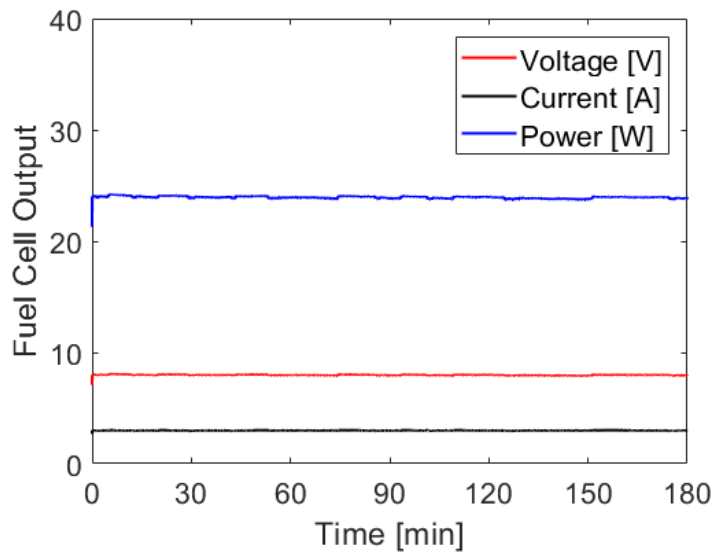


Figure 6.20. PEMFC output using during Test SBH-10.

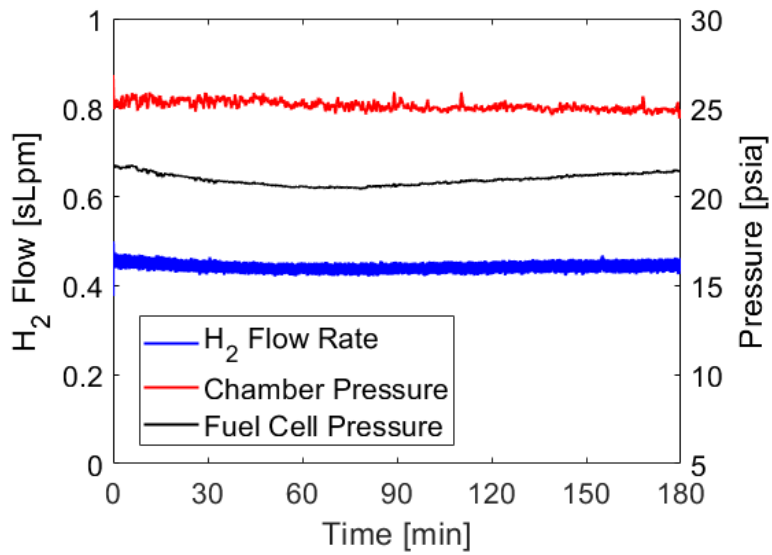


Figure 6.21. Hydrogen flow rate and pressure during Test SBH-10.

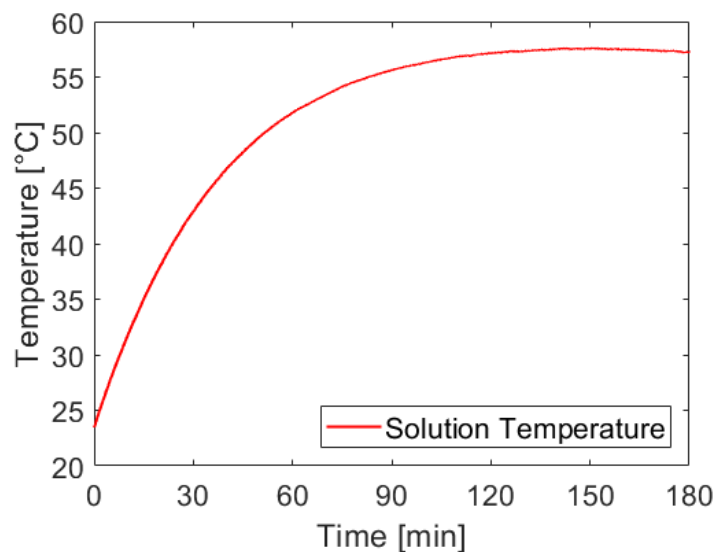


Figure 6.22. Solution temperature inside reactor during Test SBH-10.

The PEMFC power output was more stable during Test SBH-10 than Test SBH-9, with power remaining constant to within ± 0.2 W. The chamber pressure and hydrogen flow rate were again quite stable, while the fuel cell feed pressure fluctuated slightly but stayed within the operating bounds of the PEMFC. The average rate of hydrogen consumption was 0.44 sLpm.

No solid precipitate was observed at any point during the reaction. Following test completion, the solution from the reactor was allowed to cool to room temperature to determine if solids would precipitate at lower temperatures. No solids were observed. The temperature profile of the reacting solution did not have the inflection point that coincided with the formation of solid particulate during Test SBH-9 using maleic acid. Instead, the solution temperature plateaued between 55-60°C. The solution temperatures of the maleic acid and tartaric acid tests are overlaid in Figure 6.23 below to demonstrate how closely the profiles matched prior to the inflection point and how significantly they differed after. Prior to the inflection point, the two profiles never differed by more than 2°C.

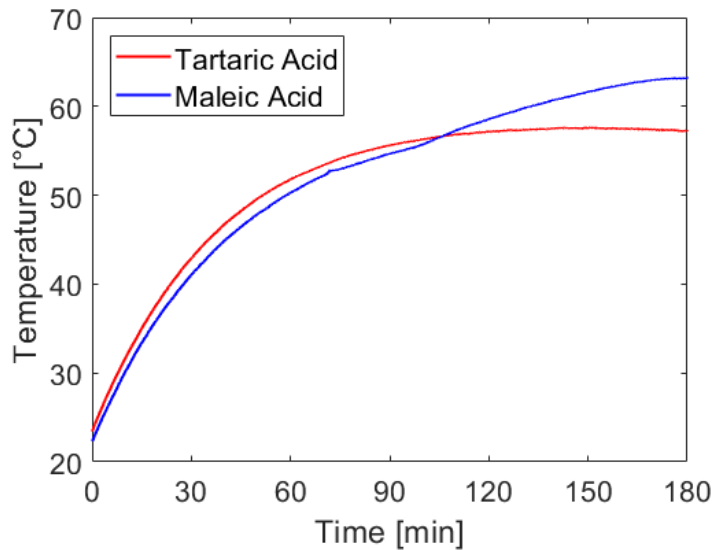


Figure 6.23. Temperature profiles from Test SBH-9 and Test SBH-10 representing solution temperatures for SBH hydrolysis using maleic acid and tartaric acid, respectively.

Several additional system level tests were conducted to confirm repeatability, iterate on operating procedures, and improve the user interface. One significant alteration that was made during this process was to decrease the molar ratio of tartaric acid to SBH from 1:1 to 0.6:1. Because tartaric acid is diprotic, this ratio still results in a surplus of acidic protons available to accelerate the reaction. Unlike the previously used 0.6:1 molar ratio of maleic acid to AB that resulted in only 80% hydrogen yield, 0.6 equivalents of tartaric acid to SBH consistently results in near theoretical yields. The decrease in acid concentration represents a greater than 30% reduction in reactant mass, which significantly increases the energy density of the system.

After conducting several successful three-hour tests using the test stand and procedures discussed above, Test SBH-11 was conducted with the intent of running for longer than five hours. The masses of sodium borohydride and tartaric acid used for the test were increased to 55 g and 131 g, respectively. The solution concentrations were held approximately constant to those used previously. Two anomalies were observed during this test, the first being chamber pressure decay occurring after 30 minutes. After several minutes of investigating the decay, it was determined that the 9 V battery used to power the pump was nearly depleted and could no longer provide the power required to transfer solution. After a new battery was installed, the chamber pressure recovered and remained at nearly 25 psia for the remainder of the test. The second off-nominal event was

that the fuel cell supply pressure decayed throughout the test, dropping to atmospheric pressure after nearly 65 minutes. A sharp drop in PEMFC power output was observed as the feed pressure reached atmospheric, and once this occurred the test had to be aborted to prevent permanent damage to the fuel cell. Because the chamber pressure held steady while the fuel cell supply pressure decreased, it appears that the issue was due to hydrogen transport from the reaction vessel to the PEMFC and not with hydrogen generation itself. The temperature profile for this test was consistent with those from previous tests, implying that there was not a leak in the system. System leaks are quite apparent in the temperature profiles as compensating for losses requires an increased rate of hydrogen generation that is accompanied by an increase of heat release. The hydrogen pressure and flow rate are shown in Figure 6.24 below.

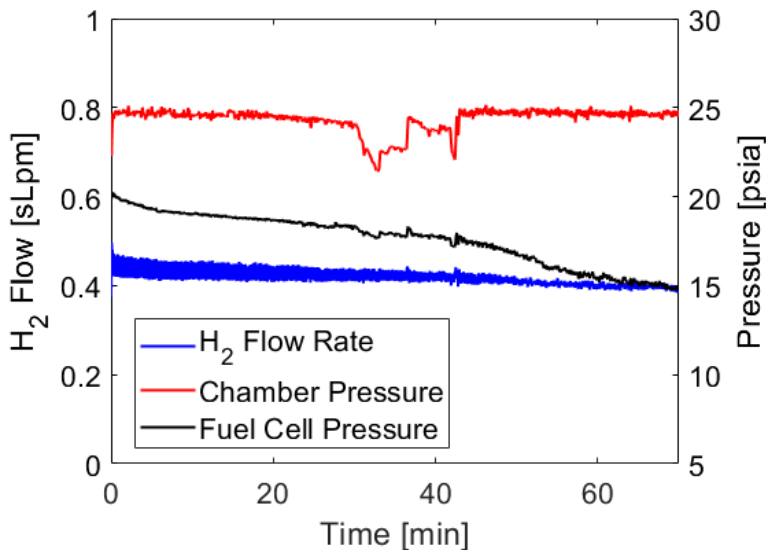


Figure 6.24. Hydrogen flow rate and pressure during Test SBH-11.

In order to better understand this unexpected outcome, the test stand was dismantled and inspected for obstructions. During inspection, a large amount of dried white debris was found inside the horizontal portions of the stand. It is expected that this debris partially blocked the flow path between the reaction chamber and fuel cell, preventing hydrogen from flowing at the rate at which the fuel cell was consuming it. At no point did the solution in the reactor overflow and flood the stand, so it appears that the deposits built up gradually over time. A sample of the solid was dissolved in water and the resulting solution was mildly acidic.

In an effort to better understand the solid deposits found in the test stand, a focused literature search was conducted to identify reports of similar debris in systems that house SBH or AB hydrolysis. The first relevant report that was found is a 2009 review paper by Liu and Li, in which the authors briefly describe “mist elimination” as one of the key challenges that must be addressed before using SBH hydrolysis to fuel a PEMFC [70]. They report that conducting SBH hydrolysis will result in mist formation, and that this mist will carry some amount of solution components such as SBH, NaOH, and NaBO₂. They argue that the mist will settle in the system and eventually result in solid deposits. While their argument is consistent with the visual observation of mist formation and solid deposits observed in the ABCharger 2.0 system, Liu and Li provide no reference to experimental evidence to support their claims.

A more recent review was published by Demirci in 2018 in which the author provides a lengthy discussion of the impacts of mist formation on hydrogen purity [71]. Several references are made to reports containing evidence or concern that solution components are being carried in the hydrogen streams generated by SBH hydrolysis [72–75]. Each of these reports are dated at least six years after the 2009 review by Liu and Li, and the individual authors report varying levels of concern over mist formation. Considering all of the reports together, Demirci concludes that hydrogen from SBH hydrolysis cannot be considered pure and predicts that mist formation could lead to system clogging, as was observed in the ABCharger 2.0.

Demirci’s discussion on the impact of mist formation is quite thorough and leaves little room for further discussion to be presented in this report. However, one of the mist mitigation techniques developed by Kwon and coworkers was discussed in detail by Demirci and is of particular interest for adoption by the ABCharger 2.0 [71,73–75]. As part of a more sophisticated and complex purification scheme, the authors used a water trap to remove water-soluble borates from the gas stream. This technique is easy to implement and adds minimal mass and complexity to the system as the water for the trap can be collected at the point of use along with reactant water.

For the present work, a water trap was added between the reaction vessel and the test stand to mitigate the effect of mist formation on system operation. Mist removal was achieved by passing hydrolysis gas products through a dip tube terminating with an 80 micron filter submerged in approximately 30 mL of room temperature water. An additional benefit to the water trap is partial dehumidification of hydrogen being fed to the fuel cell, as the partial pressure of water above the room temperature water trap will always be lower than the partial pressure of water above the

reaction solution that is heated by hydrolysis. This could prove to be increasingly valuable during longer tests that present increased potential for fuel cell flooding.

Following integration of the water trap, Test SBH-12 was conducted using seawater to observe the influence of low-quality water sources at the system level. This test used the largest acrylic reaction vessel loaded with enough acid solution to facilitate eight hours of maximum output from the H-30 stack. The test was prepared using 85 g of SBH and 8.5 g NaOH in 75 mL of seawater, and 199 g of tartaric acid in 550 mL of seawater. Additionally, this test used a new H-30 PEMFC stack to replace the unit which was previously damaged by ammonia. The results of the test can be seen in the figures below.

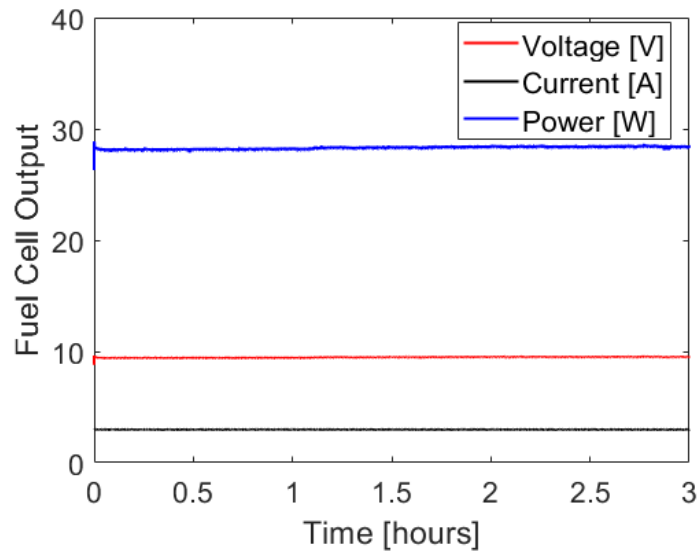


Figure 6.25. PEMFC output during Test SBH-12.

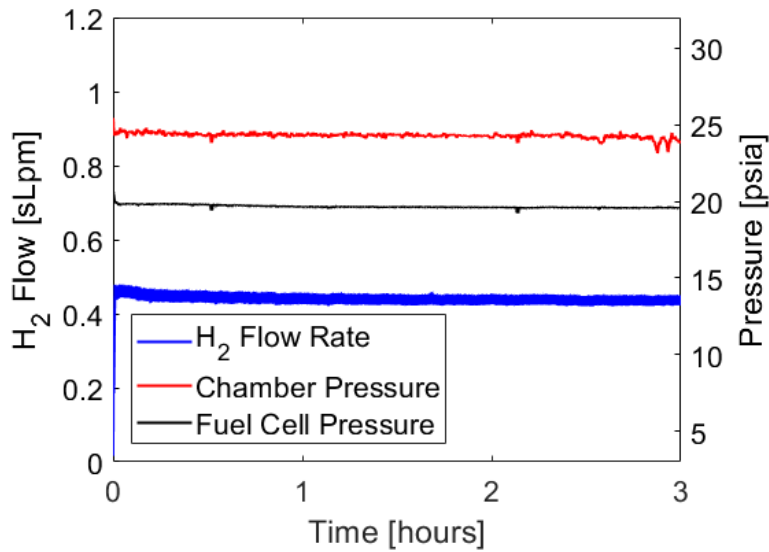


Figure 6.26. Hydrogen flow rate and pressure during Test SBH-12.

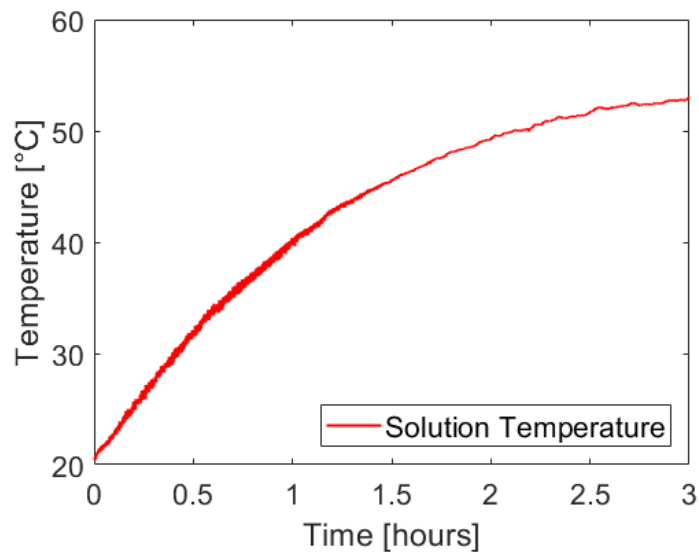


Figure 6.27. Solution temperature inside reactor during Test SBH-12.

For the first three hours of operation using seawater, the ABCharger 2.0 performance closely matches that which was observed during previous tests using deionized water. The PEMFC produced nearly 29 W of power for three hours and the pressure traces and hydrogen flow rate shown in Figure 6.26 are steady throughout the test. The only deviation from previous tests is the slower rate of temperature rise shown in Figure 6.27, which is expected due to the increase in

thermal mass from the additional acid solution. However, after three hours the chamber pressure began to drop and the test had to be aborted to protect the fuel cell. With the fuel cell disconnected and the system vented downstream of the flow meter but upstream of the pressure regulator, the pump was able to transfer enough solution to produce more than 3 sLpm of hydrogen. This is six times the amount that was being consumed by the fuel cell early in the test, implying that the drop in chamber pressure was not a reaction kinetics issue but rather a challenge with transferring SBH solution while the chamber was at pressure. Further investigation revealed that the tubing in the peristaltic pump head was worn and the pump was no longer providing enough head pressure to pump against the operating chamber pressure. The tubing in the pump head was replaced with a spare length of flex tubing that was removed from a portable version of this system that will be discussed later in this report.

Following the replacement of the tubing in the peristaltic pump, Test SBH-13 was conducted with the objective of producing enough power to match the BB-2590 battery's 225 Wh capacity. The system was loaded with 100 g of SBH in 220 mL of 1M NaOH solution and 0.6 equivalents of tartaric acid (285 g) in 600 mL of water. The test was conducted in the largest acrylic reaction vessel. Because of its limited capacity, the 9 V battery previously used to drive the peristaltic pump during shorter tests was replaced with a benchtop power supply providing a constant 10 V potential. In the envisioned final system, the SPM would allow for a portion of the PEMFC output to be supplied to the pump once the stack reaches nominal operating conditions, essentially taking on the role of the benchtop power supply used for this test.

There were periods throughout the duration of Test SBH-13 when the peristaltic pump would struggle to transfer enough SBH solution to keep up with hydrogen demand. It became apparent that there were two factors leading to this issue. The first was that trapped gas pockets were collecting near tube fittings or other restrictions in the line between the SBH storage vessel and the reaction chamber. It is unclear if the gas in the tube was due to the line not being properly primed before the test or if the SBH solution was reacting in the tube. The SBH solutions appeared to be very stable during previous tests and it is unclear why they would off gas during this test and not others. The collective volume of the gas pockets appeared to be on the order 1-2 mL and did not seem to increase after first observation. These pockets would compress during pumping cycles and expand when the pump would shut off, introducing a dampening effect to the system and

requiring the pump to operate for longer periods during each cycle. At times, the pump could not keep up with demand unless the larger bubbles were broken up by manually squeezing the line.

Approximately four hours into the test, the electronic load was disconnected and a check valve was placed in the line between the dip tube assembly (which also has a check valve) and the peristaltic pump. Trapping the gas pockets between the two check valves kept the bubbles under pressure even when the pump was not operating and seemed to improve solution transfer. The test was reinitiated with the second check valve and no additional gas pockets were observed in the line for the remainder of the test. This pause in testing can be seen in the hydrogen pressure and solution temperatures plots, Figure 6.29 and Figure 6.30, respectively. The effect is not observed in Figure 6.28 as the electronic load was shut off during this time and was therefore not recording data.

The second obstacle to maintaining hydrogen pressure seemed to be the same issue as was described following Test SBH-12. The tubing in the pump was worn and did not fit snugly in the pump head. Because the tubing was relaxed it was able to travel vertically along the pump's rollers during the test. If the alignment deviated too far from nominal, the pump's max flow rate was greatly reduced and resulted in the system's inability to maintain hydrogen pressure. The tube was closely monitored during the final four hours of testing and adjusted as necessary to maintain proper alignment. In general, the pressure was far more consistent over the latter half of the test than during the first four hours. A new pump head was purchased to prevent future tests from having issues with SBH solution transfer. The results of this test can be seen below.

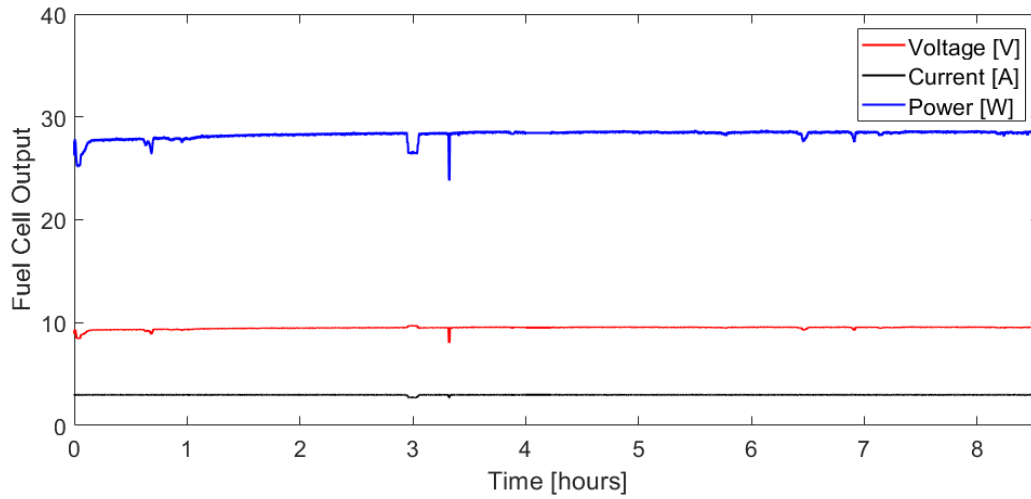


Figure 6.28. PEMFC output during Test SBH-13.

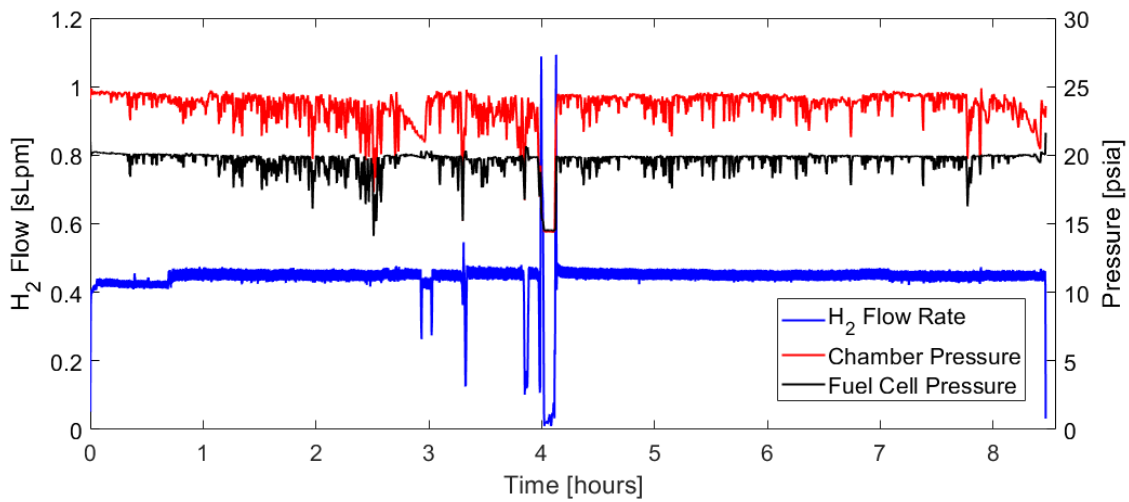


Figure 6.29. Hydrogen flow rate and pressure during Test SBH-13.

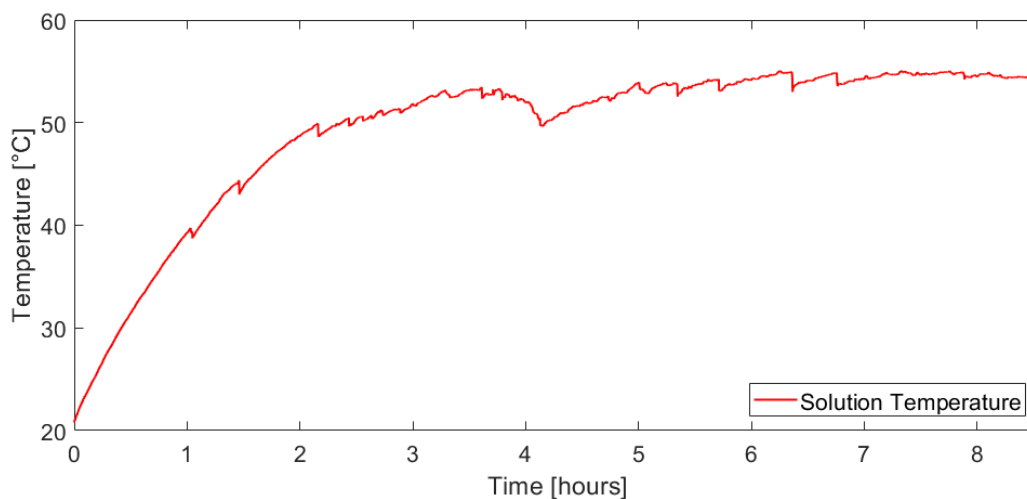


Figure 6.30. Solution temperature inside reactor during Test SBH-13.

Despite challenges with the peristaltic pump, the PEMFC output was relatively consistent throughout Test SBH-13. There are approximately five momentary power interruptions that align with drops in hydrogen pressure. However, these are brief and are expected to be avoided using the new peristaltic pump. There was also a short period approximately three hours into the test when the current draw was decreased to investigate whether that allowed the pump to keep up with hydrogen demand. However, the current demand was changed back to 3 A once the issues with the pump head were identified. The average power output actually increased during the test as the fuel cell stack warmed up and reached its steady state operating temperature. The PEMFC produced an average of 28.2 W for 8.6 hours for a total of 241.1 Wh of power. This is equivalent to the capacity of 1.1 BB-2590 batteries.

The temperature of the solution in the reaction vessel approached a steady state value just below 55°C. The sudden decreases in temperature seen periodically in Figure 6.30 are due to the reactor being shaken to mix the reactants and byproducts, and the drop at four hours is due to the test being paused to install a check valve, as discussed above. The ambient temperature in the test cell was $22^{\circ}\text{C} \pm 2^{\circ}\text{C}$ throughout the test, meaning the solution was never more than 35°C warmer than its surroundings. The temperature on the outside of the reactor was even lower, and while not directly measured, the reactor could be held by a bare hand without becoming uncomfortable.

It is extremely unlikely that an operator would ever be exposed to the liquid insides the reactor. However, if liquid to skin contact does occur, liquids at 52-56°C require 15-60 seconds of

exposure to cause significant burns [76]. This is a reasonable amount of time for a user to address the contact and prevent serious injury from occurring. Because the max operating temperature does not pose substantial risk to the user or the system, the system appears to have no need for additional thermal management. If the final system were to be used in an extremely hot environment, a thermal management strategy might become necessary. Depending on the final form factor of a fielded system, the most efficient strategy would likely be throttling of the max power output from the PEMFC. This would limit the hydrogen consumption and generation rate, in turn limiting the amount of heat being produced by hydrolysis. While this strategy would increase the time required to recharge a battery, it would not negatively impact the system's energy density or increase system complexity.

Operating at constant power output for extended periods is valuable to demonstrate system capacity, but real-world use cases often include varying loads and abrupt changes in power demand. A successful system must be able to alter its hydrogen generation rate to match these variable loads. Of particular importance is the ability to adapt to a sudden no-load situation without over-pressurization.

To demonstrate these abilities, the 8600 Series electronic load was programmed to shift abruptly across a range of loads between 0 A and 3 A. It should be noted that a small amount of hydrogen is still consumed at the 0 A load condition as the fuel cell operates at its open cell voltage and continues water management. In order to preserve the impact of abrupt changes in load, the data sets for the plots below have been smoothed over 5 second intervals, not the 30 second intervals used in previous tests. This test was prepared using 4.9 g of SBH and 0.5 g of NaOH in 30 mL of deionized water and 11.8 g of tartaric acid (0.6 equivalents to SBH) in 125 mL of deionized water. It should be noted that this test was conducted prior to Test SBH-12 and Test SBH-13, and that the issues with SBH solution transfer observed during those tests were not present during this demonstration.

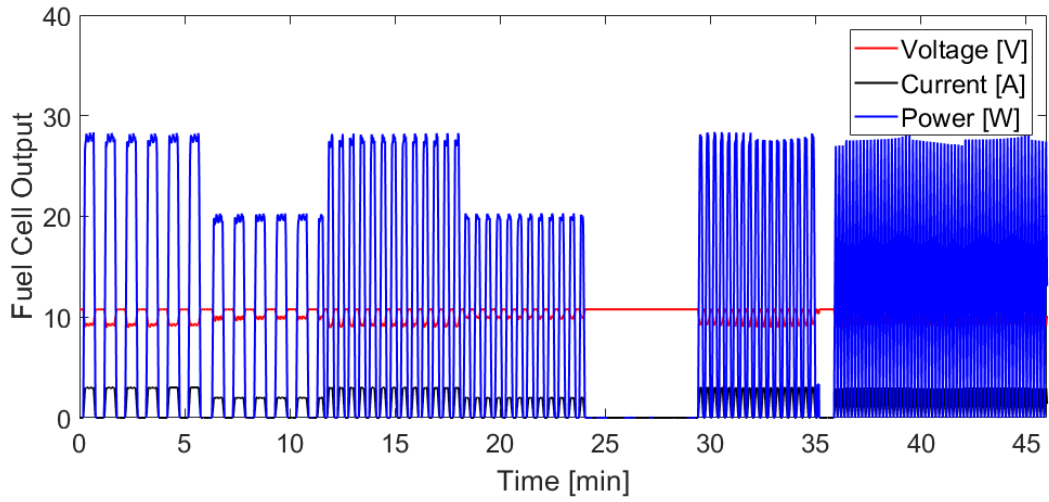


Figure 6.31. PEMFC output during Test SBH-14.

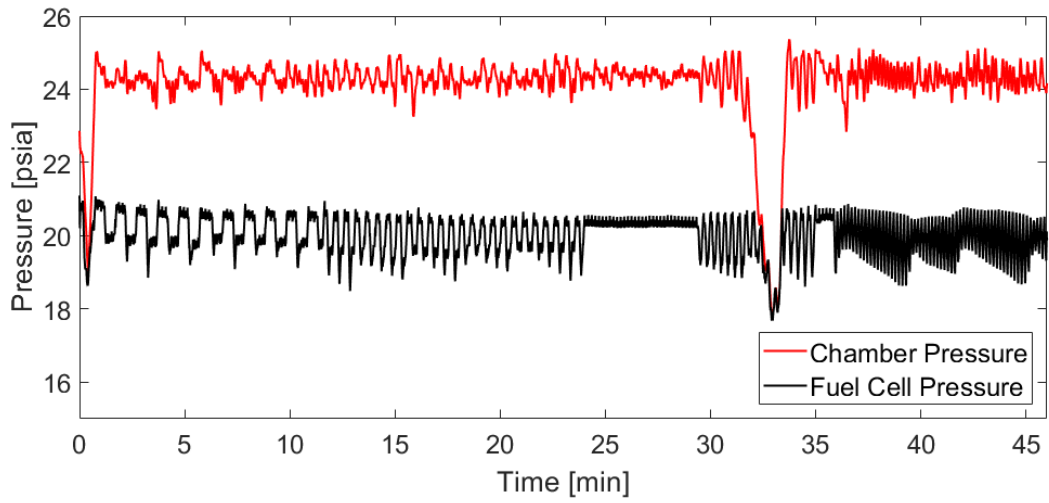


Figure 6.32. Hydrogen pressure during Test SBH-14.

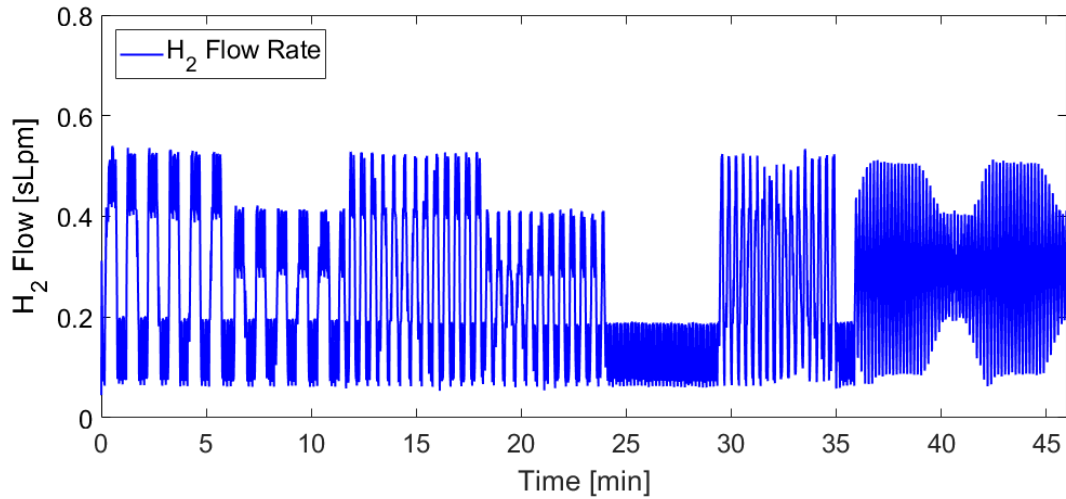


Figure 6.33. Hydrogen flow rate during Test SBH-14.

The hydrogen generation system responded well to abrupt load changes, providing the PEMFC with adequate hydrogen supply for each load that was applied. Hydrogen consumption rates varied between approximately 0.1 sLpm at no load to more than 0.55 sLpm to satisfy a 3 A load. The pressure in the system was maintained between 23 and 25 psia for the majority of the test, including throughout the entirety of the five-minute no load period. At approximately 30 minutes, the dip tube that connects the peristaltic pump to the SBH solution vessel became dislodged, preventing additional SBH from being added to the reaction vessel for just over one minute. The tube was reconnected and the pressure in the system quickly recovered. It is important to note that, despite this interruption in SBH supply, the PEMFC was not impacted and it was able to provide the target loads throughout the test.

7. BATTERY CHARGING DEMONSTRATIONS

The process for purchasing a Squad Power Manager (SPM) was initiated following the partial BB-2590 battery recharge described in Section 5.2. Procurement of the SPM took several months, during which time the testing reported in Chapter 6 was conducted using simulated loads. Once the SPM was received, testing priorities shifted to more tangible demonstrations of system capabilities. The purpose of these demonstrations was to highlight the utility of the system with respect to everyday scenarios and to observe the user-interface when operating the system outside of laboratory conditions. The SPM was used to condition the PEMFC output, typically in the range of 7-10 V and 3-4 A, and provide the voltages and currents required to recharge cell phones and BB-2590 batteries.

7.1 Cell Phone Battery Charging

The first battery charging demonstration used the ABCharger 2.0, Horizon H-30 PEMFC, and SPM to recharge a cell phone battery. The cell phone used for this test was an iPhone 6s with a nominal battery capacity of 6.9 Wh. The test was conducted using the hydrogen generation test stand to monitor and record hydrogen pressure and flow rate while charging the phone. The PEMFC was connected to the SPM using the capacitor and diode circuit shown in Figure 5.1 to provide constant power during the fuel cell's water management events, and the SPM was connected to the cell phone using a USB adapter. The phone has a built in charging controller that varies the phone's power consumption in order to satisfy the charge profile of its Li-ion battery. A flow diagram depicting the interface of the various hardware components is presented in Figure 7.1 and an image of the test stand with key elements labeled is shown in Figure 7.2.

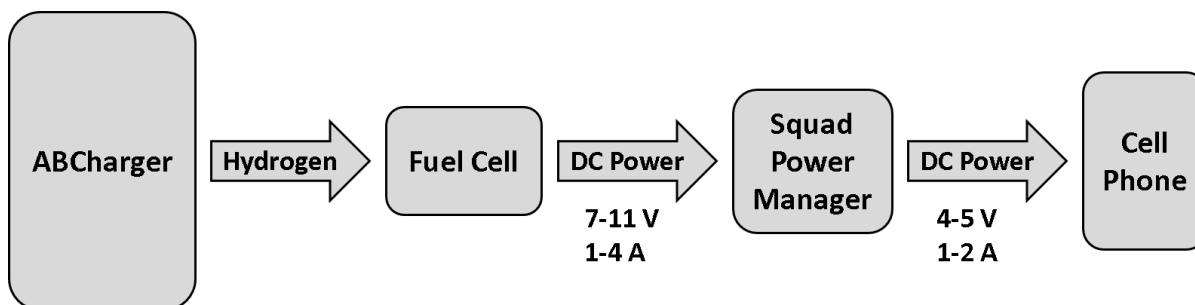


Figure 7.1. Flow diagram of the interface of key components during cell phone charging.

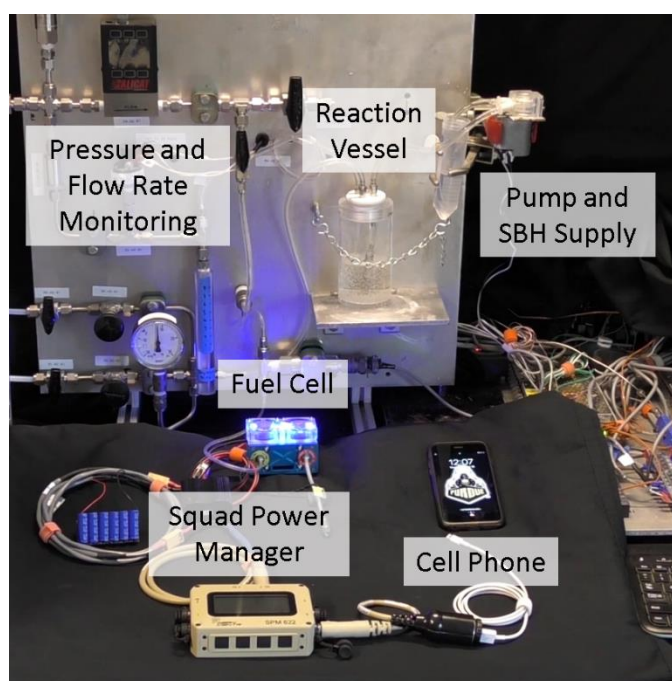


Figure 7.2. System used for charging cell phones with the ABCharger 2.0 on the hydrogen generation test stand.

For the first cell phone recharge demonstration, Test SBH-15, the ABCharger was loaded with 7.5 g of SBH and 17.9 g (0.6 molar equivalents) of tartaric acid. The SBH and acid solutions were prepared with 20 and 100 mL of deionized water, respectively. Assuming a 40% fuel cell efficiency, only 2 g of SBH is required to recharge the cell phone. However, during the approximately two-hour recharge, a relatively large amount of hydrogen is lost as the H-30 purges water from the stack by venting hydrogen. A 0.005 inch orifice was placed downstream of the purge valve to minimize losses. This orifice is smaller than those used for previous tests but still

allows for adequate water removal because charging the cell phone required less power (which produces less water) than was generated in previous tests.

As with previous tests, the system was purged with bottled hydrogen and the stack allowed to reach steady state before isolating the system from the bottled hydrogen supply. The cell phone, which had been discharged to 2% capacity, was then connected to the SPM to initiate the test. After 1 hour and 49 minutes the cell phone was charged to 100% capacity. Approximately 75% of the SBH solution was consumed during this time. Because less than 30% of the solution was required to charge the battery, it appears that nearly half of the 7.5 g of SBH was used to generate hydrogen that was lost to the water management events.

This demonstration was conducted following Test-12 and SBH-13 but prior to receiving the new peristaltic pump. The challenges with SBH transfer were lessened for this test because the cell phone has a minimal power demand compared to the simulated loads used for previous tests, but the tubing still required periodic readjustment to maintain chamber pressure. The chamber pressure never dropped below the pressure regulator set point, meaning the fuel cell supply pressure remained steady while charging the phone. Figure 7.3 shows small fluctuations in chamber pressure whenever the pump was readjusted, but throughout the test the smoothed chamber pressure never deviated by more than 2 psi from the pressure switch set point of 24 psia.

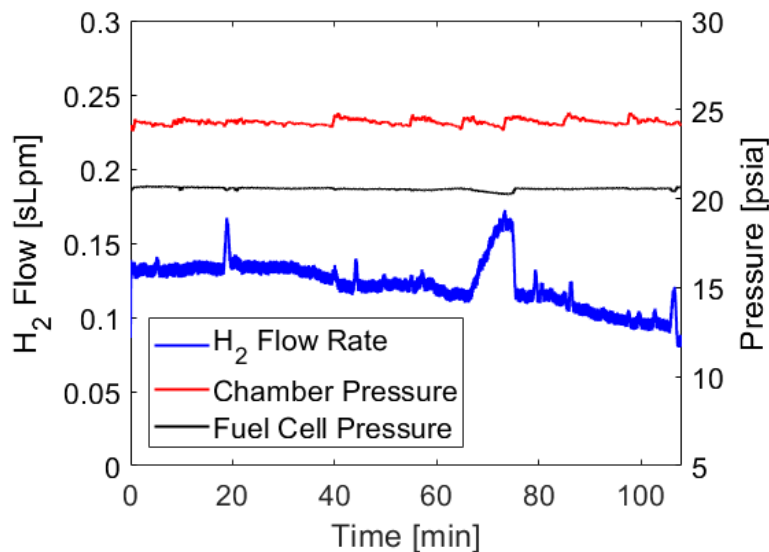


Figure 7.3. Hydrogen flow rate and pressure during Test SBH-15.

The hydrogen flow rate shown above is indicative of the charge profile for Li-ion batteries, which consists primarily of an initial constant current charge followed by a constant voltage charge with diminishing current demand. The reasonably steady hydrogen flow rate over the first 60 minutes of the test is consistent with what is expected to be relatively constant power consumption during the constant current charge. The cause of the brief spikes in flow rate, like that seen at 20 minutes, is unclear, but it appears the SPM or cell phone briefly increased power consumption. The increase in hydrogen consumption after 60 minutes is attributed to the ramp in cell voltage that occurs just prior to the end of the constant current charge. Before transitioning from constant current to constant voltage charging, the voltage is ramped from approximately 4 to 4.2 V [77]. For the remainder of the charge, the voltage is held constant while the current is decreased until the phone is completely charged. The diminishing power consumption during this period of charging agrees with the decrease in hydrogen flow rate seen in Figure 7.3.

7.2 BB-2590 Battery Recharging

The final demonstration conducted with the ABCharger 2.0 system was a recharge of a BB-2590 battery. The physical setup for this test was the same as is shown in Figure 7.2 for the cell phone charging demonstration, with the cell phone being replaced by a BB-2590 battery. The reaction vessel was loaded with 238 g of tartaric acid in 550 ml of deionized water. The SBH solution was prepared using 100 g of SBH, 10 g of NaOH, and 220 mL of deionized water. This test used a new peristaltic pump purchased from Williamson Pumps (part number 100.070.012.008/2). This new pump head had two rollers, was loaded with 0.8 mm silicone tubing, and was driven by a 12 V DC motor. The test lasted for nine hours and resulted in a 72% increase in BB-2590 battery charge level. The results of Test SBH-16 can be seen below.

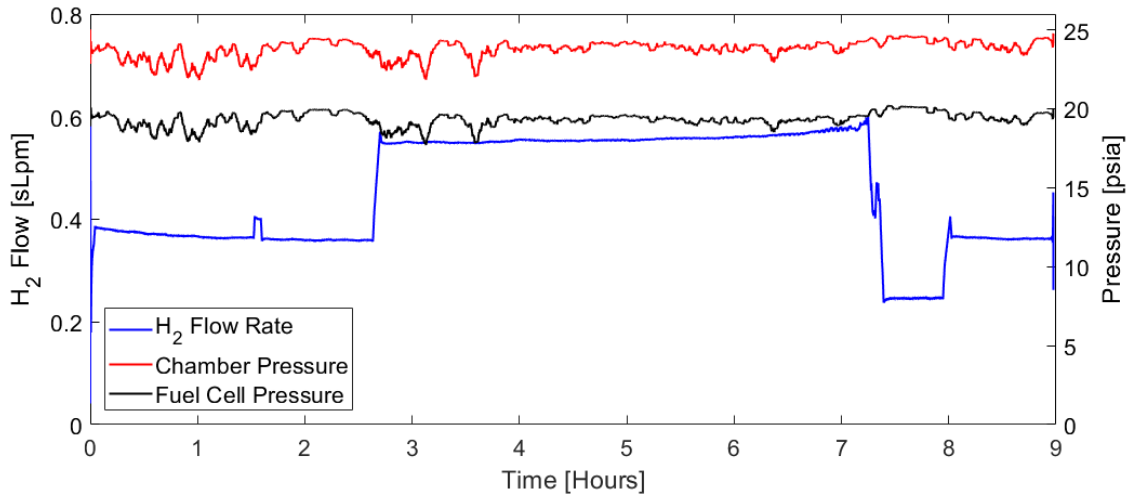


Figure 7.4. Hydrogen flow rate and pressure during Test SBH-16.

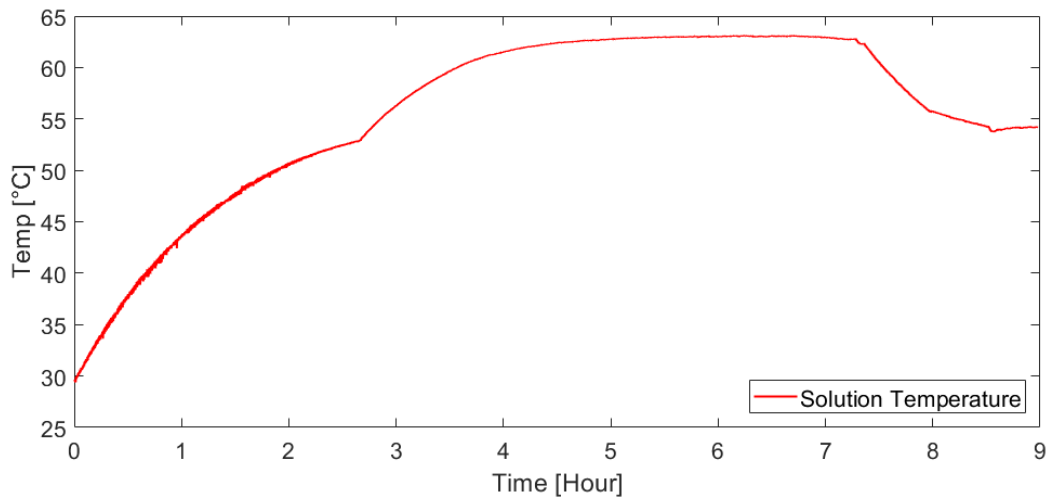


Figure 7.5. Solution temperature inside reactor during Test SBH-16

The maximum amount of power that could be delivered to the BB-2590 battery was limited to 10, 20, or 30 W by changing the max power output that the SPM would demand from the fuel cell. This was done to show that even when all of the subsystems were integrated together, the ABCharger 2.0 was capable of modifying its hydrogen generation rate to match fuel cell consumption without over-pressurization. The chamber pressure held steady at 23 psia \pm 2 psi at all power outputs. At 10 W the average hydrogen flow rate was 0.25 sLpm, compared to 0.36 and 0.55 sLpm at 20 and 30 W, respectively.

The temperature inside of the reactor appeared to approach different steady state temperatures for each of the various power outputs. This is to be expected as the fuel cell's hydrogen consumption varies at each rate of power production, and the amount of heat generation in the system is proportional to the rate of hydrogen generation. At the max power output of 30 W the temperature plateaued at 63°C. The temperature in the test cell was held reasonably constant at 30°C throughout the test.

The ABCharger 2.0 system responded well to the load demand of charging a BB-2590. The test was limited to nine hours primarily due to restrictions on testing outside of normal business hours, which limited the recharge to 72% of the BB-590's capacity. However, there was no indication from any of the collected data that implies the system could not have operated for several more hours and reached a 100% charge if more time was available. Not all of the SBH solution that was prepared was consumed during this test, but it is possible that additional reactants would have been required if the test was extended until the battery was completely recharged.

8. WASTE MANAGEMENT

The utility of the ABCharger system is derived by providing a higher energy density than currently fielded technologies. As has been described above, the features which allow for improved energy density are: 1) reusability of system hardware (i.e. reactor, pump, fuel cell, etc.), and 2) the ability to use water gathered at the point of use. As has been demonstrated in Chapters 5 and 6, the proposed hydrogen generation system is inherently reusable. The medium sized acrylic reactor has been used nearly 20 times without incurring any testing related damage, and the peristaltic pump, which was used before starting this project, facilitated even more tests than that before requiring maintenance. As such, the challenge with system reusability is not related to hardware robustness, but instead lies in the determination of how to safely dispose of spent reactants after operation.

In order for the system to be reused, the solution of water and reaction byproducts left in the reactor following use must be removed. Storing the solution and transporting it back to a central location for processing negates the energy density improvements achieved by collecting water in the field. Considering only energy density and user-friendliness, the ideal solution would be to release the reactants to the environment at the point of use. Admittedly, this would likely not be a viable option for a technology that is used at a mass scale. It is, however, worth consideration for a system that is used sparingly and only in high-risk situations where the potential benefits of the system are substantial. For the military use case being considered, carrying a lighter load has the potential to make the difference between a successful or unsuccessful mission and merits consideration of disposing the spent reactants in the field of use.

The byproducts of acid promoted SBH hydrolysis have been well documented in reported literature. Multiple authors have found that in addition to hydrogen, the reaction produces one equivalent each of boric acid and the sodium salt of the acid being used [37,40,78]. When using tartaric acid, this would mean formation of sodium tartrate ($C_4H_4Na_2O_6$). Widely used as a food additive, sodium tartrate is considered non-toxic and non-hazardous [79]. Assuming the final system uses 0.6 equivalents of tartaric acid and has nominally the same efficiency as Test SBH-13, a BB-2590 battery recharge would require roughly 84 g of SBH, and would form just over 260 g of sodium tartrate.

Acid-promoted SBH hydrolysis also results in the formation of boric acid ($B(OH)_3$). Boric acid is commonly found in cleaning products and has wide ranging industrial uses. Abbreviated

exposure to boric acid presents little to no danger to humans and it is even used in many cosmetics. There is potential for minimal acute toxicity and dermal irritation with prolonged exposure to high concentrations of boric acid, but the risk of such exposure is minor when disposing of spent reactants. Boric acid is unlikely to bio-accumulate in a body of water due to its high degree of solubility, which means it creates minimal environmental concerns [80]. Assuming once again that the final system uses 0.6 equivalents of tartaric acid and has nominally the same efficiency as Test SBH-13, each recharge of a BB-2590 battery would result in 140 g of boric acid. Under these same conditions, the solution pH is approximately 5.5.

It is proposed that the byproduct solution formed during tartaric acid-promoted SBH hydrolysis be disposed of by discharging it to the environment. This recommendation is made after careful consideration of the use cases for which this system is being designed, the benign nature of the byproducts, and the moderate pH range of the final solution. More sophisticated waste management strategies should be considered if this system is ever widely adopted for commercial applications.

9. SYSTEM ENERGY DENSITY

9.1 Comparison to BB-2590 Batteries

The utility of the system being designed is best evaluated by comparing its energy density to currently fielded technologies. As has been previously described, the BB-2590 rechargeable battery has been selected as a benchmark for comparison as it is widely used by the U.S. military and its specifications are well documented. For comparison to BB-2590 batteries, all of the components that are considered part of the overall ABCharger 2.0 system are included in Table 9.1 below. The water trap added to the system in Section 6.2 was not included in the system mass. This is because its design was motivated by the availability of materials and fabrication capabilities during the economic shut down caused by Covid-19 in the spring of 2020. Far more efficient designs could be implemented for this component as soon as a full complement of prototyping resources are available. It is important to note that the SPM is already used by the U.S. Military. The additional mass of the SPM can be neglected in situations where one is already available, bringing the total hardware mass to less than 1000 g. The target mass for the system, as defined in the design requirements in Table 4.2, was less than 1000 g. If the SPM is considered an existing part of the soldier's load, the system meets this target without further improvements.

Table 9.1. Mass breakdown of ABCharger 2.0 system.

	Component	Mass [g]	Percentage of System Mass
1	Medium-sized acrylic reactor with cap	132	10
2	Peristaltic pump	235	17
3	SBH storage vessel	15	1
4	Pressure regulator	25	2
5	Pressure switch	100	7
6	Tubing and fittings	40	3
7	Fuel cell	370	27
8	Squad Power Manager	453	33
	Total	1370	-

The reactor and SBH storage vessel were designed for single run manufacturing in a prototyping machine shop. As such, design choices including dimensions and materials were made

partially due to the availability and economics of single-unit fabrication. However, if the system were to be fabricated at scale, increased production quantities would permit for more efficient, yet costly, manufacturing techniques and material choices to be considered. For example, the SBH storage vessel and the hydrogen reactor could be replaced by polyurethane bladders, similar to those used in backpack hydration systems. This design, while not economical for prototyping, would result in significant mass savings compared to the acrylic and polycarbonate reactors used during this study. Similar savings could be achieved by purchasing ‘micro’ versions of other system components, such as the peristaltic pump and pressure switch, which are readily available but quite costly and were therefore not procured for the lab prototypes.

Based on the observed efficiency of a new H-30 fuel cell, a full BB-2590 recharge would require 84 g of SBH. Using 0.6 equivalents of tartaric acid and a 10:1 mass ratio of SBH to NaOH to stabilize the fuel solution, each recharge would require 199 g of tartaric acid and 8 g of NaOH. The total reactant mass per recharge would be 291 g. For comparison, a scenario is envisioned in which two BB-2590 batteries, weighing 1.4 kg each, are removed from a soldier’s pack and replaced with the ABCharger system and enough reactants to offset the 2.8 kg of batteries. The 2.8 kg ABCharger 2.0 system would contain 1420 g of reactants and be capable of delivering 4000 kJ of energy, or the equivalent of 4.9 BB-2590 batteries. The 1.4 kJ/g effective energy density of the ABCharger 2.0 system is more than double the 0.6 kJ/g energy density of a BB-2590, allowing for significant mass reduction in a soldier’s pack while maintaining the same level of usable power. It should be also be noted that, on average, the observed efficiency of the Horizon H-30 PEMFC is only 30%. This is considerably lower than the 40-60% efficiency that is often attributed to PEMFCs [81]. Procuring a more efficient fuel cell or identifying and mitigating inefficiencies in the implementation of the H-30 PEMFC being used could theoretically increase the system’s effective energy density by as much as 100%. This would almost certainly require a different method for removing product water, as the H-30 loses a large amount of hydrogen to water purging.

9.2 Comparison to Other Energy Storage Systems

In addition to batteries, it is important to compare the energy density of the proposed system to those of other hydrogen-based portable power systems. Many hydrogen generators have come to market in recent years, typically with underwhelming results. For example, in 2014 Gabl

reported a review of commercially marketed hydrogen-based portable power systems [51]. None of the systems discussed by Gabl had a hydrogen capacity greater than 1.2 wt. %. Of the five systems that were reported, only the Horizon Minipak is still available six years later. The rest are no longer being manufactured or sold, leaving behind a string of negatively skewed customer reviews.

The Horizon Minipak fuel cell charger is considerably smaller than the ABCharger 2.0, weighing 120 g and delivering no more than 2 W of power. The Minipak is fueled by refillable hydrogen canisters, referred to as Hydrostiks, which weigh 90 g and can deliver 50.4 kJ of energy. Considering the Minipak and a single Hydrostik, the energy density of the system is 0.24 kJ/g. If one considers a single Minipak fuel cell and enough Hydrostik cartridges to form a unit that weighs 2.8 kg, the energy density of the Horizon system increases to 0.54 kJ/g. This is comparable to the energy density of a BB-2590, but is less than half of the 1.4 kJ/g energy density of the ABCharger 2.0. The utility of the Minipak system is significantly limited by its max power output of 2 W, which renders it virtually unusable for recharging BB-2590 batteries or similarly sized applications.

As was mentioned previously, perhaps the most sophisticated SBH-based portable power system is that reported by Lapeña-Rey et al. [41]. Their system includes a commercially available hydrogen generator that uses aqueous SBH solutions and metal catalysts. The specific metal catalyst that is used was not reported. The hydrogen generator was paired with a 200 W fuel cell, which is considerably larger than the 30 W output of the Horizon H-30 stack. It is impossible to compare the energy density of their system with the ABCharger 2.0 because the authors do not report the system's energy density or operational mass. Even beyond energy density, it is difficult to compare the ABCharger 2.0 to the system developed by Lapeña-Rey et al. as they are designed for very different applications. The ABCharger 2.0 is meant to be user-friendly and light during transport, but is relatively heavy during operation once water is collected from the point of use. The system by Lapeña-Rey et al. is assumed to be relatively light during operation because it is housed on a drone during flight, but it requires what appears to be substantial pre-operation complexity and extensive system maintenance between uses. Most significantly, the authors reported decreased catalytic activity that required the entirety of the catalyst to be replaced after 8-10 hours of operation. This loss of catalyst performance was observed using pure water. Based on other literature reports, the loss is likely to be accelerated by the presence of common water

contaminants if low-quality water sources were to be used. However, their system was quite successful in powering a drone for a four-hour flight, which is a level of maturity that exceeds that of the ABCharger 2.0.

There are many reports in academic literature of potential hydrogen generation pathways for portable power systems. The technology readiness levels of these pathways vary widely, from theoretical extrapolations of benchtop experiments to more developed systems designed for specific applications. The hydrogen capacity of the most matured systems and the most efficient SBH-based hydrogen generators found in literature are between 2.5-6.5 wt. %, with these values accounting for only the stored reactants and not system hardware [71,82,83]. Considering only SBH, 0.6 equivalents of tartaric acid and a 10:1 mass ratio of SBH to NaOH, the ABCharger 2.0's reactant-only effective hydrogen capacity is 6.1 wt. %. This figure is calculated as the mass ratio of delivered hydrogen to stored reactants. The ABCharger 2.0's hydrogen capacity is slightly below those of the most highly efficient systems found in literature. The systems with higher reported capacities use metal catalysts with high turnover numbers, allowing for a much lower catalyst loading than is required with acid promoters. However, the resiliency of acid promoters towards water contaminants allows for water to be collected at the point of use and not be accounted for in the mass of stored reactants. This offsets the higher catalyst loading and provides the ABCharger 2.0 with a hydrogen content that is comparable to even the most highly-efficient reported systems. Furthermore, this author believes that the advantages provided by using acid promoters (i.e. indifference towards water contaminants, low cost, favorable byproducts, etc.) outweigh the value of the slight additional capacity attainable using metal catalysts.

10. CONCLUSIONS

The first objective of this investigation was to identify a hydrogen generation pathway that is easy to implement, resilient towards common water contaminants, and releases highly pure hydrogen gas. Ammonia borane (AB) was found to be readily hydrolyzed in the presence of an organic acid and a wide range of water sources. When AB solutions are used within several minutes of being formed, the generated hydrogen is highly pure and compatible with proton exchange membrane fuel cells (PEMFC). However, when the AB solution is exposed to air for an extended period of time, it will slowly react and generate ammonia. Sequestration techniques are required to remove ammonia and ensure fuel cell compatibility, which would add complexity and cost to the hydrogen generation system. For this reason, it is not recommended that AB solutions be used for portable fuel cell applications.

Sodium borohydride (SBH) was considered as an alternative to AB for portable hydrogen generation. Rapid hydrogen release and near theoretical hydrogen yields were attained using organic acids to accelerate hydrolysis. Evolved hydrogen was found to be highly pure when using deionized water, seawater, or a urine surrogate. Using puddle water resulted in 25 ppm of ammonia, which was attributed to ammonia dissolved in the puddle water when it was collected. It was determined that organic acid-promoted hydrolysis of SBH satisfies the target conditions for a hydrogen generation pathway and is recommended for portable applications. Based on the testing reported in this dissertation, the hydrogen generation portion of the system would likely be evaluated at a technology readiness level (TRL) 5, which requires breadboard level validation in a relevant environment. In this case, the relevant environment is achieved when hydrolysis is conducted in the ABCharger reaction vessel and evolved hydrogen is used to power a fuel cell.

The second objective of this project was to develop a robust hydrolysis control mechanism that satisfies the needs of expeditionary forces. The first attempt at designing a hydrogen reactor involved a spring-loaded piston intended to provide a constant flow rate of AB solution. Hydrogen generation was initiated by transferring AB solution to a reaction chamber filled with an acidic solution. The basic operating principle was shown to be valid during water calibration, but the system was incapable of providing a consistent and repeatable flow rate using the piston head design. The design failures appeared to be related to the extremely slow piston head velocity that is needed to achieve the target fuel solution flow rate of 1 mL/minute. Additionally, the system

was highly sensitive to particulate in the AB or SBH solution, which is problematic when water is collected from the environment at the point of use.

A second design iteration led to a more robust system that is capable of facilitating a range of hydrogen generation rates. The system controls the rate of hydrogen generation by using a peristaltic pump to move SBH solution into a reaction chamber filled with acid solution. The peristaltic pump is far more resilient towards particulate than the piston head design. The pump is controlled using a low-pressure switch that only allows SBH solution to be transferred when hydrogen pressure drops below a set point. Because of this mechanism, the system is capable of responding to abrupt changes in hydrogen demand without over-pressurization. The system has been used to conduct tests longer than eight hours and can support hydrogen demand of over 0.5 sLpm. It has also been operated using deionized water, puddle water, and seawater. Based on these results, the on-demand hydrogen generation control mechanism is likely to be evaluated at a TRL 5. In this instance, the relevant environment for testing is using the hydrogen generation system and the Horizon H-30 PEMFC stack to recharge batteries, which is the intended use application for the system.

The third objective of this project was to pair the hydrogen generator with a commercially available PEMFC in order to create a power delivery system. The fuel cell used during the testing reported in this dissertation is a Horizon H-30 PEMFC stack. The hydrogen generation scheme is able to support the H-30 in providing constant power output of more than 30 W. Demonstrations with a commercially available power conditioner have included a partial recharge of a BB-2590 battery and a complete recharge of a cell phone. The fuel cell and power conditioner are both TRL 9 as they are commercially available systems that have been proven in many applications. The integration of the hydrogen generator and these two units is likely to be evaluated at a TRL 5 or 6. This level of maturity was demonstrated when the subsystems were integrated and shown to be capable of charging batteries, which is the system's intended purpose.

Recommended future work on this project is primarily focused on updating the system for field use. The hydrogen reactors described in this document were designed for single unit fabrication in a prototyping machine shop and were limited by material and tooling availability. It is recommended that future designs consider polyurethane bladders, such as those found in backpack hydration systems, as replacements for the rigid vessels used thus far. These bladders would be lighter than the polycarbonate and acrylic vessels and are more easily adapted to being

carried during use. If these bladders could be produced at a low enough cost and with a low enough mass, it is possible that they could be considered single-use and be preloaded with tartaric acid and SBH. Using this prepackaged configuration and not requiring the user to remove the byproduct solution from the vessel would further minimize a user's exposure to chemicals during use. The use of bladders has the potential to improve portability and simplify the user-interface, both of which are critical steps towards testing in the intended use-environment and reaching TRL 7 and 8.

The system can currently generate 0.5 sLpm of hydrogen with less than a 35°C rise in temperature. However, additional heat transfer mechanisms would be required if the system was subjected to a larger hydrogen demand. It is also recommended to partner with a fuel cell manufacturer to identify a more optimal fuel cell for this application. While the Horizon H-30's nominal power output of 30 W is adequate for recharging BB-2590 batteries, using hydrogen pressure to purge product water causes the H-30 to waste a significant amount of hydrogen and negatively impacts the overall system efficiency.

Additional future work could include procedures for removing ammonia (and possibly other contaminants) from water that is collected at the point of use. It was found that the puddle water samples collected for this project contained ammonia that eventually reached the hydrogen gas stream. This ammonia could be largely removed from the system by increasing the alkalinity of the puddle water and allowing it to off gas for some time prior to use. A trade study is recommended to consider the water sources most likely to be found in a given use location, the contaminants in those sources, and the complexity required to purify them. Similarly, future work should consider the guidelines set forth by the Resource Conservation and Recovery Act (RCRA) and how they would pertain to the recommendation to discard spent reactants to the environment. While the reaction products have been found to be relatively benign and to pose minimal environmental threat, RCRA approval would be required before this practice could be implemented.

The original concept that motivated this research endeavor was to provide an emergency power source for soldiers who need to make a short radio call to request help under distress. As currently designed, the system is capable of providing far more power than was originally intended and warrants consideration as one of the primary power sources for expeditionary missions. Following completion of the recommended work listed above, the system could similarly be applied to a wide range of civilian applications.

APPENDIX A. FTIR CALIBRATION CURVES

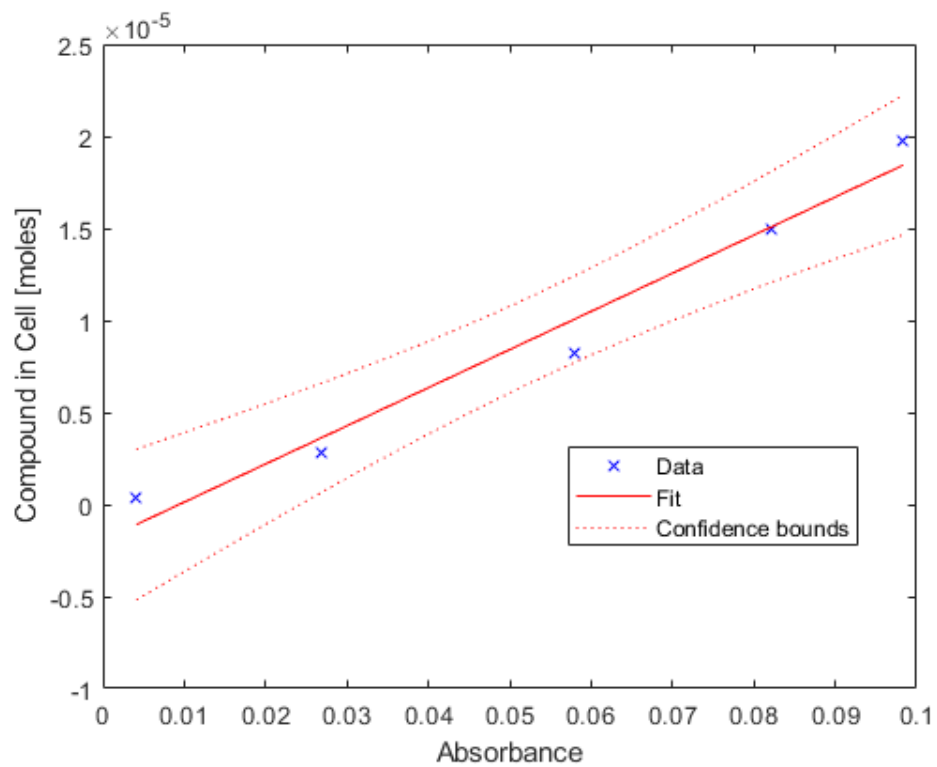


Figure A 1. FTIR calibration curve for carbon monoxide. $y = 2.07e-4x - 1.94e-6$, $R^2 = 0.970$

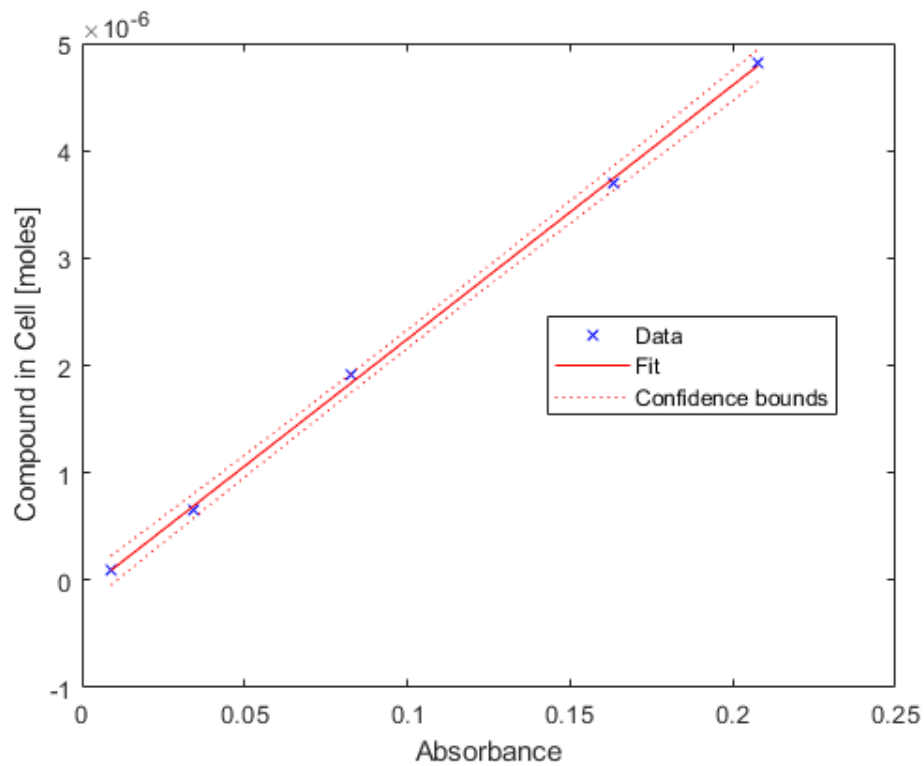


Figure A 2. FTIR calibration curve for ammonia. $y = 2.37e-5x - 1.21e-7$, $R^2 = 0.999$

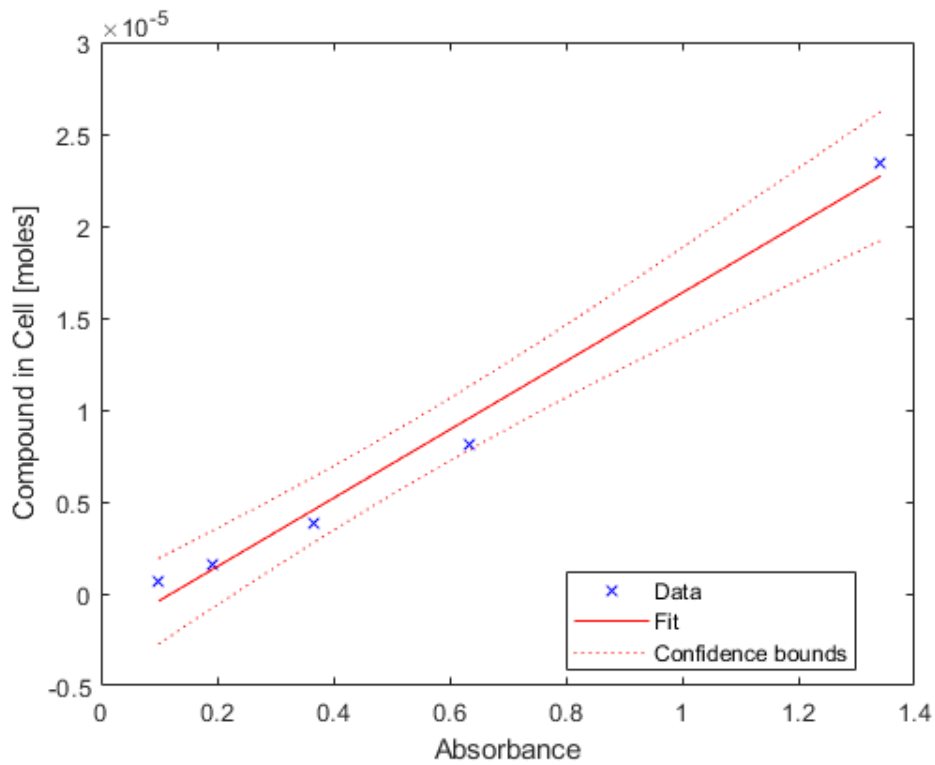
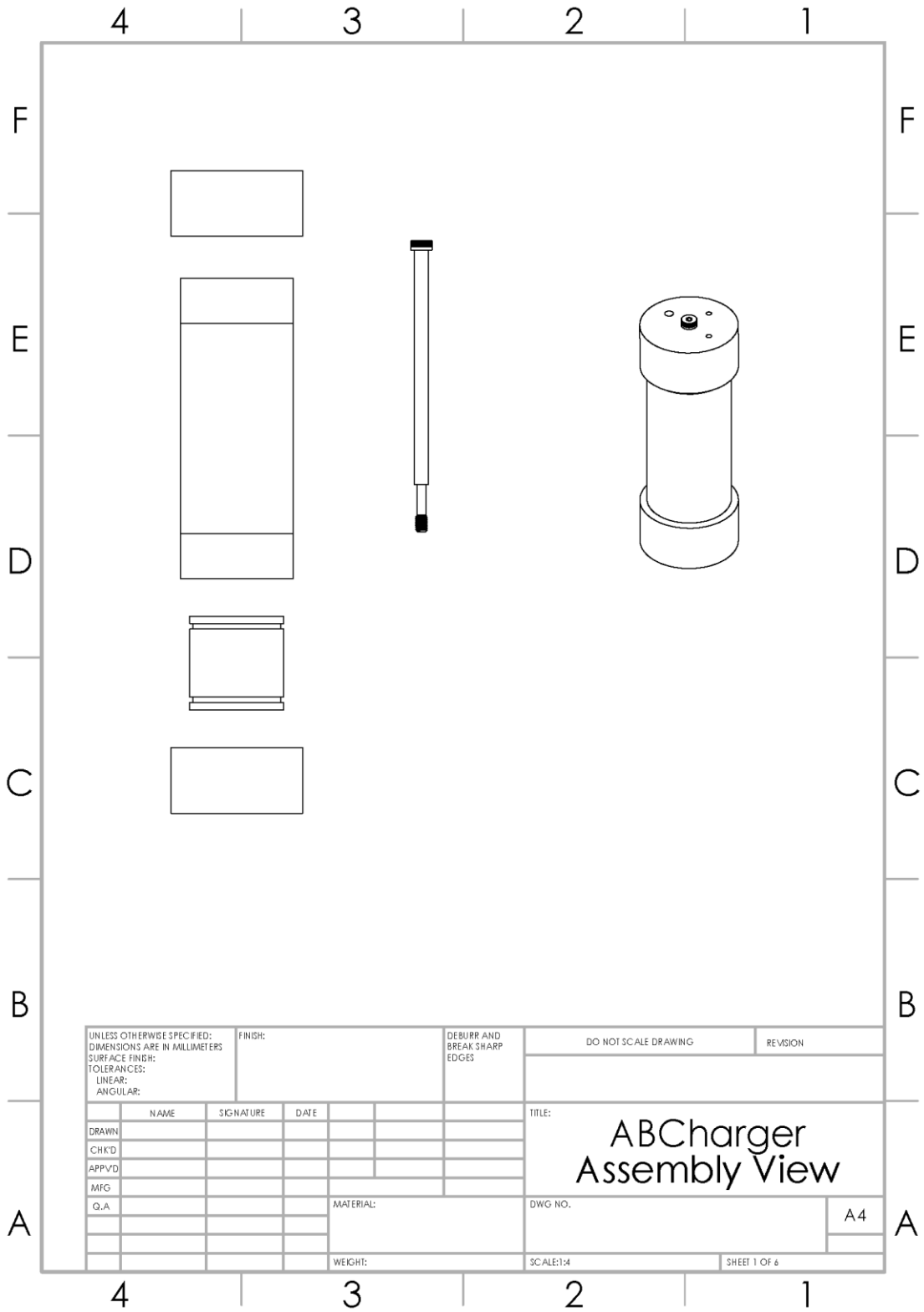
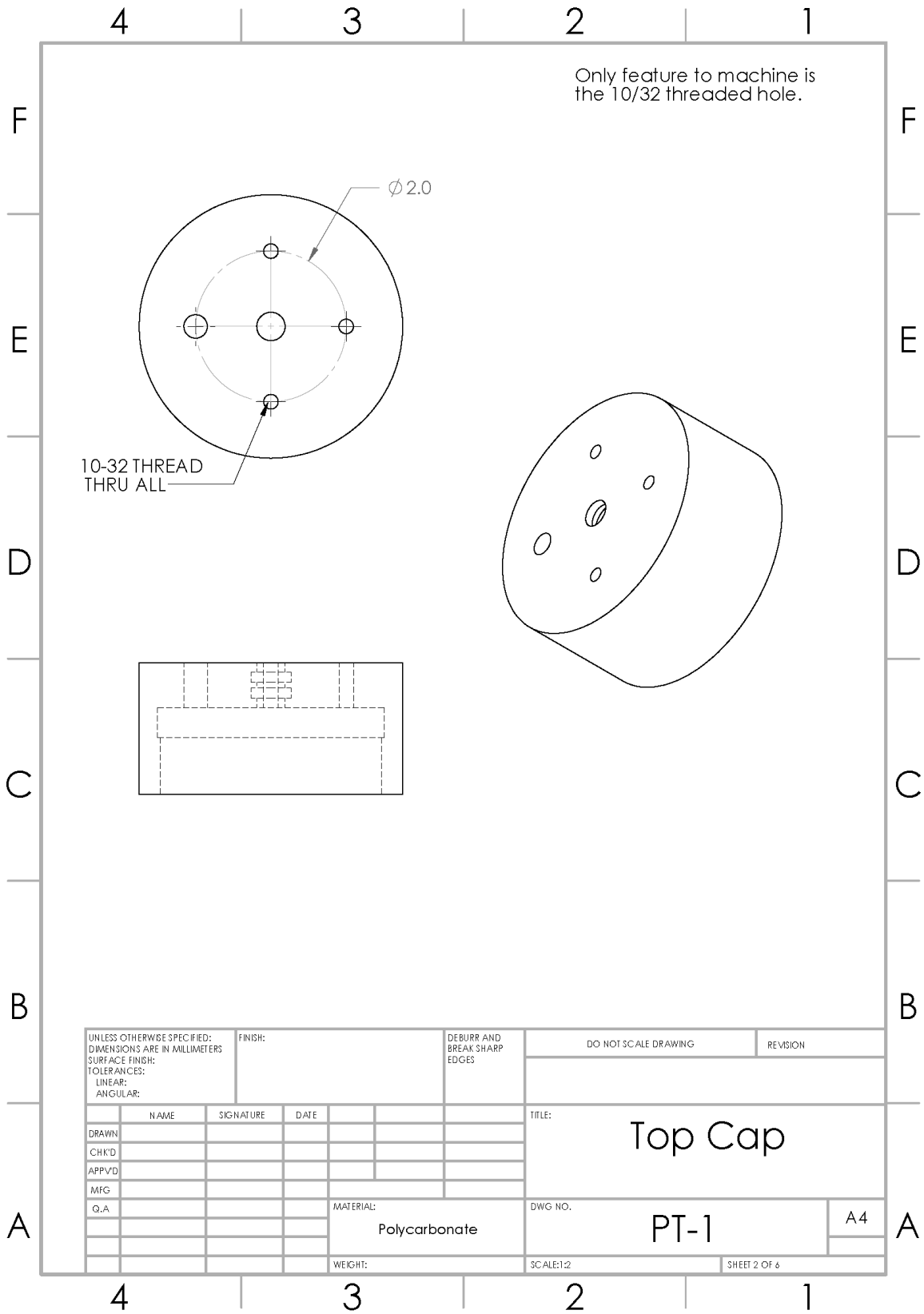


Figure A 3. FTIR calibration curve for carbon dioxide. $y = 1.86e-5x - 2.25e-6$, $R^2 = 0.988$

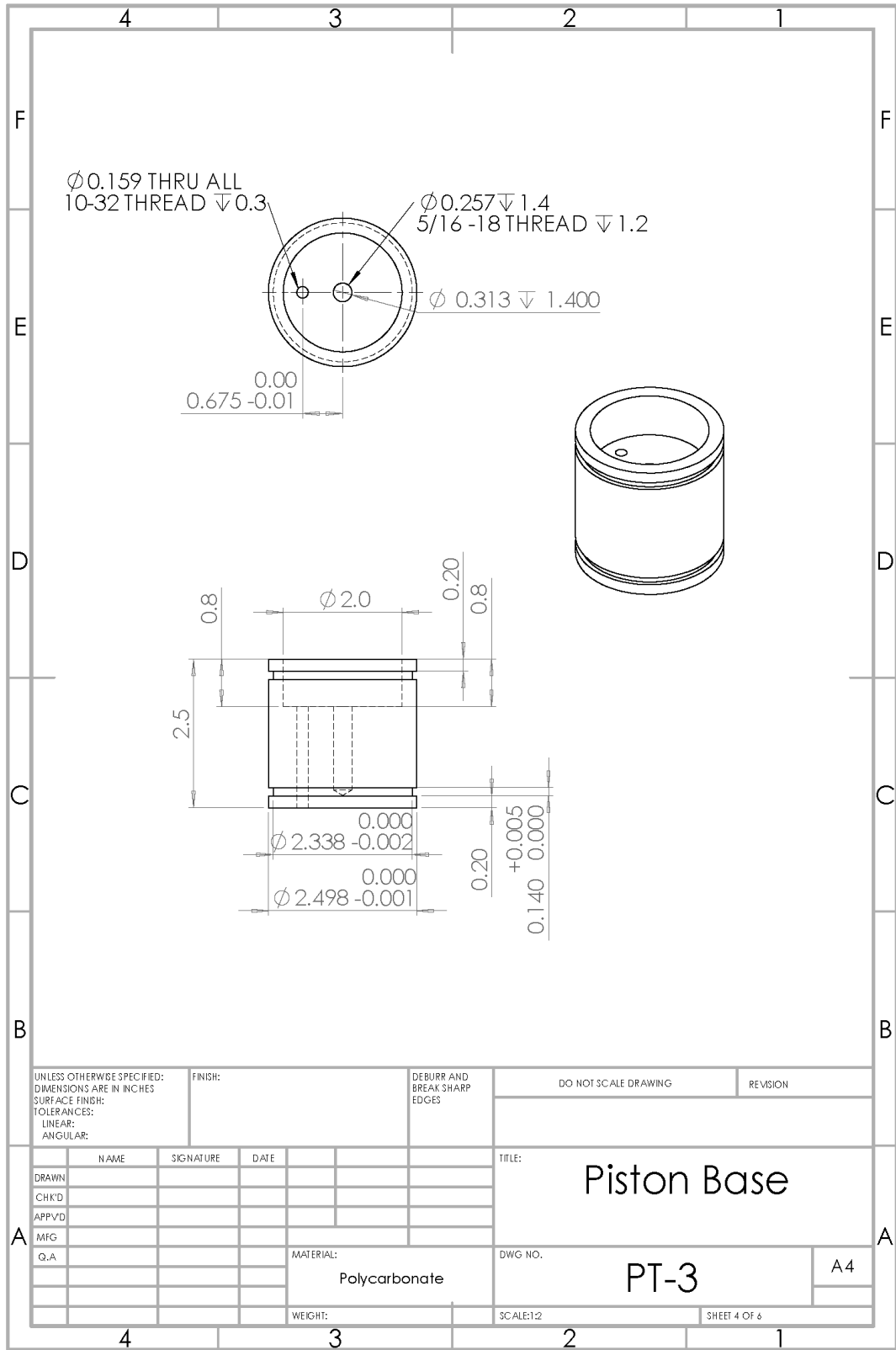
APPENDIX B. ABCHARGER MACHINE DRAWINGS



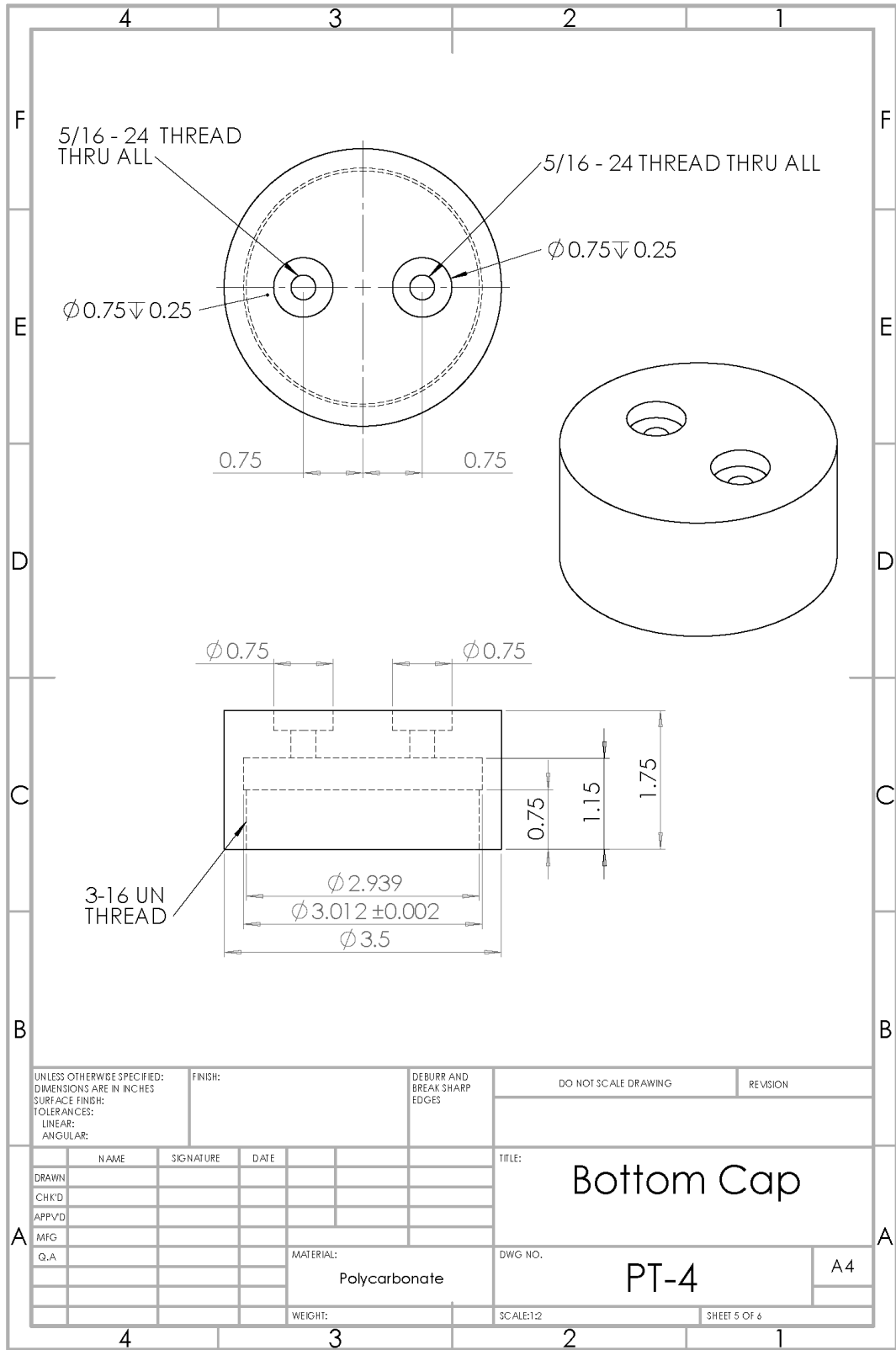
UNLESS OTHERWISE SPECIFIED: DIMENSIONS ARE IN MILLIMETERS		FINISH:		DEBURR AND BREAK SHARP EDGES		DO NOT SCALE DRAWING		REVISION	
TOLERANCES: LINEAR: ANGULAR:									
NAME		SIGNATURE		DATE		TITLE:			
DRAWN		CHK'D				ABCharger Assembly View			
APP'VD		MFG						DWG NO.	
Q.A.				MATERIAL:					
				WEIGHT:		SCALE:1:1		SHEET 1 OF 6	

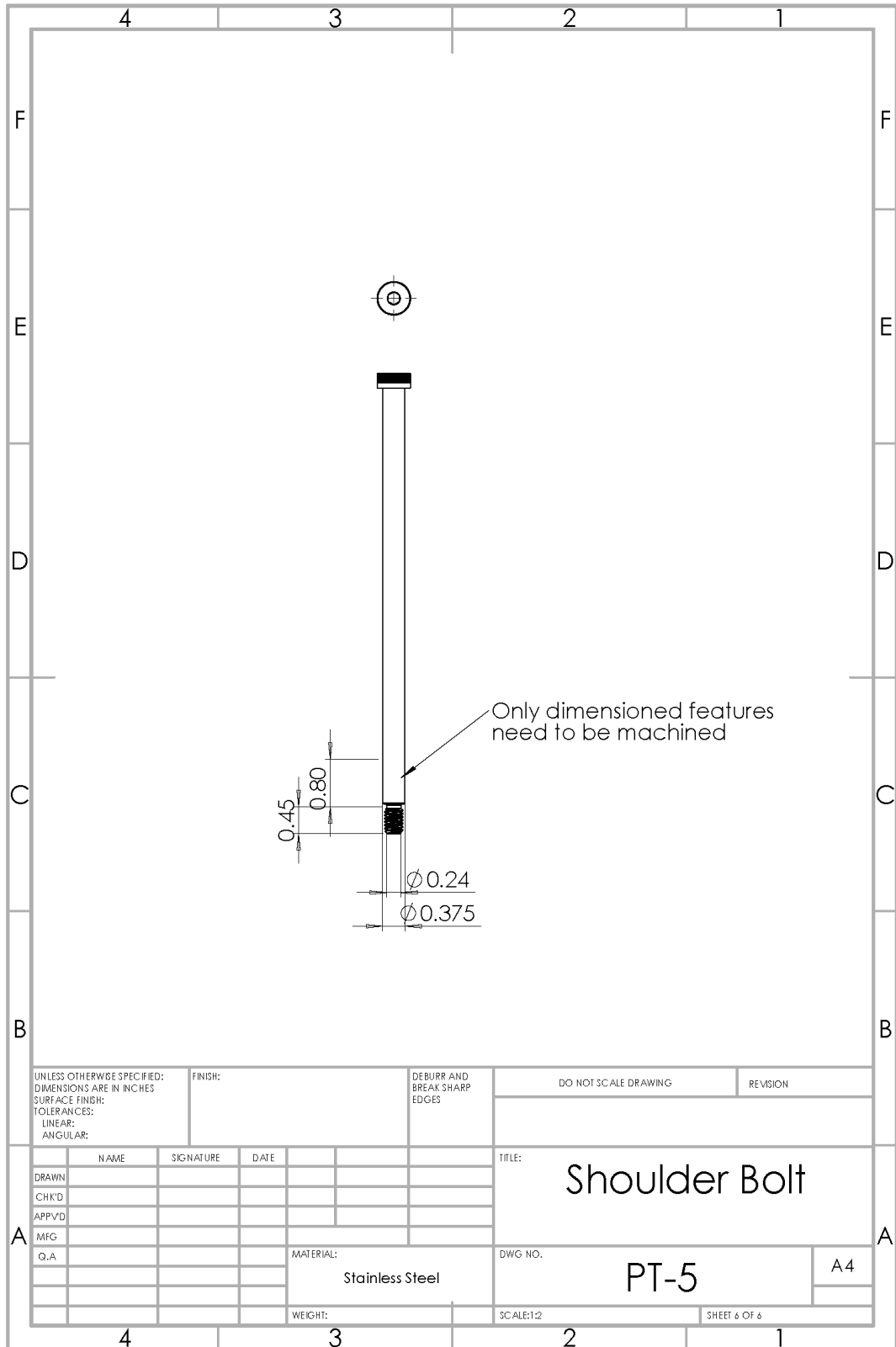


UNLESS OTHERWISE SPECIFIED: DIMENSIONS ARE IN MILLIMETERS SURFACE FINISH: TOLERANCES: LINEAR: ANGULAR:		FINISH:		DEBURR AND BREAK SHARP EDGES		DO NOT SCALE DRAWING		REVISION	
DRAWN		SIGNATURE		DATE		TITLE:		Top Cap	
CHK'D						MATERIAL:		Polycarbonate	
APP'VD						DWG NO.:		PT-1	
MFG						WEIGHT:		SCALE:1:2	
Q.A						SHEET 2 OF 6		A4	

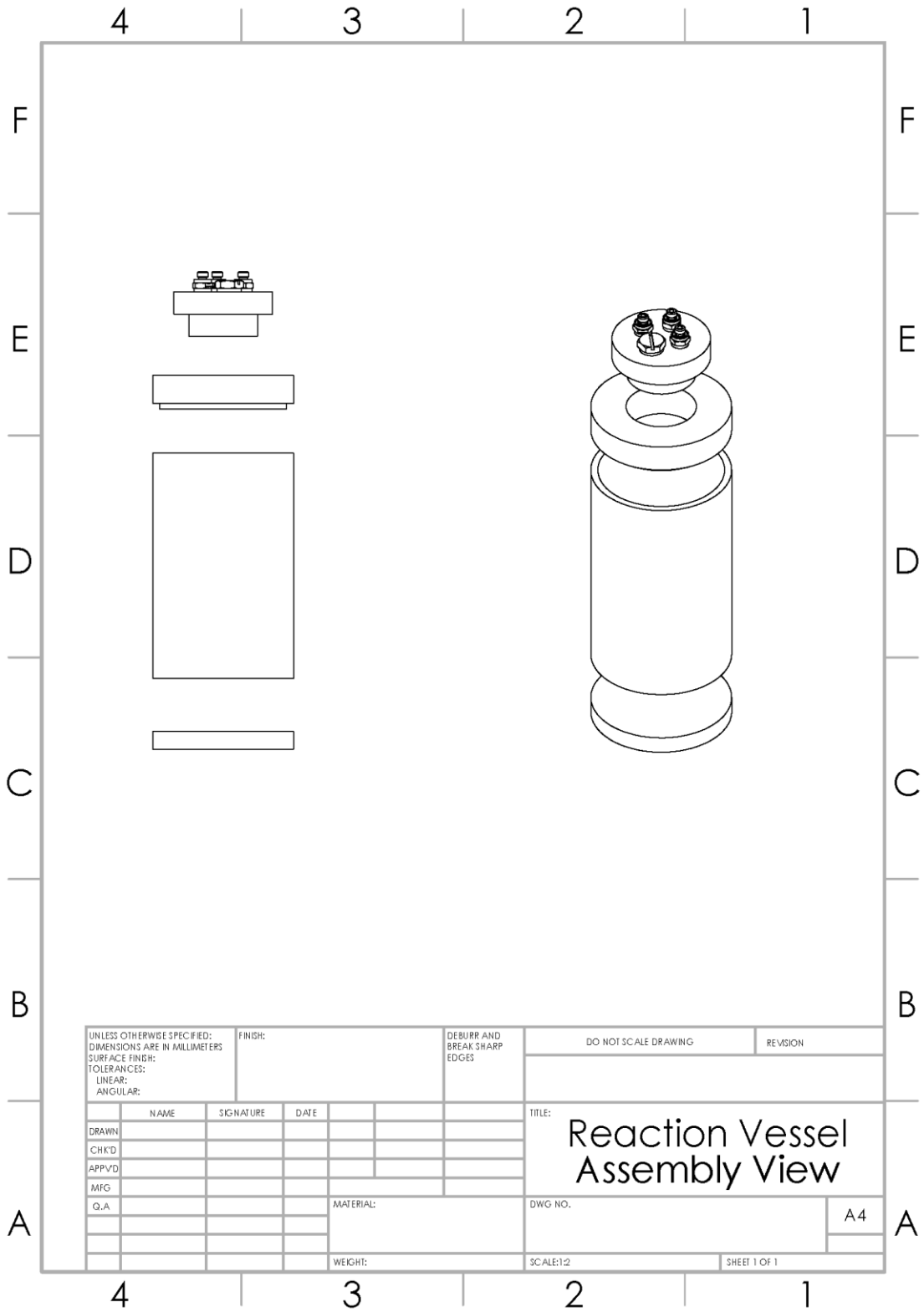


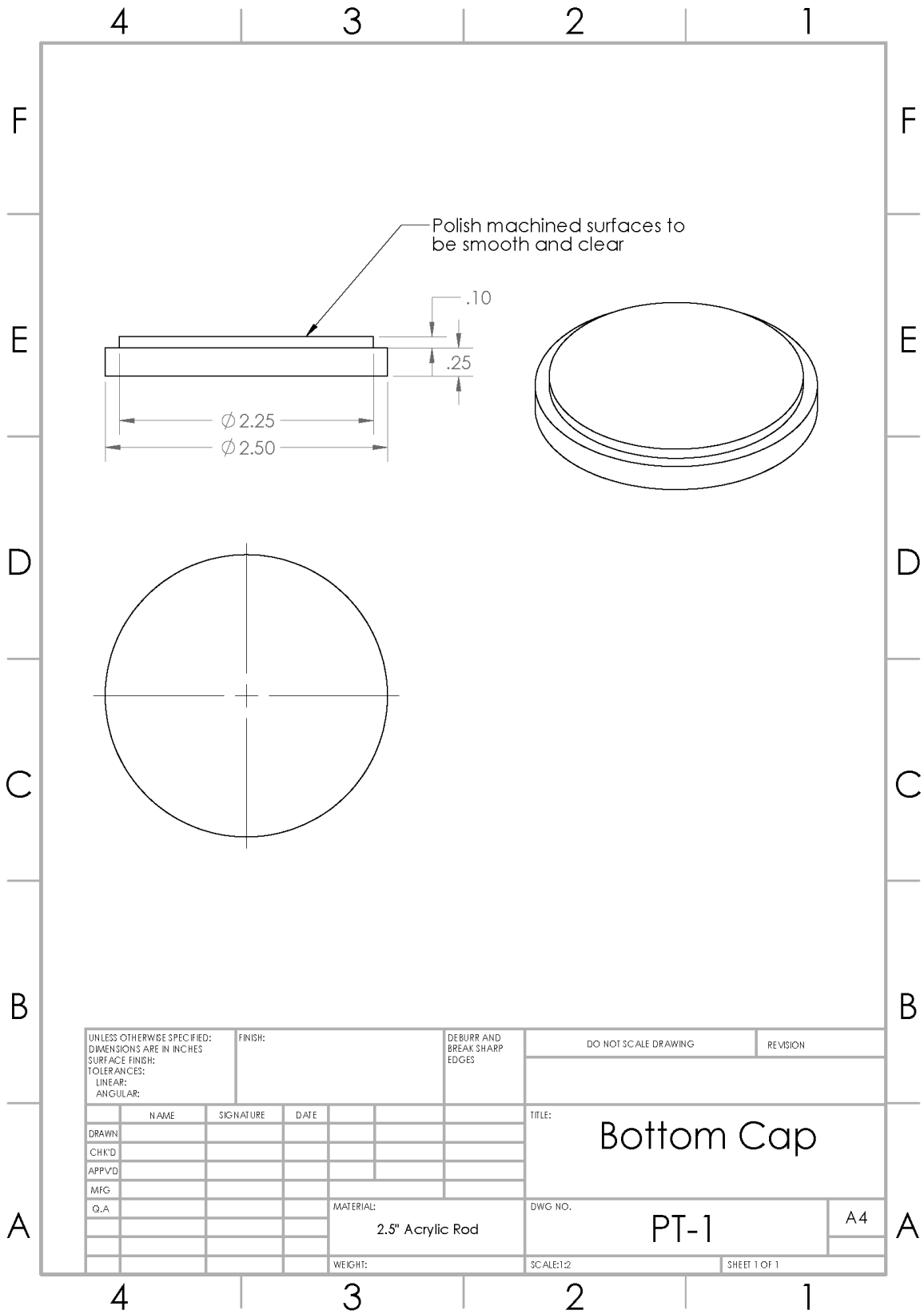
UNLESS OTHERWISE SPECIFIED: DIMENSIONS ARE IN INCHES SURFACE FINISH: TOLERANCES: LINEAR: ANGULAR:		FINISH:	DEBURR AND BREAK SHARP EDGES		DO NOT SCALE DRAWING	REVISION																								
<table border="1"> <thead> <tr> <th>NAME</th> <th>SIGNATURE</th> <th>DATE</th> <th></th> </tr> </thead> <tbody> <tr><td>DRAWN</td><td></td><td></td><td></td></tr> <tr><td>CHK'D</td><td></td><td></td><td></td></tr> <tr><td>APP'VD</td><td></td><td></td><td></td></tr> <tr><td>MFG</td><td></td><td></td><td></td></tr> <tr><td>Q.A</td><td></td><td></td><td></td></tr> </tbody> </table>				NAME	SIGNATURE	DATE		DRAWN				CHK'D				APP'VD				MFG				Q.A				TITLE: Piston Base		
NAME	SIGNATURE	DATE																												
DRAWN																														
CHK'D																														
APP'VD																														
MFG																														
Q.A																														
MATERIAL: Polycarbonate				DWG. NO. PT-3		A4																								
WEIGHT:				SCALE:1:2		SHEET 4 OF 6																								

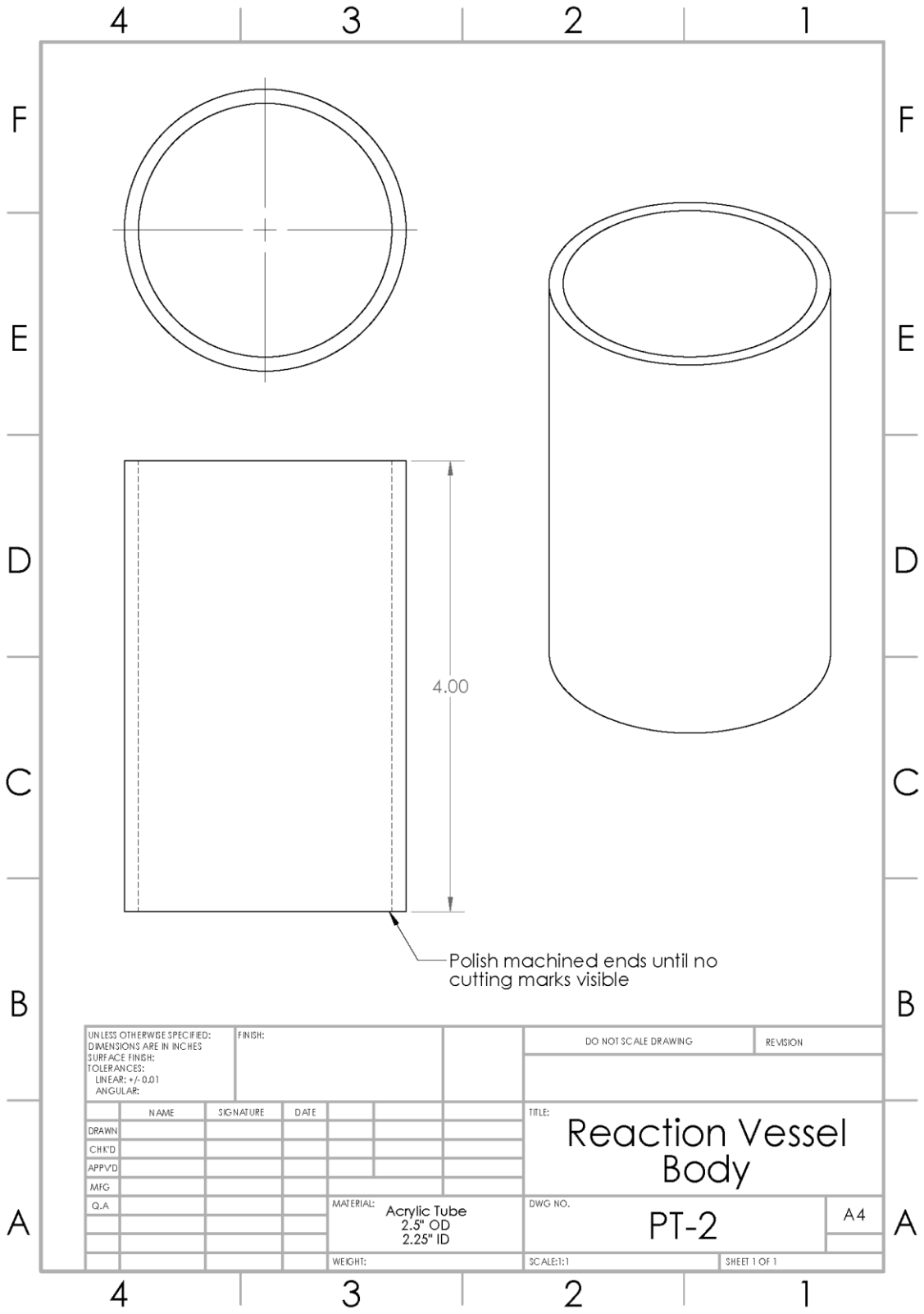


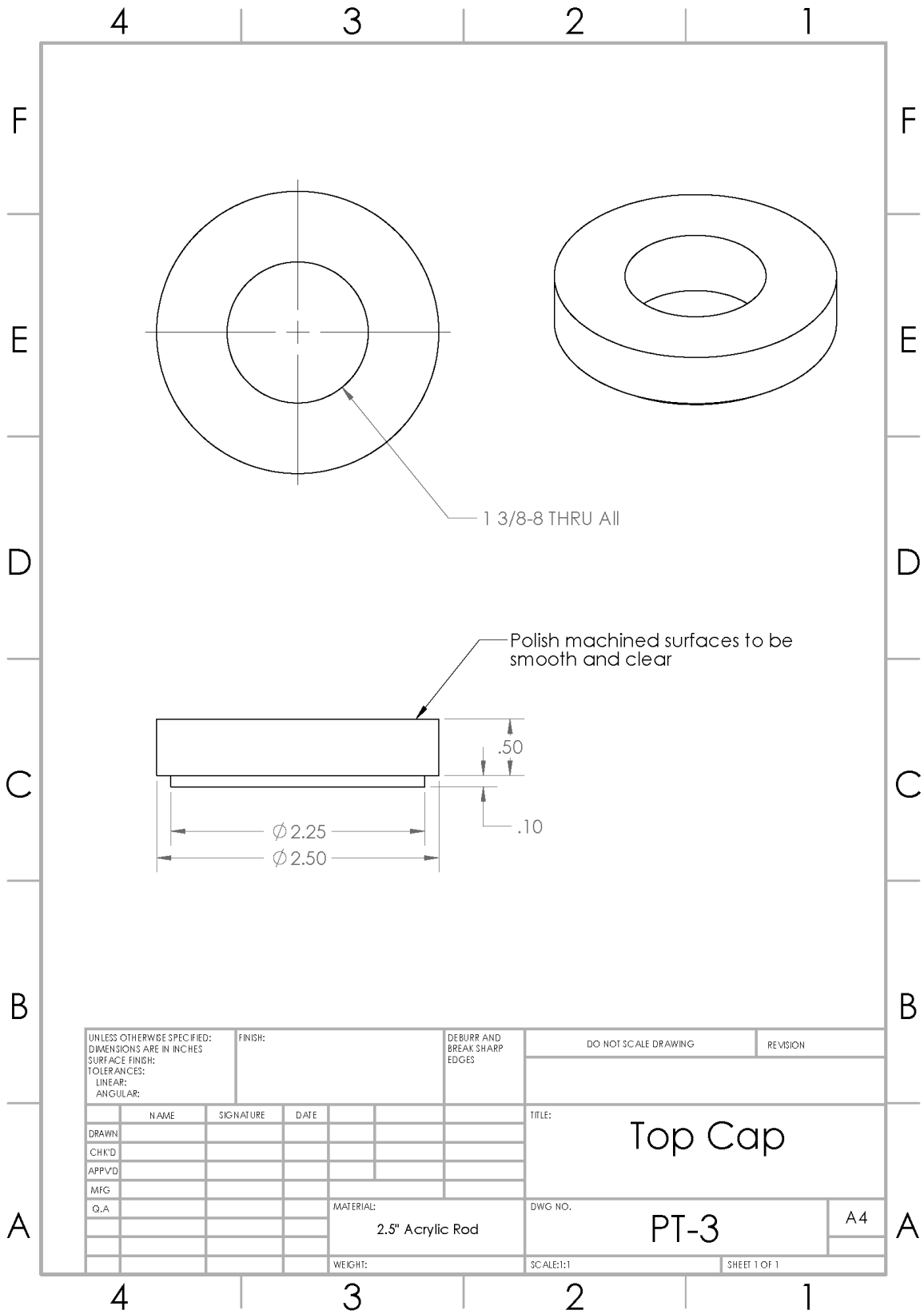


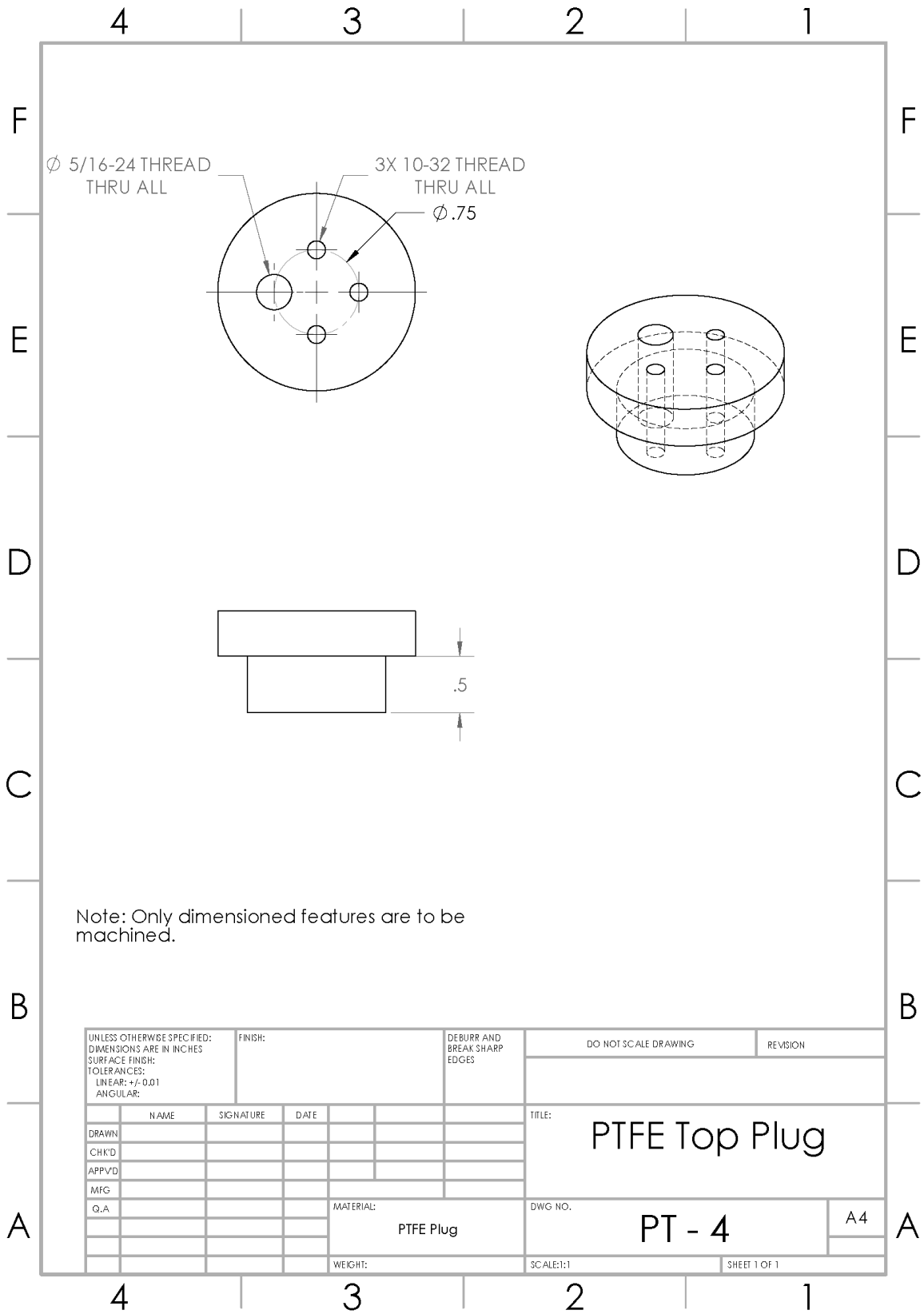
APPENDIX C. ABCHARGER 2.0 MACHINE DRAWINGS











REFERENCES

1. What Do Soldiers Carry and What Does It Weigh? | PTX Nomad.
2. Lauren Fish; Paul Scharre *The Soldier's Heavy Load*; 2018;
3. Jones, H. Special Operations Forces Tactical Energy Resource (SOFTER). 63.
4. Gironda, R.J.; Clark, M.E.; Massengale, J.P.; Walker, R.L. Pain among Veterans of Operations Enduring Freedom and Iraqi Freedom. *Pain Med* **2006**, *7*, 339–343, doi:10.1111/j.1526-4637.2006.00146.x.
5. Marine Corps Warfighting Lab Quantico Va *Guide to Employing Renewable Energy and Energy Efficient Technologies*; Defense Technical Information Center: Fort Belvoir, VA, 2012;
6. Mattis, J. Summary of the 2018 National Defense Strategy 2018.
7. National Renewable Energy Lab., Golden, CO. (US) *Hydrogen, Fuel Cells and Infrastructure Technologies Program, 2002 Annual Progress Report*; 2002;
8. Qi, Z. *Proton Exchange Membrane Fuel Cells*; CRC Press: Boca Raton, FL, 2013; ISBN 978-1-4665-1371-6.
9. Moore, J.M.; Lakeman, J.B.; Mepsted, G.O. Development of a PEM fuel cell powered portable @eld generator for the dismounted soldier. *Journal of Power Sources* **2002**, *5*.
10. Tüber, K.; Zobel, M.; Schmidt, H.; Hebling, C. A polymer electrolyte membrane fuel cell system for powering portable computers. *Journal of Power Sources* **2003**, *122*, 1–8, doi:10.1016/S0378-7753(03)00428-2.
11. Kundu, P.P.; Dutta, K. Hydrogen fuel cells for portable applications. In *Compendium of Hydrogen Energy*; Elsevier, 2016; pp. 111–131 ISBN 978-1-78242-364-5.
12. Nunes, H.X.; Ferreira, M.J.F.; Rangel, C.M.; Pinto, A.M.F.R. Hydrogen generation and storage by aqueous sodium borohydride (NaBH₄) hydrolysis for small portable fuel cells (H₂ – PEMFC). *International Journal of Hydrogen Energy* **2016**, *41*, 15426–15432, doi:10.1016/j.ijhydene.2016.06.173.
13. Cheng, X.; Shi, Z.; Glass, N.; Zhang, L.; Zhang, J.; Song, D.; Liu, Z.-S.; Wang, H.; Shen, J. A review of PEM hydrogen fuel cell contamination: Impacts, mechanisms, and mitigation. *Journal of Power Sources* **2007**, *165*, 739–756, doi:10.1016/j.jpowsour.2006.12.012.
14. Edwards, P.P.; Kuznetsov, V.L.; David, W.I.F.; Brandon, N.P. Hydrogen and fuel cells: Towards a sustainable energy future. *Energy Policy* **2008**, *36*, 4356–4362, doi:10.1016/j.enpol.2008.09.036.
15. Lubitz, W.; Tumas, W. Hydrogen: An Overview. *Chemical Reviews* **2007**, *107*, 3900–3903, doi:10.1021/cr050200z.
16. Zhang, J.; Fisher, T.S.; Ramachandran, P.V.; Gore, J.P.; Mudawar, I. A Review of Heat Transfer Issues in Hydrogen Storage Technologies. *Journal of Heat Transfer* **2005**, *127*, 1391–1399, doi:10.1115/1.2098875.
17. Petitpas, G. *Boil-off losses along LH2 pathway*; 2018; p. LLNL-TR--750685, 1466121;
18. Marrero-Alfonso, E.Y.; Beaird, A.M.; Davis, T.A.; Matthews, M.A. Hydrogen Generation from Chemical Hydrides. *Industrial & Engineering Chemistry Research* **2009**, *48*, 3703–3712, doi:10.1021/ie8016225.
19. Sakintuna, B.; Lamaridarkrim, F.; Hirscher, M. Metal hydride materials for solid hydrogen storage: A review☆. *International Journal of Hydrogen Energy* **2007**, *32*, 1121–1140, doi:10.1016/j.ijhydene.2006.11.022.

20. Kaesz, H.D.; Saillant, R.B. Hydride complexes of the transition metals. *Chemical Reviews* **1972**, *72*, 231–281, doi:10.1021/cr60277a003.
21. Voskuilen, T.G.; Waters, E.L.; Pourpoint, T.L. A comprehensive approach for alloy selection in metal hydride thermal systems. *International Journal of Hydrogen Energy* **2014**, *39*, 13240–13254, doi:10.1016/j.ijhydene.2014.06.119.
22. Visaria, M.; Mudawar, I. Experimental investigation and theoretical modeling of dehydrogenating process in high-pressure metal hydride hydrogen storage systems. *International Journal of Hydrogen Energy* **2012**, *37*, 5735–5749, doi:10.1016/j.ijhydene.2011.12.140.
23. Sakintuna, B.; Lamaridarkrim, F.; Hirscher, M. Metal hydride materials for solid hydrogen storage: A review. *International Journal of Hydrogen Energy* **2007**, *32*, 1121–1140, doi:10.1016/j.ijhydene.2006.11.022.
24. Sigma Aldrich Magnesium Hydride Safety Data Sheet 2019.
25. Thermo Fisher Scientific Lithium Hydride Safety Data Sheet 2018.
26. Stephens, F.H.; Pons, V.; Tom Baker, R. Ammonia–borane: the hydrogen source par excellence? *Dalton Trans.* **2007**, 2613–2626, doi:10.1039/B703053C.
27. Ramachandran, P.V.; Gagare, P.D. Preparation of Ammonia Borane in High Yield and Purity, Methanolysis, and Regeneration. *Inorganic Chemistry* **2007**, *46*, 7810–7817, doi:10.1021/ic700772a.
28. Peng, B.; Chen, J. Ammonia borane as an efficient and lightweight hydrogen storage medium. *Energy & Environmental Science* **2008**, doi:10.1039/b809243p.
29. Tumas, W.; Baker, R.T.; Burrell, A.; Thorn, D. IV.B.4 DOE Chemical Hydrogen Storage Center of Excellence. **2006**, *7*.
30. Moon, G.Y.; Lee, S.S.; Lee, K.Y.; Kim, S.H.; Song, K.H. Behavior of hydrogen evolution of aqueous sodium borohydride solutions. *Journal of Industrial and Engineering Chemistry* **2008**, *14*, 94–99, doi:10.1016/j.jiec.2007.08.003.
31. Santos, D.M.F.; Sequeira, C.A.C. Sodium borohydride as a fuel for the future. *Renewable and Sustainable Energy Reviews* **2011**, *15*, 3980–4001, doi:10.1016/j.rser.2011.07.018.
32. Schlesinger, H.I.; Brown, H.C.; Finholt, A.E.; Gilbreath, J.R.; Hoekstra, H.R.; Hyde, E.K. Sodium Borohydride, Its Hydrolysis and its Use as a Reducing Agent and in the Generation of Hydrogen ¹. *Journal of the American Chemical Society* **1952**, *75*, 215–219, doi:10.1021/ja01097a057.
33. Moon, G.Y.; Lee, S.S.; Yang, G.R.; Song, K.H. Effects of organic acid catalysts on the hydrogen generation from NaBH₄. *Korean Journal of Chemical Engineering* **2010**, *27*, 474–479, doi:10.1007/s11814-010-0072-3.
34. Brack, P.; Dann, S.E.; Wijayantha, K.G.U. Heterogeneous and homogeneous catalysts for hydrogen generation by hydrolysis of aqueous sodium borohydride (NaBH₄) solutions. *Energy Science & Engineering* **2015**, *3*, 174–188, doi:10.1002/ese3.67.
35. Kim, H.J.; Shin, K.-J.; Kim, H.-J.; Han, M.K.; Kim, H.; Shul, Y.-G.; Jung, K.T. Hydrogen generation from aqueous acid-catalyzed hydrolysis of sodium borohydride. *International Journal of Hydrogen Energy* **2010**, *35*, 12239–12245, doi:10.1016/j.ijhydene.2010.08.027.
36. Abdul-Majeed, W.S.; Arslan, M.T.; Zimmerman, W.B. Application of acidic accelerator for production of pure hydrogen from NaBH₄. *International Journal of Industrial Chemistry* **2014**, *5*, doi:10.1007/s40090-014-0015-7.
37. Kaufman, C.M.; Sen, B. Hydrogen generation by hydrolysis of sodium tetrahydroborate: effects of acids and transition metals and their salts. *Journal of the Chemical Society, Dalton Transactions* **1985**, 307, doi:10.1039/dt9850000307.

38. Marrero-Alfonso, E.Y.; Gray, J.R.; Davis, T.A.; Matthews, M.A. Hydrolysis of sodium borohydride with steam. *International Journal of Hydrogen Energy* **2007**, *32*, 4717–4722, doi:10.1016/j.ijhydene.2007.07.066.
39. Becker-Glad, C.A.; Glad, W.E. Acid acceleration of hydrogen generation using seawater as a reactant. *International Journal of Hydrogen Energy* **2016**, *41*, 17761–17770, doi:10.1016/j.ijhydene.2016.02.132.
40. Murugesan, S.; Subramanian, V. (Ravi) Effects of acid accelerators on hydrogen generation from solid sodium borohydride using small scale devices. *Journal of Power Sources* **2009**, *187*, 216–223, doi:10.1016/j.jpowsour.2008.10.060.
41. Lapeña-Rey, N.; Blanco, J.A.; Ferreyra, E.; Lemus, J.L.; Pereira, S.; Serrot, E. A fuel cell powered unmanned aerial vehicle for low altitude surveillance missions. *International Journal of Hydrogen Energy* **2017**, *42*, 6926–6940, doi:10.1016/j.ijhydene.2017.01.137.
42. Chandra, M.; Xu, Q. Dissociation and hydrolysis of ammonia-borane with solid acids and carbon dioxide: An efficient hydrogen generation system. *Journal of Power Sources* **2006**, *159*, 855–860, doi:10.1016/j.jpowsour.2005.12.033.
43. Kelly, H.C.; Marriott, V.B. Reexamination of the mechanism of acid-catalyzed amine-borane hydrolysis. The hydrolysis of ammonia-borane. *Inorganic Chemistry* **1979**, *18*, 2875–2878, doi:10.1021/ic50200a049.
44. Demirci, U.B. Ammonia borane, a material with exceptional properties for chemical hydrogen storage. *International Journal of Hydrogen Energy* **2017**, *42*, 9978–10013, doi:10.1016/j.ijhydene.2017.01.154.
45. Liu, C.-H.; Wu, Y.-C.; Chou, C.-C.; Chen, B.-H.; Hsueh, C.-L.; Ku, J.-R.; Tsau, F. Hydrogen generated from hydrolysis of ammonia borane using cobalt and ruthenium based catalysts. *International Journal of Hydrogen Energy* **2012**, *37*, 2950–2959, doi:10.1016/j.ijhydene.2011.05.022.
46. Brockman, A.; Zheng, Y.; Gore, J. A study of catalytic hydrolysis of concentrated ammonia borane solutions. *International Journal of Hydrogen Energy* **2010**, *35*, 7350–7356, doi:10.1016/j.ijhydene.2010.04.172.
47. T-Raissi, A. Technoeconomic Analysis of Area II/Hydrogen Production-Part II: Hydrogen from Ammonia and Ammonia-Borane Complex for Fuel Cell Applications. **2002**, *17*.
48. Ramachandran, P.V.; Kulkarni, A.S. Water-promoted, safe and scalable preparation of ammonia borane. *International Journal of Hydrogen Energy* **2017**, *42*, 1451–1455, doi:10.1016/j.ijhydene.2016.06.231.
49. Ramachandran, P.V.; Mistry, H.; Kulkarni, A.S.; Gagare, P.D. Ammonia-mediated, large-scale synthesis of ammonia borane. *Dalton Trans.* **2014**, *43*, 16580–16583, doi:10.1039/C4DT02467B.
50. Heldebrant, D.J.; Karkamkar, A.; Linehan, J.C.; Autrey, T. Synthesis of ammonia borane for hydrogen storage applications. *Energy & Environmental Science* **2008**, *1*, 156, doi:10.1039/b808865a.
51. Gabl, Jason Catalysts For Portable, Solid State Hydrogen Generation Systems, Purdue University, 2014.
52. Demirci, U.B. Ammonia borane in chemical hydrogen storage – Ammonia release during hydrolysis of ammonia borane, an issue. In Proceedings of the Advances in Nano, Biomechanics, Robotics, and Energy Research; Seoul, Korea, 2013; p. 10.

53. Uribe, F.A.; Gottesfeld, S.; Zawodzinski, T.A. Effect of Ammonia as Potential Fuel Impurity on Proton Exchange Membrane Fuel Cell Performance. *Journal of The Electrochemical Society* **2002**, *149*, A293, doi:10.1149/1.1447221.
54. Gomez, Y.A.; Oyarce, A.; Lindbergh, G.; Lagergren, C. Ammonia Contamination of a Proton Exchange Membrane Fuel Cell. *J. Electrochem. Soc.* **2018**, *165*, F189–F197, doi:10.1149/2.0761803jes.
55. Halseid, R.; Vie, P.J.S.; Tunold, R. Effect of ammonia on the performance of polymer electrolyte membrane fuel cells. *Journal of Power Sources* **2006**, *154*, 343–350, doi:10.1016/j.jpowsour.2005.10.011.
56. Lemons, A. FUEL CELLS FOR TRANSPORTATION. 14.
57. Kelly, H.C.; Marchelli, F.R.; Giusto, M.B. The Kinetics and Mechanism of Solvolysis of Amineboranes. *Inorganic Chemistry* **1964**, *3*, 431–437, doi:10.1021/ic50013a027.
58. D'Ulivo, A.; Onor, M.; Pitzalis, E. Role of Hydroboron Intermediates in the Mechanism of Chemical Vapor Generation in Strongly Acidic Media. *Analytical Chemistry* **2004**, *76*, 6342–6352, doi:10.1021/ac040078o.
59. Stephens, F.H.; Baker, R.T.; Matus, M.H.; Grant, D.J.; Dixon, D.A. Acid Initiation of Ammonia–Borane Dehydrogenation for Hydrogen Storage. *Angewandte Chemie International Edition* **2007**, *46*, 746–749, doi:10.1002/anie.200603285.
60. D'Ulivo, L.; Spiniello, R.; Onor, M.; Campanella, B.; Mester, Z.; D'Ulivo, A. Behavior and kinetic of hydrolysis of amine boranes in acid media employed in chemical vapor generation. *Analytica Chimica Acta* **2018**, *998*, 28–36, doi:10.1016/j.aca.2017.10.034.
61. Xu, Q.; Chandra, M. Catalytic activities of non-noble metals for hydrogen generation from aqueous ammonia–borane at room temperature. *Journal of Power Sources* **2006**, *163*, 364–370, doi:10.1016/j.jpowsour.2006.09.043.
62. Hu, L.; Zheng, B.; Lai, Z.; Huang, K.-W. Room temperature hydrogen generation from hydrolysis of ammonia–borane over an efficient NiAgPd/C catalyst. *International Journal of Hydrogen Energy* **2014**, *39*, 20031–20037, doi:10.1016/j.ijhydene.2014.10.032.
63. US Army Corp of Engineers Military Specification MIL-PRF-32383/3, Battery, Rechargeable, Sealed, BB-2590()/U, BB-390()/U, AND BB-3590()/U 2011.
64. BT-70791CK, BB-2590/U 7.5 Ah Rechargeable Lithium-Ion Battery Available online: <https://www.bren-tronics.com/bt-70791ck.html> (accessed on Jun 28, 2019).
65. Kim, J.; Kim, D.-M.; Kim, S.-Y.; Nam, S.W.; Kim, T. Humidification of polymer electrolyte membrane fuel cell using short circuit control for unmanned aerial vehicle applications. *International Journal of Hydrogen Energy* **2014**, *39*, 7925–7930, doi:10.1016/j.ijhydene.2014.03.012.
66. Galvion Soldier Power Solutions Available online: <https://www.galvion.com/pages/soldier-power> (accessed on Apr 7, 2020).
67. B&K 8600 Series Programmable DC Electronic Load Data Sheet Available online: https://bkpmedia.s3.amazonaws.com/downloads/datasheets/en-us/8600_Series_datasheet.pdf (accessed on Apr 8, 2020).
68. Huang, Z.-M.; Su, A.; Liu, Y.-C. Hydrogen generation with sodium borohydride solution by Ru catalyst. *International Journal of Energy Research* **2013**, *37*, 1187–1195, doi:10.1002/er.2937.

69. Marrero-Alfonso, E.Y.; Gray, J.R.; Davis, T.A.; Matthews, M.A. Minimizing water utilization in hydrolysis of sodium borohydride: The role of sodium metaborate hydrates. *International Journal of Hydrogen Energy* **2007**, *32*, 4723–4730, doi:10.1016/j.ijhydene.2007.08.014.
70. Liu, B.H.; Li, Z.P. A review: Hydrogen generation from borohydride hydrolysis reaction. *Journal of Power Sources* **2009**, *187*, 527–534, doi:10.1016/j.jpowsour.2008.11.032.
71. Demirci, U.B. About the Technological Readiness of the H₂ Generation by Hydrolysis of B(–N)–H Compounds. *Energy Technol.* **2018**, *6*, 470–486, doi:10.1002/ente.201700486.
72. Petit, E.; Miele, P.; Demirci, U.B. By-Product Carrying Humidified Hydrogen: An Underestimated Issue in the Hydrolysis of Sodium Borohydride. *ChemSusChem* **2016**, *9*, 1777–1780, doi:10.1002/cssc.201600425.
73. Kim, H.; Oh, T.H.; Kwon, S. Simple catalyst bed sizing of a NaBH₄ hydrogen generator with fast startup for small unmanned aerial vehicles. *International Journal of Hydrogen Energy* **2016**, *41*, 1018–1026, doi:10.1016/j.ijhydene.2015.11.134.
74. Oh, T.H.; Gang, B.G.; Kim, H.; Kwon, S. Sodium borohydride hydrogen generator using Co–P/Ni foam catalysts for 200 W proton exchange membrane fuel cell system. *Energy* **2015**, *90*, 1163–1170, doi:10.1016/j.energy.2015.06.055.
75. Gang, B.G.; Jung, W.; Kwon, S. Transient behavior of proton exchange membrane fuel cells over a cobalt–phosphorous/nickel foam catalyst with sodium borohydride. *International Journal of Hydrogen Energy* **2016**, *41*, 524–533, doi:10.1016/j.ijhydene.2015.11.064.
76. Moritz, A.R.; Henriques, F.C. Studies of Thermal Injury. *Am J Pathol* **1947**, *23*, 695–720.
77. Dearborn, S. Charging Li-ion Batteries for Maximum Run Times. **2005**, *9*.
78. Akdim, O.; Demirci, U.B.; Miele, P. Acetic acid, a relatively green single-use catalyst for hydrogen generation from sodium borohydride. *International Journal of Hydrogen Energy* **2009**, *34*, 7231–7238, doi:10.1016/j.ijhydene.2009.06.068.
79. Fisher Scientific *Sodium Tartrate MSDS*;
80. *Boron*; Smallwood, C., International Programme on Chemical Safety, Eds.; Environmental health criteria; World Health Organization: Geneva, 1998; ISBN 978-92-4-157204-0.
81. Dell, R.M.; Moseley, P.T.; Rand, D.A.J. Hydrogen, Fuel Cells and Fuel Cell Vehicles. In *Towards Sustainable Road Transport*; Elsevier, 2014; pp. 260–295 ISBN 978-0-12-404616-0.
82. Prosini, P.P.; Gislou, P. A hydrogen refill for cellular phone. *Journal of Power Sources* **2006**, *161*, 290–293, doi:10.1016/j.jpowsour.2006.03.072.
83. Gislou, P.; Monteleone, G.; Prosini, P. Hydrogen production from solid sodium borohydride. *International Journal of Hydrogen Energy* **2009**, *34*, 929–937, doi:10.1016/j.ijhydene.2008.09.105.